

b14016023

U.O.V.S. BIBLIOTEK

01

HIERDIE EKSEMPLAAR MAG ONDER
GEEN OMSTANDIGHEDE UIT DIE
BIBLIOTEK VERWYDER WORD NIE

University Free State



34300000933246

Universiteit Vrystaat

**SUBSTITUTION BEHAVIOUR OF WATER-
SOLUBLE ORGANOPHOSPHINE COMPLEXES OF
PALLADIUM(II)**

A thesis submitted to meet the requirements for the degree of

MAGISTER SCIENTIAE

In the

**DEPARTMENT OF CHEMISTRY
FACULTY OF NATURAL AND AGRICULTURAL SCIENCE**

At the

UNIVERSITY OF THE FREE STATE

By

Anna Magrietha Magdalena Meij

Supervisor

PROF. A. ROODT

Co-Supervisor

Dr. S. Otto

December 2001

Universiteit van die
Oranje-Vrystaat
BLOEMFONTEIN

25 APR 2002

UOVS SASOL BIBLIOTEEK

But about going further than the words given by one Shepherd, my son, be warned. Of making many books there is no end so do not believe everything you read, and much study is a weariness of the flesh. All has been heard; the end of the matter is: Fear God [revere and worship Him, knowing that He is] and keep His commandments, for this is the whole of man [the full, original purpose of his creation, the object of God's providence, the root of character, the foundation of all happiness, the adjustment to all inharmonious circumstances and conditions under the sun] and the whole [duty] of every man. For God shall bring every work into judgement, with every secret thing, whether it is good or evil.

Ecclesiastes 12:12-14

Net om dankie te sê

Graag wil ek my dank uitspreek teenoor die volgende persone:

Prof. Roodt, dankie vir Prof se leiding, hulp en motivering – vir die passie vir chemie wat so aansteeklik is. Meer nog: Vir die voorbeeld wat Prof daar stel wat nagevolg kan word.

Fanie Otto, dankie vir jou idees en raad, dat jy altyd bereidwillig was om hulp te verleen en vir die geleentheid om ook onder jou leiding hierdie studie te kon aanpak.

Aan medestudente wat bygedra het om hierdie tesis 'n werklikheid te laat word en wat morele ondersteuning gegee het – Jannie, Lang Hendrik, Fanie M. en Eleanor – baie dankie, ook vir lekker tye van lag en gesels wat ons kon deel!

Alta, dankie vir jou ondersteuning, belangstelling en hulp, veral met die laaste styftrekkings met die skryf van hierdie werk. Dankie dat ek meer as net chemie met jou kan deel. Jou vriendskap stel ek hoog op prys.

Aan Diederick en Ouma, dankie vir ondersteuning en liefde.

Aan Pa en Ma, dankie vir u onbaatsugtige liefde en opofferings – dat u my geleer het dat die lewe oor meer gaan as net dit wat ons sien. Woorde sal nie regtig my dank kan beskryf nie.

Hierdie tesis dra ek aan Pa en Ma op as 'n geringe blyk van waardering.

Aan U, o, Here Jesus, U wat die Skepper van chemie is en wat alles wat asemhaal omsluit, U wat nuwe lewe gee, aan U kom al die lof toe. U is waarlik groot!

Anneline Meij

Table of Contents

Abbreviations and Symbols	v
1. Introduction and Aim	1
1.1 Introduction	1
1.2 Aim of This Study	3
2. An Overview of Palladium Chemistry and Water-Soluble Phosphines	5
2.1 Palladium	5
2.1.1 Introduction	5
2.1.2 The (II) Oxidation State, d^8	5
2.1.2.1 Complexes of Palladium(II)	6
2.1.2.2 Palladium(II) Phosphorus Donor Complexes	7
2.1.2.3 Palladium(II) Oxygen and Sulfur Donor Complexes	9
2.1.2.4 Palladium(II) Nitrogen Donor Complexes	10
2.1.3 The (0) Oxidation State	10
2.1.3.1 Palladium(0) Phosphine Complexes	11
2.1.4 Other Oxidation States and Clusters	11
2.2 Elementary Steps in a Palladium Catalyzed Process	13
2.2.1 Palladium-Catalyzed Reactions	14
2.2.1.1 Reactions catalyzed by Palladium(II) Complexes	14
2.2.1.2 Reactions Catalyzed by Palladium(0) Complexes	18
2.3 Water-Soluble Systems	21
2.3.1 Introduction	21
2.3.2 Water-Soluble Ligands	22
2.3.3 The Water-Soluble Phosphine 1,3,5-Triaza-7-Phosphaadamantane	24
2.3.4 General Coordination Chemistry in various PTA complexes	25
2.3.5 PTA Complexes of Palladium	27

3. Synthesis and Characterization of Complexes	31
3.1 Synthesis	31
3.1.1 Introduction	31
3.1.2 Chemicals and Instruments	31
3.1.3 1,3,5-triaza-7-phosphaadamantane (PTA)	32
3.1.4 Synthesis of $(\text{NH}_4)_2[\text{PdCl}_4]$	32
3.1.5 $[\text{PdCl}(\text{PTA})_3]\text{Cl}$	33
3.1.6 $[\text{PdCl}_2(\text{COD})]$	33
3.1.7 <i>cis</i> - $[\text{PdCl}_2(\text{PTA})_2]$	34
3.1.8 <i>trans</i> - $[\text{Pd}(\text{SCN})_2(\text{PTAH})_2](\text{SCN})_2$	34
3.1.9 <i>trans</i> - $[\text{PdBr}_2(\text{PTA})_2]$	34
3.1.10 <i>trans</i> - $[\text{PdI}_2(\text{PTA})_2]$	35
3.1.11 $[\text{Pd}(\text{N}_3)_2(\text{PTA})_2]$	35
3.2 Crystallography	35
3.2.1 Introduction	35
3.2.2 Definition of a Crystal	36
3.2.3 Diffraction of X-rays	36
3.2.4 The Structure Factor	36
3.2.5 Fourier Transformation	37
3.2.6 The Patterson Synthesis	38
3.2.7 Least-Squares Refinement of a Structural Model	38
3.3 X-ray Crystal Structure Determinations of Selected complexes	39
3.3.1 Experimental	39
3.3.2 The Crystal Structure of <i>trans</i> - $[\text{Pd}(\text{SCN})_2(\text{PTAH})_2](\text{SCN})_2$	41
3.3.3 The Crystal Structure of <i>trans</i> - $[\text{PdBr}_2(\text{PTA})_2]$	46
3.3.4 Structural parameter correlation in square planar and related palladium(II) and platinum(II) complexes containing PTA as ligand	50
4. Solution Behavior and Kinetic Studies	57
4.1 Introduction	57

Table of Contents

4.2 Reaction Kinetics - Theoretical Overview	57
4.2.1 Introduction	57
4.2.2 Rate and Order of a Reaction	58
4.2.3 Pseudo-Order Reactions	60
4.2.4 Activation Parameters	62
4.3 Square Planar Substitution Reactions	64
4.3.1 Introduction	64
4.3.2 General Reaction Mechanism	65
4.3.3 General Rate Law for Square Planar Substitution Reactions	67
4.3.4 Factors Influencing the Reactivity of Square Planar Complexes	67
4.3.5 Coordination Number Four: Square Planar vs. Tetrahedral	71
4.4 NMR Kinetic Studies	71
4.5 Experimental Procedures	76
4.5.1 Multinuclear NMR	76
4.5.2 General UV-Vis Measurements	76
4.5.3 Equilibrium Constant Determination	76
4.6 Reaction Scheme/Mechanism and Rate Law	77
4.6.1 Characterization of the Starting Complexes	77
4.6.2 Stability of $[\text{PdCl}(\text{PTA})_3]^+(\text{I})$ in Aqueous Media	77
4.6.3 Stability of <i>cis</i> - $[\text{PdCl}_2(\text{PTA})_2](\text{II})$ in Aqueous Media	80
4.6.4 Multinuclear NMR	82
4.6.5 Conversion of $[\text{PdCl}(\text{PTA})_3]^+(\text{I})$ to <i>cis</i> - $[\text{PdCl}_2(\text{PTA})_2](\text{II})$ as a Function of Chloride	86
4.6.6 Protonation Behaviour of $[\text{PdCl}(\text{PTA})_3]^+(\text{I})$	87
4.6.7 Addition of Halides or Pseudo-halides	91
4.6.8 <i>Cis-Trans</i> Isomerization of $[\text{PdY}_2(\text{PTA})_2]$	92
4.6.9 Equilibrium Studies	92
4.6.10 Reactivity of Complexes	93
4.6.11 Reaction Scheme	95

Table of Contents

4.7 Results	96
4.7.1 Equilibrium Studies	96
4.7.2 Chloride Exchange	99
5. Evaluation and Future Research	106
5.1 Evaluation of The Study	106
5.2 Future Research	108
Appendix A	110
A Crystallographic data for <i>trans</i> -[Pd(SCN) ₂ (PTAH) ₂](SCN) ₂	110
B Crystallographic data for <i>trans</i> -[PdBr ₂ (PTA) ₂]	113
C Supplementary material reported for Chapter 4	116
Abstract	122
Opsomming	124



Abbreviations and Symbols

δ	Chemical shift
ρ	Electron density
θ_E	Effective cone angle
2-dqmp	2-quinolylmethylphosphonate
A_B	Absorbance of reactant
A_F	Absorbance of product
bipy	Bipyridine
Bu	Butyl
Bz	Benzene
ca.	Approximately
CO	Carbonyl
COD	1,5-cyclooctadiene
d	Doublet
DAED	2-(2-{diphenylarsino}ethyl)-1,3-dioxane
dd	Doublet of doublet
DDEP	2-(diphenylphosphino)ethanephosphonate
DMPP	1-phenyl-3,4-dimethylphosphole
DPA	Diphenylphosphinoacetic acid
DPPD	2-(2'-diphenylphosphinophenyl)-1,3-dioxalane
DTP	5,7-dimethyl-8H-[1,2,4]triazolo[1,5-5]pyrimidine
EPTA ⁺ T ⁻	1-ethyl-1-azonia-3,5-diaza-7-phosphaadamantane iodide
Eq.	Equation
Et	Ethyl
h	Planck's constant
H ₂ L	BH-alkyl-N'aroylthiourea
idaaH ₂	Iminodiacetamide
Ino	Inosine
IR	Infrared spectroscopy
K	Equilibrium constant
k	Rate constant
k_B	Boltzman's constant
k_s	Rate constant for the substitution (solvent path)
k_{obs}	Observed pseudo-first-order rate constant
k_e	Rate constant for the exchange path (direct path)

ABBREVIATIONS AND SYMBOLS

L	Ligand
m	Medium
m	Multiplet
Me	Methyl
MES	(2-[N-Morpholino]ethanesulfonic acid)
MPTA ^{+I}	1-methyl-1-azonia-3,5-diaza-7-phosphaadamantane iodide
NMR	Nuclear Magnetic Resonance spectroscopy
OMe	Methoxy
pgm	Platinum group metal
phen	Phenantroline
PMQ	2,5,6,7,8-pentamethylquinoxalin-3-yl
PPh ₃	Triphenylphosphine
PPK	Phenyl-2-pyridyl ketone
ppm	Unit of chemical shift - Parts per million
ppq	<i>p</i> -quinonyldiphenylphosphine
PTA	1,3,5-triaza-7-phosphaadamantane
py	Pyridine
RDS	Rate determining step
s	Singlet
s	Strong
SCN	Thiocyanate
t	Triplet
TMP	1,3,4-trimethyl-phosphole
TP	2-(2'-thienyl)pyridine
TPPMS	meta-sulphonatophenyldiphenylphosphine
TPPTS	tris-meta-sulphonatophenylphosphine
TQ	Terquinoxaliny
TW	This work
UV	Ultraviolet
w	Weak

1 Introduction and Aim

1.1 Introduction^{1,2}

Wollaston discovered palladium in 1802 in the course of refining platinum. It is the second most abundant platinum group metal (pgm), accounting for 38% of pgm reserves. Russia produces over 50% of the world's palladium, which is more than double that produced by South Africa. Braggite, a mixed sulfide of platinum, palladium and nickel, and michenerite (PdBi_3), are two major sources of the metal.

Remarkable advances have been made in the applications of various transition metal compounds in organic synthesis, particularly as homogeneous catalysts. Amongst many transition metals used in organic synthesis as catalysts, palladium is the most versatile and is particularly useful for carbon-carbon bond formation reactions (Heck reaction).

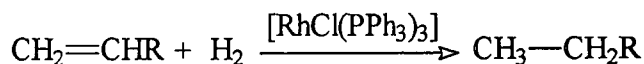
For many years palladium has been used mainly in laboratories and industrial processes as a supported catalyst for hydrogenation of unsaturated compounds. The renaissance of palladium chemistry started in 1958 when the Wacker process was invented and since then it has found industrial usage. Formerly palladium was only used for redox reactions, but recently it achieved a prominent role in synthesis due to the manifold and unique transformations that it is capable of mediating, often in a catalytic mode. In conjunction with the above the heterogeneous combination of palladium alloys found other application in catalytic converters of automotive exhaust fumes.

Palladium is now widely used in both chemical laboratories and in the chemical industry. The number of industrial processes catalysed by palladium compounds is increasing, particularly for the production of fine chemicals. Palladium is a somewhat expensive metal, but can be tolerated economically as a catalyst if it is an efficient one. In addition, palladium compounds are usually stable, easy to handle and toxicity is not a problem.

Some of the most important processes, where palladium catalysts are employed, include:

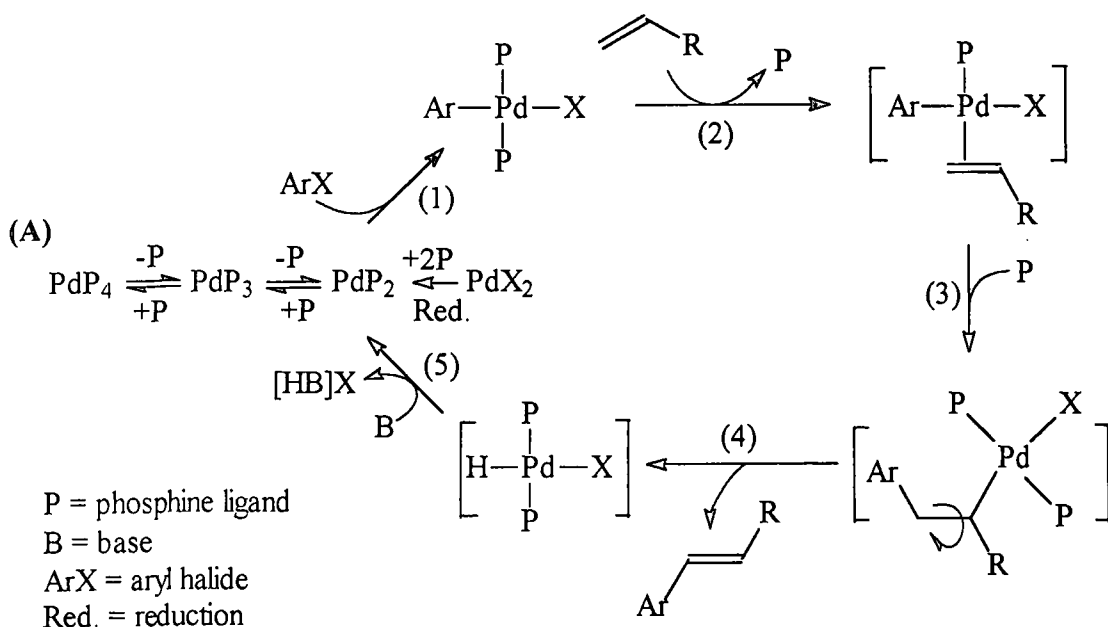
- hydroformylation of olefins (Wacker process), *e.g.*, PdCl₂;
- carbonylation of olefins, amines and alcohols, *e.g.*, PdCl₂, Pd(OAc)₂, Pd-C;
- oxidative coupling of aromatic compounds, *e.g.*, Pd(OAc)₂;
- acetoxylation of aromatic compounds, *e.g.*, Pd(OAc)₂;
- C-C coupling reactions of aryl and alkenyl halides (Heck reactions), *e.g.*, Pd(PPh₃)₃, Pd(OAc)₂/PPh₃.

Wilkinson's catalyst, [RhCl(PPh₃)₃], is a very useful catalyst that hydrogenates a wide variety of alkenes at pressures of hydrogen close to 1 atm and a general reaction is given as:



Similarly, palladium analogues of Wilkinson's compound can also be synthesized. The mechanism³ of the Heck C-C coupling is given in Scheme 1.1 as example were palladium-phosphine complexes are used:

Scheme 1.1 Mechanism of Heck C-C coupling.



It is clear from the mechanism that the phosphine ligands play an important role in the reactions, since the equilibrium distribution in (A) is dependent on the properties of these ligands. Step (1) is the oxidative addition of ArX to the metal centre and it is critically dependent on ArX and on PdP₂, but PdP₂ is primarily determined by the properties of the

phosphines ligand, since it is the only ligands in the coordination sphere. Step (2) is the insertion of the olefin and the dissociation of the phosphine ligand; again the phosphine ligand plays a significant role. In step (3) a C-C coupling reaction occurs during which a phosphine ligand is re-introduced to the metal center. Elimination occurs in step (4) to form the final olefin C-C coupling product. The catalyst reactivation follows in step (5) *via* HX-elimination by the base. Three of the five steps mentioned above in the catalytic cycle are thus closely interlinked to the properties of the specific phosphine ligand employed during the process.

It is also well known that the medium in which the reaction is performed has a significant effect on the rate of the reaction and product distribution. In this context water-soluble catalysts^{3,4} combine the following advantages of homogeneous and heterogeneous catalysis:

- (i) simple separation of the product from the catalyst, and
- (ii) high activity and regioselectivity.

Furthermore, the use of water as a solvent, if possible, has advantages, since it is economical, non-toxic and environmentally acceptable. However, water is also a highly polar solvent with the ability to form strong hydrogen bonds, and therefor may affect the mechanism of the catalysis intricately.

Today, environmental factors in addition to economic motives are more and more taken into consideration as a driving force for technological innovations in the chemical industry. In this regard, homogeneous catalysis can be regarded as particular attractive. The development of water-soluble, and therefor polar, ligands and their incorporation into organometallic complexes, play a mayor role in the field of aqueous homogeneous catalysis.

1.2 Aim of This Study

Wilkinson's complex is an important square planar complex and catalyst and the aim of this study is to prepare palladium analogues thereof, since palladium-phosphine complexes play a significant role in many catalytic reactions. The phosphine ligand that will be employed is PTA (PTA = 1,3,5-triaza-7-phosphaadamantane), since it is soluble in water.

Prior to the experimental investigation an extensive literature survey, covering different aspects to be investigated, was done and is reported in Chapter 2 and Chapter 4.

The aim of this study was the following:

- (i) The preparation and characterization of the palladium analogue of Wilkinson's complex, $[\text{PdCl}(\text{PTA})_3]\text{Cl}$, as well as related complexes^{5,6}.
- (ii) Investigation of the stability of these complexes in aqueous solution as well as the effect of pH and hydrolysis on the stability and composition of the complexes.
- (iii) Investigation of the solution behaviour of the complexes with respect to other halides/pseudo-halides. These reactions will also be investigated kinetically and thermodynamically to gain information on the stability, as well as the product distribution in order to construct a mechanism for the reactions.
- (iv) Characterization of the starting complexes, intermediates and products with the techniques available, such as IR- and UV-Vis spectrophotometry, multinuclear NMR (^1H , ^{31}P and ^{35}Cl) spectrometry and if possible, X-ray crystallography.
- (v) Construction of a complete reaction scheme of the aqueous solution behaviour of the $[\text{PdCl}(\text{PTA})_3]^+$ complex in the presence of halide/pseudo-halide.

¹ G. Wilkinson, R. D. Gillard, J. A. McCleverty, *Comprehensive Coordination Chemistry – Volume 5*, Pergamon Press, 1987, 1099.

² J. Tsuji, *Synthesis*, 1990, 739.

³ W. A. Herrmann, B. Cornils, *Applied Homogeneous Catalysis with Organometallic Compounds*, Wiley-VCH Publishers, Weinheim, 2000, p575, p719.

⁴ M. Karlsson, M. Johansson, C. Andersson, *J. Chem. Soc. Dalton. Trans.*, 1999, 4175.

⁵ D. J. Darensbourg, T. J. Decuir, N. W. Stafford, J. B. Robertson, J. D. Draper, J. H. Reibenspies, A. Kathó, F. Joó, *Inorg. Chem.*, 1997, **36**, 4218.

⁶ D. J. Darensbourg, J. B. Robertson, D. L. Larkins, J. H. Reibenspies, *Inorg. Chem.*, 1999, **38**, 2473.

An Overview of Palladium Chemistry

2 and Water-Soluble Phosphines

2.1 Palladium

2.1.1 Introduction^{1,2}

Palladium is a $4d$ transition element and has the electronic configuration of $[\text{Kr}] 4d^{10}$. The most characteristic feature of its chemistry is its similarity with platinum, its $5d$ congener, but it differs from platinum in that it is much more reactive. Palladium exists in various oxidation states that are of typical importance in catalytic processes.

The dominant oxidation state of palladium is II. Palladium(IV) complexes are less stable than the corresponding platinum compounds and are readily reduced to palladium(II). Where Pd-Pd bonds are involved the I and III oxidation states are found, but it is rare. The 0 oxidation state is found where PR_3 , CO, olefins and other π -acid ligands are present, while the higher oxidation state V occurs only in a few fluoro compounds. In some compounds mixed oxidation states also occur, usually II and IV, but some with III.

2.1.2 The (II) Oxidation State, d^8

Palladium(II) is generally regarded as a class b (soft) metal and this is reflected in the rich chemistry with sulfur and phosphorus donor ligands. Palladium(II) complexes can be of all possible types, for example $[\text{PdL}_4]^{2+}$, $[\text{PdL}_3\text{X}]^+$, *cis*- and *trans*- $[\text{PdL}_2\text{X}_2]$, $[\text{PdLX}_3]^-$ and $[\text{PdX}_4]^-$ (L = neutral ligand; X = negative ligand). The Pd^{2+} ion occurs in $[\text{PdF}_2]$ and $[\text{PdCl}_2]$ and is paramagnetic. In aqueous solution, however, the $[\text{Pd}(\text{H}_2\text{O})_4]^{2+}$ ion is diamagnetic and is presumably square planar. In general, palladium(II) complexes are four or five-coordinate (square planar or trigonal bipyramidal) and are diamagnetic. Palladium(II) have a preference for halogens and ligands that can π bond such as PR_3 , SR_2 , CN^- , NO_2^- , alkenes, and alkynes. Strong bonds that form with ligands with heavier donor atoms is the result of metal-ligand π -bonds that forms. Palladium shows low affinity for F^- and O donor ligands.

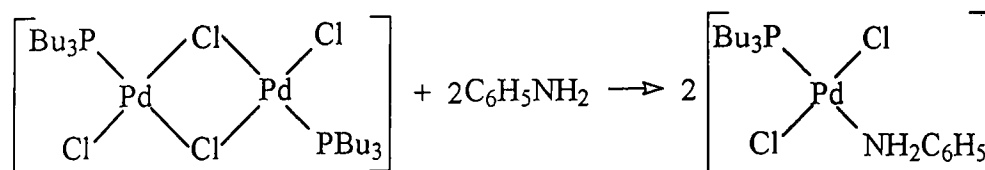
The formation of cationic species even with non- π -bonding ligands and anionic species with halide ions contrasts with the chemistry of the isoelectronic rhodium(I) and iridium(I) where most of the complexes involve π bonding. The difference is presumably a reflection on the higher charge. Palladium(II) species bond with neutral molecules to form five- and six-coordinate species, but they do so with less ease. Oxidative-addition reactions that is characteristic of d^8 complexes, have a tendency to form equilibrium reactions, except with strong oxidants. This is presumably because more energy of activation is needed for $M(\text{II}) \rightarrow M(\text{IV})$ than for $M(\text{I}) \rightarrow M(\text{III})$.

Palladium(II) complexes are usually similar to their platinum(II) analogues, although the palladium complexes are somewhat less stable in the thermodynamic and the kinetic sense than platinum.

2.1.2.1 Complexes of Palladium(II)

For the preparation of palladium(II) or palladium(0) complexes salts of the ions $[\text{MCl}_4]^{2-}$ are a common source. The yellowish $[\text{PdCl}_4]^{2-}$ ion is formed when $[\text{PdCl}_2]$ is dissolved in aqueous HCl or when $[\text{PdCl}_6]^{2-}$ is reduced with Pd sponge. A disadvantage of starting with this complex is that the sodium salt cannot be obtained pure. Furthermore, in contrast to platinum, the $[\text{PdCl}_4]^{2-}$ and $[\text{Pd}(\text{phen})_2]^{2+}$ ions associate with Cl^- in solution to form five-coordinate species.

Bridged complexes of palladium can also be formed. Bridges like SCN^- may form linkage isomers. Bridged species are generally subject to cleavage⁶ by various nucleophiles giving mononuclear species, for example in Eq. 2.1:



2.1

The equilibria generally lie toward the mononuclear complexes when the bridges are Cl^- or Br^- . Such bridge-splitting reactions should give *trans* products supposedly, and the *trans* isomers probably are the initial products of most cleavage reactions. However, depending

on the identities of L and X, the relative stabilities of the *cis* and *trans* isomers of $[\text{PdL}_2\text{X}_2]$ and $[\text{PtL}_2\text{X}_2]$ vary greatly. A major difference between square planar complexes of the two metals is that for $[\text{PtX}_2(\text{PR}_3)_2]$ complexes *cis-trans* isomerization normally proceed extremely slowly unless catalyzed by excess PR_3 , whereas the analogous isomerization of palladium(II) complexes proceeds rapidly to give equilibrium mixtures. Many substitution and isomerization reactions of square planar complexes normally proceed by association involving distorted five-coordinate intermediates (trigonal bipyramidal transition states). The *cis-trans* isomerization of $[\text{PdL}_2\text{X}_2]$ complexes where the isomerization is immeasurably slow in the absence of an excess phosphine, is very fast when phosphine is present. The isomerization doubtlessly proceeds by pseudorotation of the five-coordinate state. Weakly bound solvent molecules may of course occupy the "vacant" positions on square planar species, while interaction between suitably placed atoms on the ligand may lead to blocking of one or more positions.

2.1.2.2 Palladium(II) Phosphorus Donor Complexes

Amongst the most intensively studied complexes with palladium, both chemically and spectroscopically are the complexes with the tertiary phosphine ligands (π -bonding as well as σ donor ligands). Not only are they important in chemistry in the II oxidation state, but also of the 0 and I oxidation state.

Palladium(II) phosphine complexes with hydrides may be of the types $[\text{PdXH}(\text{PR}_3)_2]$ (X = halide, alkyl, aryl, *etc.*) and $[\text{PdH}_2(\text{PR}_3)_2]$ with both the *cis* and the *trans* isomers existing. The stable dihydrides are usually *trans*, but for PMe_3 and PEt_3 the isomers are in equilibrium with the *cis* isomers where the ratio is very dependent on the solvent. Phosphines, phosphites and arsines give similar complexes. They are obtained from dihalides (the *cis* isomer is usually the most reactive) by the action of hydride transfer agents such as KOH in ethanol, 90% N_2H_4 , Na naphthalenide under H_2 , *etc.* Palladium(II) phosphine complexes with alkyls and aryls (σ -bonding ligands) may be of the type $[\text{PdXR}(\text{PR}'_3)_2]$ and $[\text{PdR}_3(\text{PR}'_3)_2]$. These complexes have also been intensively studied because of interest in decomposition pathways such as reductive-elimination and β -hydride transfers.

Palladium(II) phosphine dihalide complexes $[\text{PdX}_2(\text{PR}_3)_2]$ are formed when solutions of $[\text{PdX}_4]^{2-}$ ($\text{X} = \text{Cl}, \text{Br}$ or I) are treated with two equivalents of a tertiary phosphine:

$[\text{PdX}_4]^{2-} + 2\text{PR}_3 \longrightarrow [\text{PdX}_2(\text{PR}_3)_2] + 2\text{X}^-$. The products are generally yellow air stable crystalline solids. Arsines and stibines react in a similar manner and the thermal stability decreases in the order $\text{PR}_3 > \text{AsR}_3 > \text{SbR}_3$.

With these types of complexes it is important to distinguish between *cis* and *trans* isomers. In a solution a *cis-trans* equilibrium is rapidly established. Usually only one form is obtained on working up (in contrast to the chemistry of the analogous platinum(II) compounds). In general the *cis* isomer is more stable than the *trans* isomer; the amount of *trans* isomer in solution decreasing with basicity of the ligand and increasing dipole moment of the solvent. The halide complexes $[\text{PdX}_2(\text{PR}_3)_2]$ are precursors to a wide variety of derivatives, which may be prepared by simple substitution reactions.

The pseudo-halide complexes $[\text{PdX}_2(\text{PR}_3)_2]$ ($\text{X} = \text{N}_3, \text{NCO}, \text{SCN}$ or CN) may be prepared by metathesis of the chloro complexes with NaX or LiX . The thiocyanate complexes are especially interesting since the mode of coordination of the ambidentate ligand is markedly influenced by the other ligands present. Isomerization can be brought about in a number of cases by heating the solid complex or by dissolution in an appropriate solvent. The type of coordination found in a particular complex may in general only be rationalized by consideration of both electronic and steric factors. As an example of steric factors is given the complex *trans*- $[\text{Pd}(\text{NCS})_2(\text{PPh}_3)_2]$ which contains N-bonded, linear NCS groups, but in the analogous complex containing the less sterically demanding triphenyl phosphite ligand, *trans*- $[\text{Pd}(\text{SCN})_2\{\text{P}(\text{O}^i\text{Ph})_3\}_2]$, the thiocyanate ligand is S-bonded and non-linear.

Five-coordination is much less common for palladium(II) than for nickel(II). Nonetheless, ligands with suitable steric requirements can, under favourable conditions, yield $[\text{PdX}_2(\text{PR}_3)_3]$ complexes, e.g., $[\text{PdCl}_2(\text{PPhMe}_2)_3]$. Stibines in particular seem to favour higher coordination numbers.

2.1.2.3 Palladium(II) Oxygen and Sulfur Donor Complexes

Palladium(II), as a soft metal ion, does not form strong bonds with oxygen donors and therefore the ligands can readily undergo substitution. Oxygen-containing solvents such as water, alcohols or ethers are such poor donors that few complexes with palladium(II) have been isolated. The most important class of complexes of this type consists of those containing water. They are formed as intermediates in the substitution reactions of palladium(II) when carried out in aqueous solution. In these reactions their formation are in competition with the second order reaction of the complex with the incoming ligand. The reaction of halo complexes with silver salts containing non-coordinating anions (e.g., NO_3^- , ClO_4^- , BF_4^-) in water can also form the aqua complexes. These complexes are acidic and are in equilibrium with hydroxo complexes in neutral or basic media.

Although palladium(II) are generally viewed as having a low affinity for oxygen donors there are some notable exceptions. Hydroxo complexes are in equilibrium with aqua complexes in water, but they have rarely been isolated. In a non-aqueous medium hydroxo complexes can prove quite stable. There are various μ -OH dimers and trimers that have outstanding stability. For example, reaction of $[\text{PdCl}_2(\text{PPh}_3)_2]$ with AgBF_4 in moist acetone yields the hydroxo-bridged dimer $[\text{Pd}_2(\text{OH})_2(\text{PPh}_3)_4](\text{BF}_4)_2$. There are also sulfoxide complexes in which, depending on the particular sulfoxide used, there may be *S*-bonded, *O*-bonded, or a mixture of *S*- and *O*-bonded ligands. One of the most important palladium compounds is palladium(II) acetate which is used as a source for other palladium compounds. It also have been greatly studied in a wide variety of palladium catalyzed reactions of organic compounds. Brown crystals of palladium(II) acetate is readily obtained by dissolving palladium in acetic acid containing some concentrated HNO_3 . The acetate readily undergoes cleavage with donors to give yellow *trans* compounds, $[\text{Pd}(\text{O}_2\text{CMe})_2\text{L}_2]$. In the crystal the acetate is trimeric, but it dissociates in hot benzene.

Palladium, considered a soft metal ion, generally forms stronger complexes with sulfur donors than with oxygen donors. The π back-donation of electron density from the metal atom to the empty, relative low energy *d* orbitals on sulfur, contribute to the strength of the palladium(II)-sulfur bonds. Ligands such as sulfite ions, thiosulfate ions, thiourea and

dialkyl thioethers that bind to palladium(II) through a sulfur atom generally exhibit a high *trans* effect while the *trans* influence is negligible. Complexes of palladium(II) with sulfur, selenium or tellurium donor ligands generally exhibit similar stabilities, though the actual stability sequence within this group of donor atoms depends on the nature of the other ligands bound to the metal.

2.1.2.4 Palladium(II) Nitrogen Donor Complexes

Palladium(II) also forms complexes with amines, nucleotides and related complexes. There are a wide variety of organic compounds that contains nitrogen atoms that are capable of acting as donors in coordination complexes. The strength of the palladium-nitrogen bond has led to a large number of stable compounds being prepared. The bonds being exclusively σ in character in the majority of complexes, because of the absence of low-lying *d* orbitals for nitrogen. In consequence these ligands lie low in the *trans* influence and *trans* effect series, which is reflected in the stability of these compounds.

The largest class of amine complexes are of the type $[\text{PdX}_2\text{L}_2]$ (X = halide or pseudo-halide; L = amine). The complexes is readily prepared by addition of the amine to $[\text{PdCl}_2]^{2-}$ in aqueous solution or by the reaction of the amine with $[\text{PdCl}_2]$ or $[\text{PdCl}_2(\text{PhCN})_2]$ in organic solution.

The inclusion of the nitrogen donor atom in an aromatic heterocycle allows the possibility of π -bonding with the metal centre, giving these ligands some similarities to tertiary phosphines. For example, the pyridyl and bipyridyl ligands form very stable organometallic complexes with palladium.

2.1.3 The (0) Oxidation State

Palladium(0) compounds have a d^{10} configuration. Unlike most of the transition metals, phosphine complexes rather than carbonyls dominate this oxidation state. In fact palladium complexes with binary carbonyls are unstable at room temperature. The highest coordination number known for Pd^0 is four and $[\text{PdL}_4]$ have a tetrahedral structure. The complexes undergo displacement reactions with CO , C_2H_4 , dienes and other donors, but the

important chemistry is of the oxidative-addition reactions to yield Pd^{II} species. They form hydrido, chloro or dichloro species with HCl and also react with alkyl and aryl halides.

2.1.3.1 Palladium(0) Phosphine Complexes

These complexes are readily prepared by the reduction of palladium(II) compounds in the presence of excess phosphine. Typical reducing agents include copper, hydrazine, borohydride, propoxide ions and alkylaluminium compounds. Triphenylphosphine has been the most widely employed phosphine, however complexes incorporating PF_3 , phosphites, arsines and stibines have also been prepared.

Dissociation of ligands from PdL_4 complexes ($\text{L} = \text{phosphine}$) occurs readily, giving the three-coordinate, 16-electron species, PdL_3 and the two-coordinate, 14-electron species, PdL_2 in solution. PdL_3 is trigonal planar and PdL_2 has a linear geometry. The species distribution depends mainly on the cone angle of the phosphine and on electronic factors. For triaryl and alkyl diaryl phosphines dissociation is extensive, whereas for trialkyl or dialkylaryl phosphines it is not. With very bulky phosphines, *e.g.*, P^tBu_3 , $\text{P}(\text{C}_6\text{H}_{11})_3$, $\text{P}^t\text{Bu}_2\text{Ph}$, the PdL_2 species can be isolated. The lability of the ligands in PdL_n is a convenient tool which has been used in the synthesis of mixed ligand complexes.

2.1.4 Other Oxidation States and Clusters

Palladium(I) complexes should be paramagnetic, having a d^9 configuration; generally, however, those characterized complexes are diamagnetic and multinuclear. In 1971 only two complexes of palladium(I) had been identified. Although the area has grown significantly, the relative small amount of palladium cluster compounds can be attributed, in part, to the surprising weakness of palladium-carbon monoxide bonds and particular those where CO is bound terminally.

Palladium(IV) is a relatively rare oxidation state and although it exists, the complexes are generally less stable than those of platinum(IV). The coordination number is invariably six and include halides, nitrogen and phosphorus donor ligands.

The complexes are mainly the octahedral halide anions, apart from $[\text{Pd}(\text{NO}_3)_2(\text{OH})_2]$. The fluoro complexes of Ni, Pd and Pt are all very similar and are rapidly hydrolyzed by water. The chloro and bromo ions are stable to hydrolysis but are decomposed by hot water to give the Pd^{II} complex and halogen. When palladium is dissolved in aqua regia or when $[\text{PdCl}_4]^{2-}$ solutions are treated with chlorine, the red $[\text{PdCl}_6]^{2-}$ ion is formed. $[\text{PdF}_4]$ has been prepared by the fluorination of $[\text{PdF}_3]$ under pressure.

$[\text{PdCl}_4(\text{NH}_3)_2]$ has been synthesized by the chlorination of $[\text{PdCl}_2(\text{NH}_3)_2]$ in water, CHCl_3 or CCl_4 . On heating it decomposes to the palladium(II) starting material, while on standing a partial reduction to $[\text{PdCl}_2(\text{NH}_3)_2][\text{PdCl}_4(\text{NH}_3)_2]$ occurs. Pyridine and bipyridine complexes such as $[\text{PdpyX}_5]^-$ and *cis*- $[\text{PdbipyCl}_4]$ and similar complexes with PR_3 and AsR_3 donors can be obtained by halogen oxidation of the Pd^{II} complex.

The yellow cationic compound, $[\text{PdCl}_2(\text{NH}_3)_4]\text{Cl}_2$, has been formed in the chlorine oxidation of $[\text{Pd}(\text{NH}_3)_4]\text{Cl}_2$. This is also thermally unstable and reverts to palladium(II) in aqueous solution or on heating.

A particular problem in the palladium(IV) complex systems containing monodentate phosphine and arsine ligands, is that an excess of oxidant, *e.g.*, Cl_2 , results in the formation of $[\text{PdCl}_6]^{2-}$ together with the oxidized ligand, *e.g.* PPh_3O , AsPh_3O , AsPh_3Cl_2 . The complexes *trans*- $[\text{PdCl}_4\text{L}_2]$ ($\text{L} = \text{PMe}_2\text{Ph}$, PPh_3 , PPr^i_3 , AsEt_3 , AsMe_2Ph , SbMe_3) have borderline stabilities and are difficult to purify.

The yellow salt $\text{K}_2[\text{Pd}(\text{CN})_6]$ is formed by the oxidation of $\text{K}_2[\text{PdCl}_4]$ by persulfate in the presence of KCN.

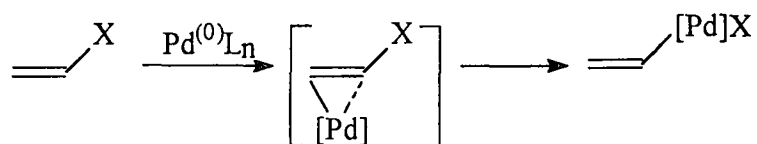
Many square planar complexes of palladium(II) or platinum(II) have crystal packings where infinite chains of metal atoms are formed. A related class of compound with chainlike structures contains both palladium(II) and palladium(IV) but differs from the above in that the metal units are linked by halide bridges. Both show high electrical conductivity along the direction of the $-\text{Cl}-\text{Pd}^{\text{II}}-\text{Cl}-\text{Pd}^{\text{IV}}$ chains, for example, in $[\text{Pd}^{\text{II}}(\text{NH}_3)_2\text{Cl}_2][\text{Pd}^{\text{IV}}(\text{NH}_3)_2\text{Cl}_2]$.

2.2 Elementary Steps in a Palladium Catalyzed Process^{3,4}

When a transition metal is involved in a reaction three main stages exist:

- (i) initial activation of the organic fragment by palladium (C-Pd activation)
- (ii) generation of the new organometallic bond (modification(s) of the Pd complex organic fragments), and
- (iii) removal of the metal from the modified organic molecule with possible recycling (C-Pd cleavage).

In the first stage there is interaction between the inorganic palladium derivative and the organic ligand. The ligand coordinates, which, depending on the oxidation state of the palladium complex, may be followed either by oxidative addition or by oxidative coupling. Two distinct processes can then occur depending on whether palladium(0) or palladium(II) is implicated, and palladium(II) complexes are formed in both cases. Transformations that result take place independently of the original oxidation state of the complex. Thus, transformations that require palladium(0) actually use palladium(II) complexes, which are reduced *in situ* as illustrated below.



Palladium(0) and palladium(II) are both capable of interacting with unsaturated compounds, such as alkenes or alkynes *via* coordination. Palladium(0) however differs from palladium(II). Palladium(0) is highly electron rich and back donates to the ligand ($\text{Pd} \rightarrow \text{L}$), while palladium(II) is electrophilic, and its main interaction is represented by σ -donation from the organic system to an empty orbital on the palladium.

The second stage may involve addition of nucleophiles, either to the palladium (ligand exchange) or to the coordinated ligand, followed by intramolecular migratory insertion. All these transformations are characterized by the electrophilic nature of palladium(II). Finally, the third stage may take place *via* ligand dissociation, reductive elimination, dehydropalladation or oxidative cleavage.

2.2.1 Palladium-Catalyzed Reactions

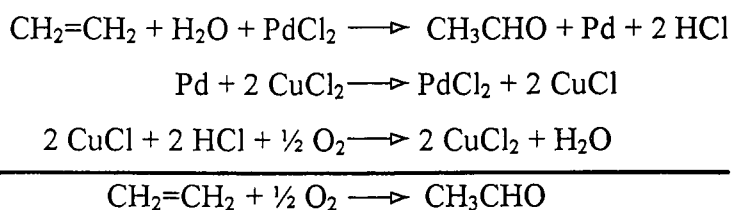
Industrial applications of palladium catalysts as homogeneous and heterogeneous catalysts are rapidly growing. Palladium-catalyzed reactions can be divided into two groups. The first is the oxidative reaction of palladium(II) compounds, which are reduced to palladium(0). A reaction can be carried out catalytically with palladium in either homogeneous and heterogeneous phase in the cases when palladium(0) is reoxidized *in situ* to palladium(II) with proper reoxidants. Usually readily available palladium(II) chloride or acetate are used as the palladium(II) compounds. The first catalytic cycle developed was the Wacker process, in which copper(II) chloride is used as the reoxidant of palladium(0). Hydrogen peroxide and some organic reagents are also good reoxidants.

2.2.1.1 Reactions Catalyzed by Palladium(II) Complexes

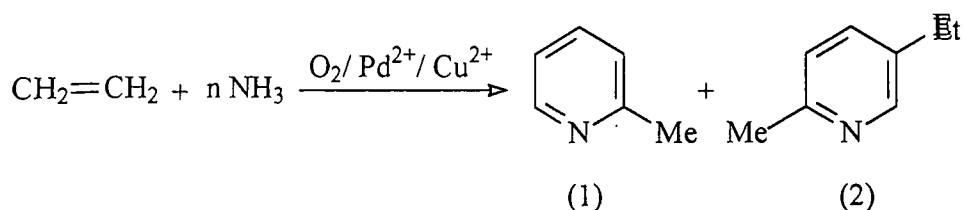
Oxidative Reactions of Olefins

An example of a reaction that is catalyzed by a palladium(II) salt is the Wacker process. In the Wacker process acetaldehyde is produced by the oxidation of ethylene using palladium(II) chloride (PdCl₂) and copper(II) chloride (CuCl₂) as catalysts (Scheme 2.1). This process was the first large scale commercial process catalyzed by palladium and it consists of three consecutive reactions. Acetaldehyde is mainly further converted to acetic acid, however most companies use the Monsanto process to produce acetic acid by the rhodium-catalyzed carbonylation of methanol.

Scheme 2.1 The Wacker Process



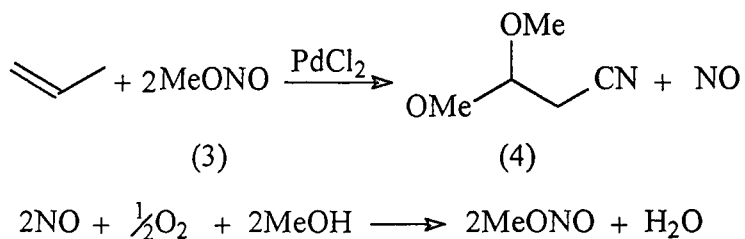
Related to the Wacker process is the oxidation of ethylene in ammonia, catalyzed by palladium(II) chloride and copper(II) chloride, to give a mixture of 2-methylpyridine (1) and 5-ethyl-2-methylpyridine(2) *via* acetaldehyde in one step, in high yield, and with higher than 80% selectivity.



This process was developed by the Nippon Steel Chemical Company as a possible commercial process⁵. 2-Methylpyridine (1) is an important intermediate in the production of 2-vinylpyridine, which has a sizable market. The catalytic oxidation of 5-ethyl-2-methylpyridin (2) to yield nicotinic acid, was also developed.

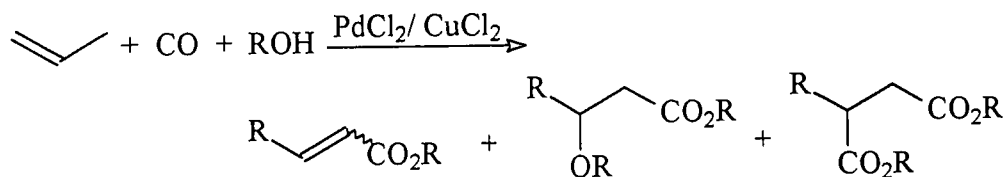
It is interesting to note that these oxidation reactions are carried out in ammonia to give the pyridine derivatives and the reactions proceeds smoothly, whilst the Wacker process is carried out in concentrated hydrochloric acid.

Acetals of aldehydes or ketones are produced by the oxidation of olefins with palladium(II) chloride in pure alcohols⁶. The oxidation of acrylonitrile in methanol⁷ for the commercial production of 3,3-dimethoxypropionitrile (4) was developed by Ube Industries. 3,3-Dimethoxypropionitrile (4) is converted to the pyrimidine derivative, which is then used for vitamin B₁ production



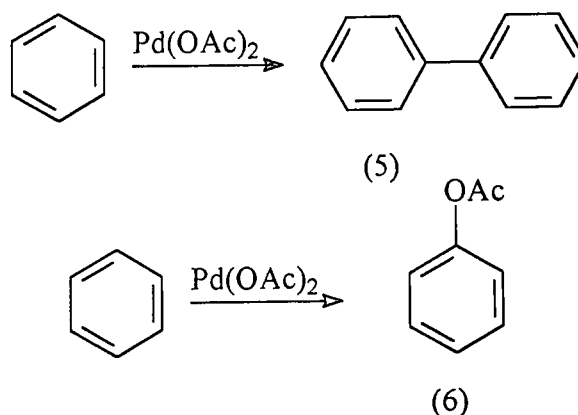
Unique to this two-step process is the reoxidation of Pd(0), by methyl nitrite (3). Methyl nitrite (3) is a gas and can easily be separated from water and recycled. The nitrite (3) is regenerated by the reaction of nitrogen oxide with oxygen and methanol.

Oxidative carbonylation of olefins in alcohols affords α,β -unsaturated esters, β -alkoxy esters and succinate derivatives depending on the reaction conditions⁸, as illustrated in the following scheme:

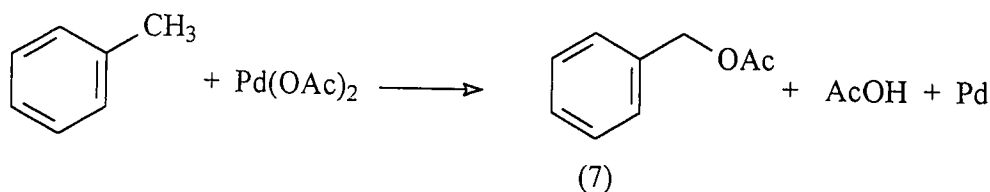


Oxidative Reactions of Aromatic Compounds

Interesting oxidative reactions of aromatic compounds are possible with Pd(II) complexes. Palladium(II) acetate is normally used in the reactions, since palladium(II) chloride is not a good oxidant of aromatic compounds. An example of these type of reactions is the reaction of benzene with palladium(II) acetate. Two competitive reactions can take place; *i.e.*, oxidative coupling to give biphenyl⁹ (5) and acetoxylation of benzene to give acetoxybenzene¹⁰ (6). The selectivity is dependent on the reaction conditions.



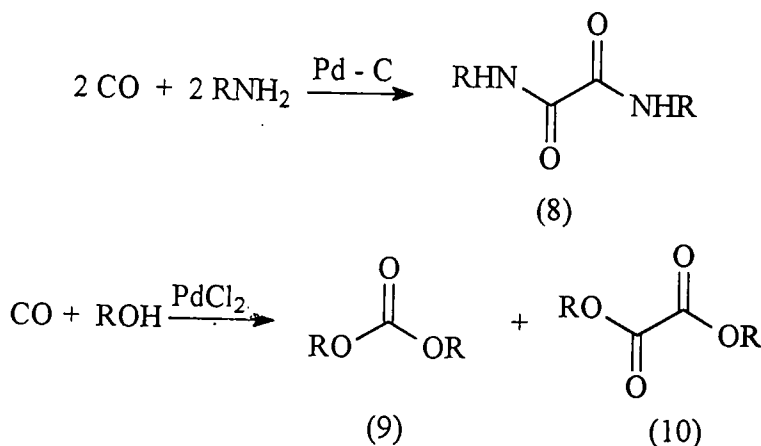
In the reaction of toluene with palladium(II) acetate, ring acetoxylation and coupling are the competing reactions. In addition, acetoxylation of the methyl group to afford benzyl acetate (7) is another possibility, but when stannous acetate is added¹¹, it was found that the formation of benzyl acetate (7) becomes the main pathway. Benzyl acetate is a useful compound in the perfume industry, which is presently produced commercially *via* benzyl chloride.



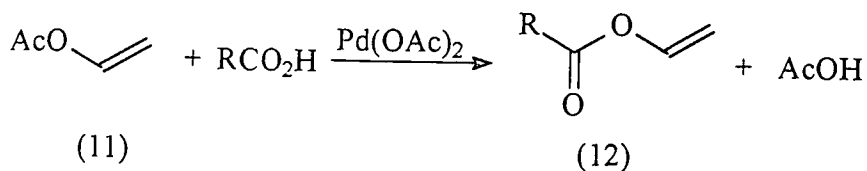
Oxidative Carbonylation and Other Reactions

Oxamide (8) is formed¹² in the oxidative carbonylation of amines, while carbonates (9) and oxalates (10) are formed by the oxidative carbonylation of alcohols¹³.

The palladium-catalyzed reaction of an alcohol with carbon monoxide is a promising phosgene-free method for the production of dialkyl carbonates (9), which currently has an increasing demand.



The exchange reaction of the vinyl group between vinyl acetate (11) and other carboxylic acids is catalyzed by palladium(II) acetate, although it is not an oxidative reaction¹⁴. The reaction of readily available vinyl acetate (11) with various carboxylic acids gives various vinyl esters (12).



Vinyl acetate is the basis of a broad spectrum of polymers and copolymers mainly used as emulsions for adhesives, paints, concrete admixers, coatings, and binding agents for paper, textiles, etc.

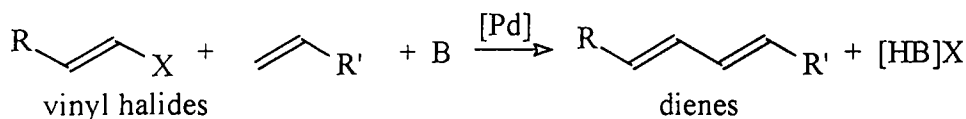
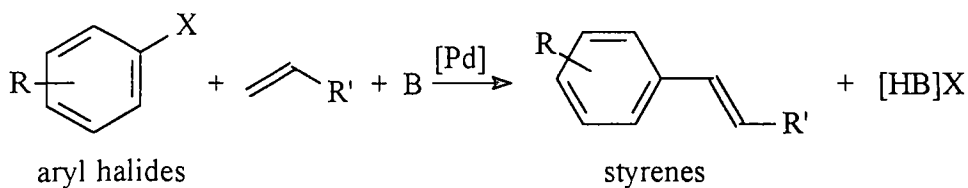
2.2.1.2 Reactions Catalyzed by Palladium(0) Complexes

The second type of reaction are those catalyzed by $\text{Pd}^{(0)}\text{L}_n$ complexes (L = ligand, usually phosphine) which are carried out in homogeneous phase without the addition of the reoxidant. Many useful reactions are catalyzed by especially palladium(0) phosphine complexes. Tetrakis(triphenylphosphine)palladium, $[\text{Pd}(\text{PPh}_3)_4]$, is an air sensitive catalyst which is nonetheless commercially available. Therefore, $[\text{Pd}(\text{PPh}_3)_n]$ as an active catalytic species is often prepared *in situ* by mixing palladium(II) acetate and triphenylphosphine in solution.

Currently, the two most useful reactions in industrial processes that are catalyzed by palladium(0) complexes are reactions of aryl and alkenyl halides and reactions via π -allylpalladium complexes.

Reactions of Alkenyl and Aryl Halides

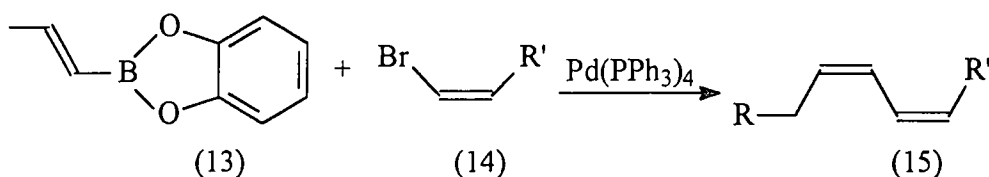
In transition-metal-catalyzed reactions halides attached to sp^2 carbons are more reactive than those attached to sp^3 carbons, while in organic chemistry it is well-known that it is the other way around. Thus, in palladium-catalyzed reactions, alkenyl or aryl halides are very reactive, they undergo so-called oxidative addition reactions and Mizoroki¹⁵, Heck¹⁶ and respective co-workers reported the reactions of these halides with olefins. The olefins¹⁷ were converted into vinylic C–C coupling products, and this type of reactions are now called “Heck reactions”. The term “Heck reaction” summarises catalytic C–C coupling processes, such that a vinylic hydrogen is replaced by a vinyl, aryl or benzyl group, with the latter being introduced from a halide or related precursor compound. Therefore, the final step of product formation is the elimination of a hydrogen halide, and a base is thus required to bind the acid. The olefinic (vinylic) double bond is retained throughout the Heck reaction. Palladium is practically the only metal catalyst successfully used in these type of reactions. Both *intra*- and (more commonly) *inter*-molecular Heck reactions have been reported, which has found widespread use in organic synthesis for the preparation of substituted olefins.



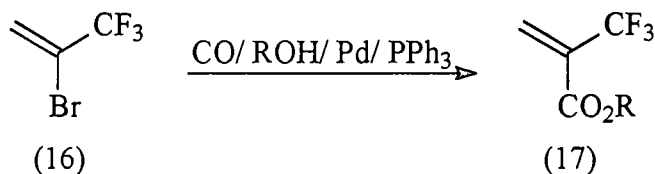
$\text{X}^- = \text{I}, \text{Br}, \text{N}_2\text{BF}_4, \text{C}(=\text{O})\text{Cl}, \text{CF}_3\text{SO}_3$

$\text{B} = \text{base: NR}_3, \text{K}_2\text{CO}_3, \text{NaOAc}$

Palladium-catalyzed coupling reactions of aryl and alkenyl halides with alkyl, aryl and alkenyl compounds of main group elements such as boron, aluminum, zinc, tin and silicon are useful for the synthesis of aryl and alkenyl compounds. As a typical example, the coupling reaction of vinyl boron compounds (13) with vinyl halides (14) is useful for the synthesis of conjugated dienes¹⁸ (15). Particularly, *E* or *Z* stereochemistry of the conjugated diene (15) can be controlled cleanly by this method.

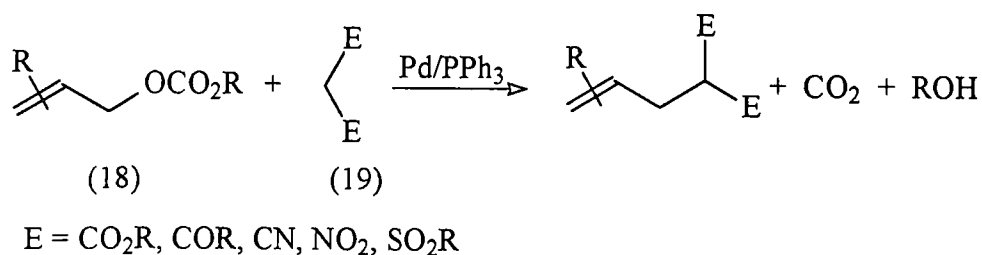


The carbonylation reaction of aryl and alkenyl halides under low pressure offers a good preparative method for aromatic or α,β -unsaturated esters. For example, methyl trifluoromethylacrylate¹⁹ (17) is produced by the carbonylation of 2-bromo-3,3,3-trifluoropropylene (16) catalyzed by dichlorobis(triphenylphosphine)palladium, $[\text{PdCl}_2(\text{PPh}_3)_2]$, in the presence of triethylamine.

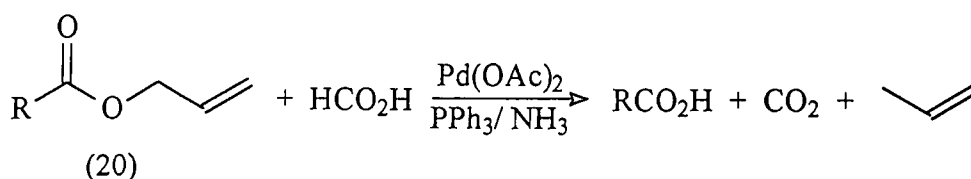


Reactions of Allylic Compounds and Conjugated Diene

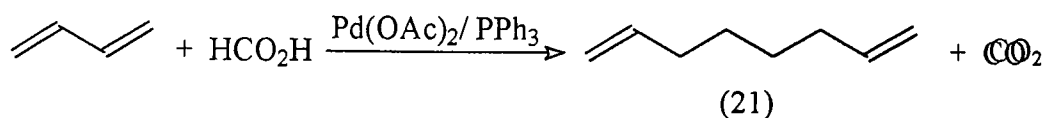
Allylic compounds and conjugated dienes react with Pd(0) complexes to form π -allylpalladium moieties. Depending on the reaction conditions, the π -allylpalladium complex can undergo various transformations. Carbon-carbon bond formation by the reaction with carbonucleophiles²⁰ and the corresponding catalytic process^{21,22} are particularly well known. The reaction of allylic carbonates (18) with carbonucleophiles (19) takes place under mild, neutral conditions²³ and no base or acid is required for the carbon-carbon bond formation, while allyl carbonates are much more reactive than the allyl acetates.



The allyl and allyloxycarbonyl group can be useful protecting groups in organic chemistry. Carboxylic acids are protected as allyl esters (20), while amines and alcohols are protected as allyl carbamates and carbonates. These protecting groups can readily be removed by palladium catalysts. For example, in the presence of ammonium formate, the allyl group is removed by forming propylene^{24,25}, while the palladium-catalyzed deprotection of allyl esters proceeds under mild conditions without using acid or base.

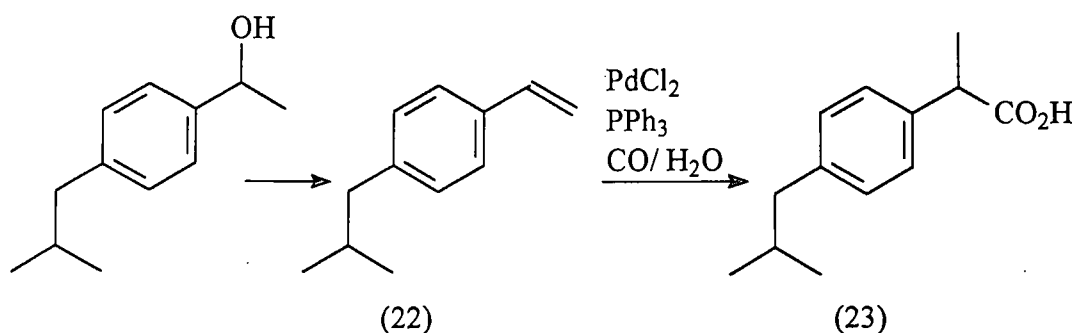


Another example of these reactions is that of butadiene with ammonium formate, which produces 1,7-octadiene²⁶ (21).



Carbonylation of olefins

The carbonylation of olefins catalyzed by palladium complexes gives saturated esters²⁷. Regioselectivity between linear and branched esters is a problem and usually a mixture of regioisomers is obtained in the carbonylation of terminal olefins. But the carbonylation of 4-isobutyl-1-vinylbenzene (22) in ethanol proceeded regioselectively to give ethyl 2-(4-isobutylphenyl)propionate²⁸ in a high yield. When the reaction is carried out in a mixture of benzene and water, 2-(4-isobutylphenyl)propionic acid (23) is obtained. Therefore the reaction is useful for the synthesis of the important anti-inflammatory drug, Ibuprofen.



2.3 Water-Soluble Systems

2.3.1 Introduction

The introduction^{29,30} of the aqueous two-phase ("biphase") technique is one of the most important developments of the past 15 years in homogeneous catalysis. In a biphasic system two immiscible liquids are used, usually an organic layer that contains the substrate(s) and product(s) and an aqueous phase that contains the homogeneous catalyst dissolved in it. The reaction can take place in either layer or at the interface region – where the two layers are in contact. By simple phase separation (decantation) the catalyst and reactants/products are separated after the reaction took place, at approximately the same temperature and without any chemical stress.

2.3.2 Water-Soluble Ligands

Aqueous homogeneous catalysts depend on the development of polar, and therefore water-soluble, ligands, and their incorporation into organometallic complexes. Many homogeneous catalysts are not soluble in water, or they are moisture sensitive and decompose in the presence of water to form metal oxides and hydroxides. Therefore, the history of biphasic homogeneous catalysis begins with preparatory work on various water-soluble ligands. Solubility of transition metal complexes in aqueous media is usually achieved by introduction of charged or highly polar substituents such as $-\text{SO}_3\text{H}$, $-\text{COOH}$, $-\text{OH}$, $-\text{NH}_2$, or $-\text{PO}_3\text{H}_2$, to phosphine ligands. Almost any desired ratio of hydrophilic and hydrophobic properties may be obtained. This is done by variation of the nature and number of suitable substituents and by choice of the conditions of the aqueous phase. For example, sulfophenylphosphines dissolve in aqueous media at any pH, while carboxy- or amino-substituted phosphines dissolve only in basic or acidic solutions, respectively. Phosphine complexes with functionalized ligands are especially interesting due to their catalytic activity.

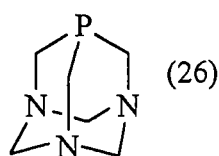
For substrates of high hydrophobicity there are an inherent drawback with water-soluble catalysts with regard to reaction rates: the rate is largely controlled by the rate of phase-boundary mass transfer. The addition of co-solvents or surfactants may however solve this problem. Although both facilitate transfer of the substrate into the aqueous phase, it also limits the recycling of the catalyst. A better solution to both catalyst separation and slow phase boundary mass transfer is by using amphiphilic ligands and complexes thereof. An amphiphilic catalyst has the property of being soluble in aqueous or organic phase, depending on the pH. Through simple pH adjustments the amphiphilic catalysts can thus be transferred between an aqueous and an organic solvent phase. The reaction then runs homogeneously in an organic solvent, thus avoiding mass transfer problems and after completion of the reaction the catalyst is easily extracted into the aqueous phase.

The solubility of a complex is largely governed by the charge to molecular mass ratio, and to achieve a high water solubility two strategies can be employed: protonation/deprotonation of a number of chargeable substituents or protonation/deprotonation of a single, multiple

Engineering difficulties have prevented industrial utilization of many advances in the field of homogeneous catalysis in large-scale synthesis. The industrial scene is still strongly dominated by heterogeneous catalysis: about 85% of all known catalytic processes.

2.3.3 The Water-Soluble Phosphine 1,3,5-Triaza-7-Phosphaadamantane

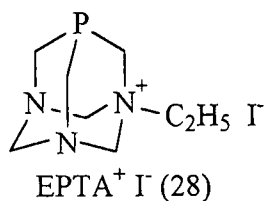
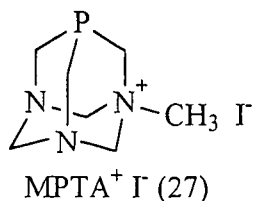
There is thus a need for a wider range of water-soluble phosphine ligands, covering a range of steric and electronic properties. In 1974 Daigle and co-workers³⁵ synthesized the water-soluble phosphine, 1,3,5-triaza-7-phosphaadamantane (PTA) (26).



The potentially quadridentate PTA ligand coordinates to the metal only through the P atom and PTA³⁶ finds use as a neutral P-donor ligand and it is made water-soluble by virtue of H-bonding to the tertiary amine nitrogens. PTA is a nonionic, air-stable aliphatic phosphine, and because it is small it has low steric demand. It typically binds more strongly to the metal centers than do the phenylsulfonated phosphine ligands. The Tolman cone angle for PTA³⁷ is similar to the 118° of PMe₃³⁸. Therefore, PTA is an air-stable, water-soluble version of PMe₃³⁹.

PTA is a strong σ -donor⁴⁰ as well as a strong π -acceptor, and protonation of PTA occurs at one nitrogen atom, and not at the phosphorus atom. PTA is not a pronounced surfactant⁴¹ as are the sulfonated phosphines, and therefore it provides better phase separations during catalysis in biphasic aqueous/organic media.

Alkylated derivatives of PTA can also be prepared. Methyl iodide reacts with PTA to form the ligand 1-methyl-1-azonia-3,5-diaza-7-phosphaadamantane iodide (MPTA⁺I⁻) (27). The alkylated derivatives coordinates less strongly to a metal centre than does the PTA ligand, since the alkyl functionality withdraws electron density from the aliphatic phosphine. 1-ethyl-1-azonia-3,5-diaza-7-phosphaadamantane iodide (EPTA⁺I⁻) (28) is another alkylated derivative of PTA.



2.3.4 General Coordination Chemistry in various PTA complexes

Many complexes have been synthesized using PTA as a ligand, some of which are discussed below:

The first metal³⁹ complexes synthesized containing PTA as ligand were [Mo(CO)₅(PTA)], [Cr(CO)₅(PTA)] and [W(CO)₅(PTA)]. Since then, many complexes with other metals have been synthesized, and many of them have been characterized crystallographically.

[RuCl₂(PTA)₄]^{41,42} have been prepared by the reduction of RuCl₃ in ethanol in the presence of an excess of PTA. This water-soluble complex is catalytically quite active for the conversion of unsaturated aldehydes to unsaturated alcohols using biphasic aqueous-organic medium with formate or hydrogen gas as the source of hydrogen. [RuCl₂(PTA)₄]⁴³ was also used as catalyst precursor for the hydrogenation of CO₂ and HCO₃⁻ in aqueous solution.

An analogue to Wilkinson's catalyst, [RhCl(PTA)₃]^{42,44,45} have been prepared by the reduction of RhCl₃ in ethanol in the presence of an excess PTA. [RhCl(PTA)₃] is an active catalyst for the hydrogenation of various olefinic and oxo-acids, as well as of allyl alcohol and selective reduction of unsaturated aldehydes to saturated aldehydes. In these studies it was suggested that water strongly assists the dehydrochlorination of [RhCl(PTA)₃] to yield the catalytically active monohydrido species [HRh(PTA)₃].

[RhCl(PTA)₃] was also successfully employed for hydrogenation of phospholipid liposomes⁴⁶ as model membranes in aqueous media under mild conditions. A Rh analogue of Vaska's compound, *trans*-[RhCl(CO)(PTA)₂], which catalyzes the reduction of CO₂ with H₂, has also been prepared.

In the reaction of PTA with $[\text{IrCl}(\text{COD})]_2$ (COD = 1,5-cyclooctadiene), under CO atmosphere, PTA ligated iridium⁴⁷ compounds have been formed. The reaction produces an inseparable mixture of $[\text{IrCl}(\text{CO})(\text{PTA})_3]$ and the PTA analogue of Vaska's compound $[\text{IrCl}(\text{CO})(\text{PTA})_2]$. The complex $[\text{Ir}(\text{PTA})_4(\text{CO})]\text{Cl}$ is prepared *via* ligand substitution reactions of PTA with Vaska's compound, *trans*- $[\text{IrCl}(\text{CO})(\text{PTA})_2]$. The complex $[\text{Ir}(\text{PTAH})_3(\text{PTAH}_2)(\text{H})_2]\text{Cl}_6$ have been synthesized and characterized.

Insoluble mercury(II) complexes⁴⁸ with PTA have been reported. For example $[\text{PTAHgX}_2]$, where X = halide, SCN^- , CN^- . Other complexes isolated are $[(\text{PTA})_2\text{Hg}(\text{NO}_3)_2]$ and $[(\text{PTA})_4\text{HgX}_2]$ where X = Cl^- , Br^- or NO_3^- .

Gold complexes⁴⁹ of PTA have been prepared by mixing PTA with (dimethyl sulfide)gold(I) chloride in a molar ratio 1:1 in aprotic solvents affording $[(\text{PTA})\text{AuCl}]$ of which the protonated product can also be formed. Three coordinated gold complexes do exist and the complex $[(\text{PTA})_2\text{AuCl}]$ has been reported⁵⁰.

A variety of Group 10 metal complexes of PTA have been synthesized and characterized. Complexes of low-valent Group 10 metals are some of the most important complexes used as catalyst precursors in homogeneous catalysis. The general catalytic activity follows the trend $\text{Pd} > \text{Pt} > \text{Ni}$. Treatment of $[\text{Ni}(\text{NO}_3)_2]$ with NaNO_2 and PTA provides the nitrosyl complex⁵¹ $[\text{Ni}(\text{NO})(\text{PTA})_3]\text{NO}_3$. The zerovalent⁵² complex, $[\text{Ni}(\text{PTA})_4]$ have been prepared in good yields by the ligand exchange reaction of $[\text{Ni}(\text{COD})_2]$ with PTA. $[\text{Ni}(\text{CO})_{4-n}(\text{PTA})_n]$ derivatives have also been reported for $n = 3, 2$ and 1 . The complex⁵³ $[\text{Ni}(\text{CN})_2(\text{PTA})_3] \cdot 4.3\text{H}_2\text{O}$ has also been isolated.

The⁵² zero-valent complex $[\text{Pt}(\text{PTA})_4]$ have been prepared by the reduction of PtCl_2 with hydrazine in the presence of PTA or by the ligand exchange reaction of $[\text{Pt}(\text{PPh}_3)_4]$ with PTA. The *cis*- $[\text{Pt}(\text{PTA})_2\text{Cl}_2]$ were obtained by the metathesis reaction of K_2PtCl_4 with PTA in refluxing ethanol. Treatment⁵⁴ of $[\text{PtCl}_2(\text{SMe}_2)_2]$ with 2 equivalents of PTA in water also leads to *cis*- $[\text{Pt}(\text{PTA})_2\text{Cl}_2]$, while the complexes *trans*- $[\text{Pt}(\text{PTA})_2(\text{CN})_2]$ ⁵⁵ and *trans*- $[\text{Pt}(\text{PTA})_2(\text{I})_2]$ ⁵⁶ are also known. The five-coordinate³⁷ complex, $[\text{PtI}_2(\text{PTA})_3]$, were isolated from the reaction mixture of $[\text{PtCl}(\text{PTA})_3]\text{Cl}$ and NaI in aqueous methanol.

2.3.5 PTA Complexes of Palladium

PTA complexes of palladium^{51,52,57} that have been synthesized and characterized crystallographically are *cis*-[PdCl₂(PTA)₂], [PdCl(PTA)₃]Cl and [Pd(PTA)₄].

The cis-[PdCl₂(PTA)₂] complex

The two crystal structures that have been reported for the four coordinated bis-PTA complex, are *cis*-[PdCl₂(PTA)₂]·6H₂O and {*cis*-[PdCl₂(PTA)₂]}₂·H₂O.

The synthesis⁵¹ of *cis*-[PdCl₂(PTA)₂]·6H₂O was achieved by the metathesis reaction of (NH₄)₂[PdCl₄] and 2 equivalents of PTA in refluxing ethanol. The complex was isolated as a greenish-yellow powder in 83% yield. The ³¹P NMR spectrum of the complex exhibited one sharp peak at -23.2 ppm, which shifted downfield to -21.0 ppm in aqueous 0.10 M HCl. Interestingly, the crystal did not contain the expected 2 equivalents of HCl (see Par. 3.3.2)

The greenish-yellow {*cis*-[PdCl₂(PTA)₂]}₂·H₂O complex was synthesized⁵⁷ by the reaction of solid PdCl₂ with an excess of PTA in water. This square planar complex contains rare intermolecular C···H···Pd interactions; such C···H···M interactions is possible examples of agostic bonding, and is best described as three-center-four-electron (3c-4e) hydrogen bonds⁵⁸. It is reported that this complex is unstable in water, but it is relatively stable in the presence of an excess of PTA. The ³¹P NMR spectra in [(CD₃)₂SO] gives a peak at -18.3 ppm.

A third method to synthesize the *cis*-[PdCl₂(PTA)₂] complex is the reaction of [PdCl₂(COD)] with three equivalents of PTA in a methanol/water mixture (See Par 3.1.7).

The [PdCl(PTA)₃]Cl complex

A bright yellow solid^{51,52} was isolated in an attempt to prepare the zerovalent [Pd(PTA)₄] complex from the reduction of PdCl₄²⁻ in the presence of an excess of PTA (5 equivalents) in refluxing ethanol. The bright yellow solid was identified primarily as a mixture of Pd(II) species, [PdCl₂(PTA)₂] and [PdCl(PTA)₃]Cl. The ³¹P NMR spectrum of the reaction mixture consisted of two broad signals, one centered at -25.0 ppm, due to [PdCl₂(PTA)₂],

and the other at -43.6 ppm assigned to the $[\text{PdCl}(\text{PTA})_3]^+$ cation. The broadness of these ^{31}P resonances is due to ligand exchange occurring with free phosphine in solution.

The $[\text{Pd}(\text{PTA})_4]$ complex

The $[\text{Pd}(\text{PTA})_4]$ complex^{51,52} is similarly prepared from PdCl_2 and 4–5 equivalents of PTA in an aqueous solution in a yield of 57–79%. A longer reaction period of about 12 h is needed for this derivative. ^{31}P NMR reported resonances for the complex are at -58.7 ppm, in D_2O , and at -54.2 and -56.5 ppm respectively, in 0.1 M $\text{HCl}/\text{D}_2\text{O}$.

It is also reported that for the small, tight-binding PTA ligand in Group 10 $\text{M}(\text{PTA})_4$ species, there is little or no dissociation and slow exchange, which has been shown to be governed by steric rather than electronic effects.

¹ G. Wilkinson, R. D. Gillard, J. A. McCleverty, *Comprehensive Coordination Chemistry – Volume 5*, Pergamon Press, 1987, p.1099.

² F. Cotton, G. Wilkinson, *Advanced Inorganic Chemistry*, 5th Edition, John Wiley and Sons Inc, 1988, p. 917.

³ G. Poli, G. Giuliano, A. Heumann, *Tetrahedron*, 2000, **56**, 5959.

⁴ J. Tsuji, *Synthesis*, 1990, 739.

⁵ Y. Kusunoki, H. Okazaki, *Hydrocarbon Process*, 1974, **11**, 129.

⁶ W. G. Lloyd, B. J. Luberoff, *J. Org. Chem.*, 1969, **34**, 3949.

⁷ K. Matsui, S. Uchiumi, A. Iwayama, T. Umezu, *Japanese Patent Kokai* 106635, 1982; *Eur. Patent Appl.* EP 55108, Ube Industries, Ltd., C. A. 1982, **97**, 162364.

⁸ D. M. Fenton, P. J. Steinwand, *J. Org. Chem.*, 1969, **34**, 738.

⁹ R. van Helden, G. Verberg, *Rec. Trav. Chim.*, 1965, **84**, 1263.

¹⁰ J. M. Davidson, C. Triggs, *Chem. Ind. (London)*, 1966, 457.

¹¹ D. R. Bryant, J. E. MeKeon, B. C. Ream, *J. Org. Chem.*, 1968, **33**, 4123, and 1969, **34**, 1106.

¹² J. Tsuji, N. Iwamoto, *J. Chem. Soc., Chem. Commun.*, 1966, 380.

¹³ D. M. Fenton, P. J. Steinwand, *J. Org. Chem.*, 1974, **39**, 701.

- ¹⁴ J. Smidt, W. Hafner, R. Jira, R. Sieber, J. Sedlmeier, A. Sabel, *Angew. Chem.*, 1963, **74**, 93.
- ¹⁵ T. Mizoroki, K. Mori, A. Ozaki, *Bull. Chem. Soc. Japan*, 1971, **44**, 581.
- ¹⁶ R. F. Heck, J. P. Nolley, *J. Org. Chem.*, 1972, **37**, 2320.
- ¹⁷ W. A. Herrmann, B. Cornils, *Applied Homogeneous Catalysis with Organometallic Compounds – Volume 2*, Wiley-VCH Publishers, Weinheim, 1996, 712.
- ¹⁸ N. Miyaoura, K. Yamada, H. Sugimoto, A. Suzuki, *J. Am. Chem. Soc.*, 1985, **107**, 972.
- ¹⁹ T. Fuchikami, I. Ojima, *Tetrahedron Lett.*, 1982, **23**, 4099.
- ²⁰ J. Tsuji, H. Takahashi, M. Morikawa, *Tetrahedron Lett.*, 1965, 4381.
- ²¹ G. Hata, K. Takahashi, A. Miyake, *J. Chem. Soc., Chem. Commun.*, 1970, 1392.
- ²² K. E. Atkins, W. E. Walker, R. M. Manyik, *Tetrahedron Lett.*, 1970, 3821.
- ²³ J. Tsuji, I. Shimizu, I. Minami, T. Ohashi, T. Sugiura, K. Takahashi, *J. Org. Chem.*, 1985, **50**, 1523.
- ²⁴ J. Tsuji, T. Yamakawa, *Tetrahedron Lett.*, 1979, 613.
- ²⁵ I. Minami, T. Ohashi, I. Shimizu, J. Tsuji, *Tetrahedron Lett.*, 1985, **26**, 2449.
- ²⁶ P. Rofia, G. Gregorio, F. Conti, G. F. Fregalia, R. Ugo, *J. Organometal. Chem.*, 1973, **55**, 405.
- ²⁷ K. Bittler, N. V. Kutepow, K. Neubauer, H. Reis, *Angew. Chem.*, 1968, **80**, 352, *Angew. Chem. Int. Ed. Engl.*, 1968, **7**, 359.
- ²⁸ M. Takeda, M. Uchide, H. Iwane, *Japanese Patent Kokai*, 51338, 1977, and 18533, 1978, *German Patent (DOS)*, 2646792, Mitsubishi Petrochemical Co., C. A., 1977, **87**, 67848.
- ²⁹ W. A. Herrmann, B. Cornils, *Applied Homogeneous Catalysis with Organometallic Compounds*, Wiley-VCH Publishers, Weinheim, 2000, 575.
- ³⁰ M. Karlsson, M. Johansson, C. Andersson, *J. Chem. Soc. Dalton. Trans*, 1999, 4175.
- ³¹ Y. Tokito, N. Yoshimura (Kuraray Corp.), U. S. Pat. 4,808,756, 1989.
- ³² L. Cassar, *Chem. Ind. (Milano)*, 1985, **57**, 256; *Ger. Pat.* 2,035,902, 1979.
- ³³ D. Morel, (Rhône Poulenc Ind.) *French Pat.* 2,486,525, 1980; Rhône Poulenc Ind. *French Pat.* 2,505,322, 1981; Rhône Poulenc Ind. *French Pat.* 2,541,675, 1983.
- ³⁴ W. A. Hermann, J. A. Kulpe, J. Kellner, H. Piepl, H. Barhmann, W. Konkol, *Angew. Chem., Int. Ed. Engl.*, 1990, **29**, 391.
- ³⁵ D. J. Daigle, A. B. Pepperman (Jr.), S. L. Vail, *J. Heterocycle. Chem.*, 1974, **17**, 407.
- ³⁶ D. J. Daigle, *Inorg. Synth.*, 1998, **32**, 40.
- ³⁷ S. Otto, A. Roodt, *Inorg. Chem. Commun.*, 2001, **4**, 49.

- ³⁸ C. A. Tolman, *Chem Rev.*, 1977, **77**, 313.
- ³⁹ M. Y. Darensbourg, D. J. Daigle, *Inorg. Chem.*, 1975, **14**, 1217.
- ⁴⁰ E. C. Alyea, K. J. Fisher, S. Foo, B. Philip, *Polyhedron*, 1993, **12**, 489.
- ⁴¹ D. J. Darensbourg, F. Joó, M. Kannisto, A. Katho, J. H. Reibenspies, D. J. Daigle, *Inorg. Chem.*, 1994, **33**, 200.
- ⁴² D. J. Darensbourg, F. Joó, M. Kannisto, A. Katho, J. H. Reibenspies, *Organometallics*, 1992, **11**, 1990.
- ⁴³ G. Luarency, F. Joó, L. Nadasdi, *Inorg. Chem.*, 2000, **39**, 5038.
- ⁴⁴ F. Joó, L. Nadasdi, A. Cs. Bényei, D. J. Darensbourg, *J. Organomet. Chem.*, 1996, **512**, 45.
- ⁴⁵ D. J. Darensbourg, N. W. Stafford, F. Joó, J. H. Reibenspies, *J. Organomet. Chem.*, 1995, **488**, 99.
- ⁴⁶ L. Nadasdi, F. Joó, *Inorg. Chim. Acta*, 1999, **293**, 218.
- ⁴⁷ D. A. Krogstad, J. A. Halfen, T. J. Terry, V. G. Young, *Inorg. Chem.*, 2001, **40**, 463.
- ⁴⁸ E. C. Alyea, K. J. Fisher, S. Johnson, *Can. J. Chem.*, 1989, **67**, 1319.
- ⁴⁹ Z. Assefa, B. G. McBurnett, R. J. Staples, J. P. Fackler, *Inorg. Chem.*, 1995, **34**, 75.
- ⁵⁰ Z. Assefa, R. J. Staples, J. P. Fackler, *Acta Cryst.*, 1996, **C52**, 305.
- ⁵¹ D. J. Darensbourg, T. J. Decuir, N. W. Stafford, J. B. Robertson, J. D. Draper, J. H. Reibenspies, A. Kathó, F. Joó, *Inorg. Chem.*, 1997, **36**, 19.
- ⁵² D. J. Darensbourg, J. B. Robertson, D. L. Larkins, J. H. Reibenspies, *Inorg. Chem.*, 1999, **38**, 2473.
- ⁵³ E. C. Alyea, G. Ferguson, S. Kannan, *Polyhedron*, 1998, **17**, 2727.
- ⁵⁴ S. Otto, A. Roodt, W. Purcell, *Inorg. Chem. Commun.*, 1998, **1**, 415.
- ⁵⁵ Z. Assefa, B. McBurnett, R. J. Staples, J. P. Fackler, *Acta Cryst.*, 1995, **C51**, 1742.
- ⁵⁶ S. Otto, A. Roodt, *Acta Cryst.*, 2001, **C57**, 540.
- ⁵⁷ E. C. Alyea, G. Ferguson, S. Kannan, *Chem. Commun.*, 1998, 345.
- ⁵⁸ (a) L. Brammer, J. M. Charnock, P. L. Goggin, R. J. Goodfellow, A. G. Orpen, T. F. Koetzle, *J. Chem. Soc., Dalton Trans.*, 1991, 1789; (b) A. Albinati, P. S. Pregosin, F. Wombacher, *Inorg. Chem.*, 1990, **29**, 1812; (c) R. H. Crabtree, *Angew. Chem., Int. Ed. Engl.*, 1993, **32**, 789.

3 Synthesis and Characterization of Complexes

3.1 Synthesis

3.1.1 Introduction

The synthesis and characterization of complexes investigated in this study are discussed in this chapter and a schematic presentation is given in Scheme 4.2 (Chapter 4). Wilkinson's compound, $[\text{RhCl}(\text{PPh}_3)_3]$, is well known; this study deals with the palladium 1,3,5-triaza-7-phosphaadamantane (PTA) analogue thereof, $[\text{PdCl}(\text{PTA})_3]\text{Cl}$, and related complexes. The complexes were characterized by means of multinuclear NMR spectroscopy, UV-Vis spectrophotometry, X-ray crystallography and infrared spectroscopy.

3.1.2 Chemicals and Instruments

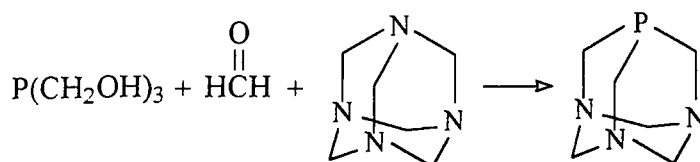
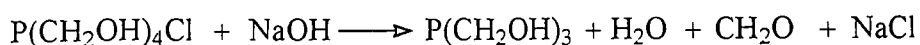
All common laboratory reagents were of analytical grade and double-distilled water was used in all the experiments unless stated otherwise. An aqueous solution of *tetrakis*-(hydroxymethyl)phosphonium chloride (Aldrich), 1,5-cyclooctadiene (Aldrich), hexamine (Aldrich), PdCl_2 (Next Chemica), NaCl (Merck), NaI (Merck), KSCN (Aldrich), LiBr (Aldrich) and NaN_3 (Merck) were commercial products.

All the reagents were used without further purification.

The NMR data were obtained in $\text{H}_2\text{O}/\text{D}_2\text{O}$ solutions on a 300 MHz Bruker spectrometer operating at 300 MHz for ^1H and 121.497 MHz for ^{31}P . The ^1H spectra were calibrated relative to the residual H_2O peak at 4.60 ppm and the ^{31}P spectra relative to 85% H_3PO_4 in a capillary at 0 ppm. UV-Vis spectra were recorded in 1.00 cm^3 quartz cells on a Varian Cary (model 50 conc). The spectrophotometer was equipped with constant temperature cell holders (accurate within 0.1 °C). IR data were recorded on a Hitachi 270-50 Infrared spectrophotometer in KBr disks in the range 4000-250 cm^{-1} .

3.1.3 1,3,5-triaza-7-phosphaadamantane (PTA)

PTA was synthesized according to the procedure developed by Daigle and co-workers¹.

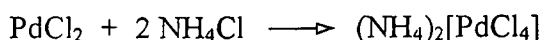


A solution of *tetrakis*(hydroxymethyl)phosphonium chloride, THPC, (80% solution in water; 17 cm³; 95 mmol) was neutralised (pH 7) by a solution of sodium hydroxide (50% w/w; 3.19g; 80 mmol) followed by the addition of formaldehyde (40 g; 37%; 500 mmol) and hexamethylenetetramine (14.0 g; 100 mmol). The solution was stirred overnight at room temperature (17 hours) followed by evaporation of the water in a fume hood. Recrystallisation of PTA from ethanol results in the formation of a white crystalline solid. Yield: 69%; 10.3 g.

¹H NMR: D₂O: δ 3.74 (*d*, 6H, ²J_{H-H} = 9 Hz); 4.39 (*dd*, 6H, ²J_{H-H} = 9 Hz, ²J_{P-H} = 13 Hz)

³¹P NMR: D₂O: δ -94.10

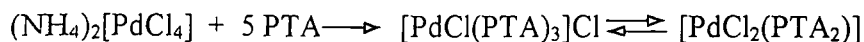
IR (KBr): 1616(w); 1438(w); 1414(w); 1366(w); 1296(m); 1242(m); 1104(w); 1036(w); 1014(m); 970(s); 796(m); 756(w); 578(m) cm⁻¹

3.1.4 Synthesis of (NH₄)₂[PdCl₄]

Palladium(II)chloride (100 mg; 0.056 mmol) was added to water/methanol (1:1) (10 cm³). NH₄Cl (60.4 mg; 1.13 mmol) was dissolved in a water/methanol mixture (1:1) (10 cm³) and added to the PdCl₂ suspension. The reaction mixture was stirred for 30 minutes, filtered and any unreacted palladium(II) chloride stayed on the filter paper and the filtrate contained the product. The filtrate was evaporated to collect the red brown crystalline product. Yield: 96%; 154 mg.

3.1.5 [PdCl(PTA)₃]Cl

Chlorotrakis(1,3,5-triaza-7-phosphaadamantane)palladium(II)chloride, [PdCl(PTA)₃]Cl, was synthesized according to the procedure described by Darensbourg² and co-workers.



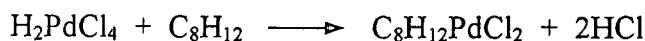
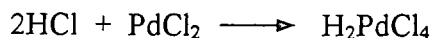
(NH₄)₂[PdCl₄] (150 mg; 0.53 mmol) was dissolved in ethanol (10 ml) under a nitrogen atmosphere and the solution was heated to 60 °C. To the resulting light brown solution, containing residual undissolved [PdCl₄]²⁻, was added PTA (415 mg; 2.6 mmol). Heating was continued for 3 hours during which time the solution became bright yellow and a precipitate formed. After cooling the solution to room temperature the precipitate was filtered and washed with several small aliquots (3 x 5 ml) of diethyl ether. The ³¹P spectrum of the complex consisted of two singlets, at -26.0 ppm due to [PdCl₂(PTA)₂] and the other at -42.7 ppm assigned to [PdCl(PTA)₃]Cl. The ratio of the signals is 1:3 and the broadness of the singlets is dependent on the preparation. See Fig. 4.9 and Par. 2.3.5. Yield: 65%; 220 mg.

³¹P NMR: δ - 26.0; - 42.7

¹H NMR: δ 4.6(m); δ 3.5 (m); δ 3.12(s)

UV-Vis: ε₂₄₆ = 24580; ε₃₀₆ = 12070 M⁻¹cm⁻¹

IR (KBr): 1618(w); 1442(w); 1420(w); 1288(m); 1242(m); 1102(w); 1012(s); 972(s); 944(s); 804(m); 736(m); 576(m) cm⁻¹

3.1.6 [PdCl₂(COD)]³

Palladium(II) chloride (2.0 g; 11.3 mmol) was dissolved in concentrated hydrochloric acid (5 ml) by warming the mixture. The solution was cooled to room temperature and diluted with ethanol (150 ml), filtered, and the residues on the filter paper washed with ethanol (1 x 20 ml). To the combined filtrate and washing was added 1,5-cyclooctadiene (COD) (3.0 ml; 24.4 mmol) with stirring. The yellow product precipitated immediately and after 10 minutes

it was filtered and the precipitate washed with diethyl ether (3 x 30 ml). Yield: 3.1 g; 96% based on PdCl₂.

¹H NMR: δ 6.3 (s, 4H); δ 2.9 (dd, 4H); δ 2.55 (dd, 4H)

3.1.7 *cis*-[PdCl₂(PTA)₂]

[PdCl₂(COD)] (100 mg; 0.35 mmol) was added to methanol (15 ml). PTA (165 mg; 0.81 mmol) was dissolved in the minimum amount of a water/methanol mixture (1:1) (30 ml) and added to the [PdCl₂(COD)] suspension. The mixture was stirred for 30 minutes and filtered, the precipitate was washed with methanol (3 x 15 ml) to remove unreacted PTA followed by washing with diethyl ether (2 x 15 ml). See Fig. 4.10 and Par. 2.3.5. Yield: 85%; 146 mg.

³¹P NMR: δ - 20.7

¹H NMR: δ 4.4(m); δ 3.8 (d); δ 3.4 (m); δ 3.12(s); δ 2.0(s), δ 0.9(t)

UV-Vis: ε₂₄₂ = 22300; ε₃₀₆ = 6900 M⁻¹cm⁻¹

IR (KBr): 1620(w); 1425(w); 1281(s); 1239(m); 1164(w); 1098(w); 1011(m); 972(s); 942(m); 798(m); 738(m); 539(s) cm⁻¹

3.1.8 *trans*-[Pd(SCN)₂(PTAH)₂](SCN)₂

To a solution of *cis*-[PdCl₂(PTA)₂] (2.5 mg; 100 ml) at pH 3–4 (HClO₄) in water, was added an excess (> 10 x) of KSCN (100 mg; 1.03 mmol). Evaporation of the solution gave red crystals suitable for X-ray analysis in yields < 20% (5.1 mg). See Par. 3.3.2 for the crystal structure determination.

IR (KBr): 2044(s); 1413(m); 1293(w); 1113(w); 1011(m); 978(w); 933(m); 762(w); 603(w) cm⁻¹

UV-Vis: ε₂₈₃ = 29000; ε₃₇₅ = 7700 M⁻¹cm⁻¹

3.1.9 *trans*-[PdBr₂(PTA)₂]

[PdCl(PTA)₃]Cl (7.4 mg; 0.011 mmol) was dissolved in the minimum amount of water (*ca.* 10 ml) and an excess of LiBr (300 mg; 3.45 mmol) was added. Evaporation of the solution gave yellow crystals suitable for X-ray analysis in yields > 55% (3.8 mg). See Par. 3.3.3 for the crystal structure determination.

IR (KBr): 1416(m); 1274(m); 1238(m); 1206(w); 1098(m); 1012(s); 968(s); 936(s); 894(w); 794(m); 668(m); 618(w) cm^{-1}

UV-Vis: $\epsilon_{275} = 28000$, $\epsilon_{330} = 10300 \text{ M}^{-1}\text{cm}^{-1}$

3.1.10 *trans*-[PdI₂(PTA)₂]

[PdCl(PTA)₃]Cl (10.0 mg; 0.015mmol) was dissolved in water (*ca.* 100 ml) and an excess NaI (50.0 mg; 0.334 mmol) was added. Evaporation of the solvent gave yellow crystals suitable for X-ray analysis in yields > 60% (6 mg).

IR (KBr): 1616(s); 1418(w); 1280(w); 1126(w); 1096(w); 1010(m); 968(m); 944(m); 806(w); 612(s); 472(m); 408(m) cm^{-1}

UV-Vis: $\epsilon_{288} = 15000$; $\epsilon_{400} = 6300 \text{ M}^{-1}\text{cm}^{-1}$

The crystal structure for the complex was done, but it is not reported in this work.

3.1.11 [Pd(N₃)₂(PTA)₂]

cis-[PdCl₂(PTA)₂] (4.3 mg; 0.07mmol) was dissolved in water (*ca.* 50 ml) and an excess NaN₃ (300 mg; 4.7 mmol) was added.

UV: $\epsilon_{295} = 19700 \text{ M}^{-1}\text{cm}^{-1}$

3.2 Crystallography^{4,5,6}

3.2.1 Introduction

Crystal structure determination is a two-part process. First is the determination of the lattice parameters, that is the size and shape of the unit cell, from the geometry of the diffraction pattern and the determination of the crystal system. This is in principle a straightforward process and the information can be obtained with the Weissenberg method. Secondly, is the determination of the lattice type and the distribution of the atoms in the structure from the relative intensities of the diffraction spots. This is a very complex process, as will be discussed in the following paragraphs.

3.2.2 Definition of a Crystal

A crystal⁷ is a substance that is periodic in three dimensions and is bound by plane faces. In crystallography the term "lattice" refers to a regular, infinite three dimensional collection of points with exactly the same surroundings (identical points). From this stems the unit cell which is defined as the "smallest arrangement of atoms that is repeated throughout the crystal". The size and shape of a unit cell is defined by the lengths a , b and c of the three independent edges and the three angles α , β and γ between these edges, α is the angle between the b and c axis, β the angle between a and c and γ the angle between the a and b axis.

3.2.3 Diffraction of X-rays

X-ray diffraction is a very powerful tool to study molecular structures. X-rays constitute of electromagnetic waves and atoms surrounded by electron clouds are capable of being disturbed by these electromagnetic waves. Each atom is associated with a number of electrons that absorb the X-rays and re-emit them at the same frequency. Therefore, when matter is in the path of waves, it may under appropriate conditions, scatter the waves. If the wavelength of the X-rays is in the same order of magnitude as the inter atomic distances in a crystal, the waves scattered in the same direction combine with one another in such a way that in some directions the scattered waves reinforce one another and in others they annul each other and this is called the diffraction of waves. The characteristics of the diffraction pattern can be used to deduce information about the geometry of the molecule/atoms that produces it.

3.2.4 The Structure Factor

When a X-ray beam strikes a lattice array of atoms, all the atoms scatter the X-rays, but the scattered wavelets do not interfere unless certain conditions are satisfied. An actual crystal is ordinarily made up of several parallel, displaced lattice arrays. The geometry of reflections from such a composite lattice array is exactly the same as that for one of the component lattice arrays, but the amplitudes of the reflections are functions of the relative displacements of arrays and of the scattering power of the atoms (*i.e.* Scattering factor).

Therefore, the directions of the diffraction maxima depend on the geometry of the cell, while their amplitudes depend on the arrangement of the atoms of the cell. The specific combination of amplitude and phase of the diffracted X-rays, by one unit cell, in any direction where there is a diffraction maxima, is known as the structure factor, F_{hkl} .

$$\text{structure factor } F_{hkl} = \frac{\text{amplitude scattered by all the atoms in the unit cell}}{\text{amplitude scattered by a single electron}}$$

F_{hkl} express the amplitude of scattering from a reflecting plane with Miller indices hkl , and also the phase angle of the scattered wave. The indices h , k and l are integers and describe the orientation of naturally occurring crystal faces. F_{hkl} is therefore a vector or a complex number.

3.2.5 Fourier Transformation

In the introduction of crystallography (Par. 3.2.1) it was said that it is a complex process to determine the lattice type and the distribution of the atoms in the structure. The reason being that films and counters record intensities which are proportional to the squares of the amplitude of the structure factor. The relationship is given in Eq. 3.1:

$$I \propto |F|^2 \tag{3.1}$$

The square of a complex number, F_{hkl} , is always real (simple number) and hence the information about the phase angles of the diffracted beams is lost.

The electron density, that is the number of electrons per unit volume, is the same in all the cells; therefore it can be expressed as a periodic function. A periodic function can be expressed as a Fourier series in which the series is a sum of terms representing a wave and its harmonics, having various amplitudes. Fourier transformation is used for the conversion of the intensity data provided by the experimental diffraction of X-rays by the crystal to produce the image of the structure. The Fourier transformation of the electron density (ρ) at any point (x, y, z) is given by Eq. 3.2:

$$\rho_{(x,y,z)} = \frac{1}{V} \sum_h \sum_k \sum_l F_{(hkl)} e^{-2\pi i (hx+ky+lz)} \tag{3.2}$$

where V is the volume of the unit cell, and F_{hkl} the structure factor for the particular set of Miller indices h , k and l . The amplitude of F_{hkl} can be determined from the intensity of the reflection, but the phase angle is not known. Thus there is no way of finding the Fourier coefficients experimentally; the Fourier series cannot be summed to find the electron distribution (therefore, the locations of atoms in the structure) in a crystal directly from its X-ray diffraction pattern. This is known as the phase problem.

3.2.6 The Patterson Synthesis

The Patterson function is one of the methods used to solve the phase problem. Patterson used the phaseless squares of the structure amplitude, $|F|^2$, as coefficients in a Fourier series, instead of the structure factor as shown in Eq. 3.3:

$$\rho_{(u,v,w)} = \frac{1}{V} \sum_h \sum_k \sum_l |F_{(hkl)}|^2 e^{-2\pi i (hu+kv+lw)} \quad 3.3$$

The Patterson synthesis shows peaks that correspond with interatomic distances in contrast with the Fourier synthesis that gives only the distribution of electron density in the unit cell. If there is a peak with position (u, v, w) it means that there are atoms whose coordinates, (x, y, z) and (x', y', z') , differ by these values: $u = x-x'$; $v = y-y'$; $w = z-z'$. If the two atoms have atomic numbers of Z_A and $Z_{A'}$ respectively, a peak height of approximately $Z_A Z_{A'}$ can be expected. The Patterson function thus gives a map of vectors between atoms with a Patterson peak for each interatomic vector. If an atom with a relatively high atomic number is present in the unit cell, the vector peak will stand out strongly. The position of the atom can therefore be determined easily. If the coordinates of the heavy atoms are known the approximate phase angle can be determined and be correlated with the experimental F_{hkl} so that the positions of the lighter atoms can be determined.

3.2.7 Least-Squares Refinement of a Structural Model

After all the atoms have been identified, approximately positioned and given rough amplitudes of thermal vibration the coordinates of the atoms are calculated more accurately with the least squares method. The isotropic and anisotropic temperature factors are refined simultaneously with the atom coordinates. For all the reflection indices, a measure of

reliability of the experimentally observed structure factors, F_{obs} , to the structure factors calculated for the model, F_{cal} , is expressed by the reliability index, given by Eq. 3.4:

$$R = \frac{\sum || F_{\text{obs}} || - |F_{\text{cal}} ||}{\sum |F_{\text{obs}}|} \quad 3.4$$

If the reliability index, or R -value, is 0.10 or less, it means that there is good agreement between the observed and calculated F values. A low R value alone is not a guarantee that the atomic positions are placed correctly. Very accurate values for both the atomic coordinates and the parameters that specify the thermal motion of the atoms will be obtained if a large number of reflections are available. In updated versions of crystallographic programs⁸, the principles of refinement against F^2 are introduced, given by Eq. 3.5:

$$R = \frac{\sum [w(F_{\text{obs}}^2 - F_{\text{cal}}^2)^2]}{\sum |F_{\text{obs}}|} \quad 3.5$$

3.3 X-ray Crystal Structure Determinations of Selected Complexes

X-ray crystal structure determinations are reported for the complexes *trans*-[Pd(SCN)₂(PTAH)₂](SCN)₂ and *trans*-[PdBr₂(PTA)₂] Scheme 4.2 (Chapter 4) shows the relevance of these structure determinations.

3.3.1 Experimental

The reflection data for *trans*-[Pd(SCN)₂(PTAH)₂](SCN)₂ was collected at -100 °C on a Nonius Kappa CCD diffractometer using monochromated Mo K_{α} radiation ($\lambda = 0.7107 \text{ \AA}$). The reflection data for *trans*-[PdBr₂(PTA)₂] were collected at 293(2) K on a Siemens Smart CCD diffractometer. Both structures were solved by direct-method techniques by using the SHELX 97 computer program⁸, which yielded the position of the palladium atom, followed by successive Fourier methods. The structures were refined through full matrix least squares calculations using by using the SHELX 97 computer program⁸, with F^2 being minimized. All non-hydrogen atoms were refined anisotropically while the positions of the hydrogen atoms were calculated as riding on the adjacent carbon (alkyl C-H = 0.97 Å). For *trans*-[Pd(SCN)₂(PTAH)₂](SCN)₂ the position of the hydrogen bonded to the nitrogen was placed

from the final electron map. The experimental densities of the crystals were determined by flotation in diiodomethane/benzene.

A summary of the general crystal data and refinement parameters are given in Table 3.1 while figures showing the numbering schemes and thermal ellipsoids are given in Figs. 3.1 and 3.2, respectively. Supplementary data with complete lists of atomic coordinates, bond distances and angles, anisotropic displacement parameters as well as hydrogen coordinates are given in Appendix A. Selected interatomic bond distances for the complexes are given in Table 3.2 and Table 3.4, respectively.

Table 3.1 Crystal data and refinement parameters for *trans*-[Pd(SCN)₂(PTAH)₂](SCN)₂ and *trans*-[PdBr₂(PTA)₂]

	[Pd(SCN) ₂ (PTAH) ₂](SCN) ₂	<i>trans</i> -[PdBr ₂ (PTA) ₂]
Empirical formula	C ₁₆ H ₂₆ N ₁₀ S ₄ P ₂ Pd	C ₁₂ H ₂₄ N ₆ Br ₂ P ₂ Pd
Molecular weight	655.05	580.53
Crystal system	Monoclinic	Monoclinic
Space group	<i>P</i> 2 ₁ / <i>n</i>	<i>P</i> 2 ₁ / <i>n</i>
<i>a</i> (Å)	7.5170(15)	7.2755(15)
<i>b</i> (Å)	12.733(3)	11.808(2)
<i>c</i> (Å)	12.956(3)	10.317(2)
β (°)	94.96(3)	94.99(3)
<i>V</i> (Å ³)	1235.4(4)	883.0(3)
<i>Z</i>	2	2
ρ_{exp} (g.cm ⁻³)	1.746	2.167
ρ_{calc} (g.cm ⁻³)	1.761	2.184
μ (mm ⁻¹)	1.247	5.765
<i>F</i> (000)	664	568
Crystal size (mm)	0.16 x 0.22 x 0.30	0.06 x 0.09 x 0.18
Theta range (°)	2.25 to 27.45	2.63 to 31.78
	-9 ≤ <i>h</i> ≤ 9	-10 ≤ <i>h</i> ≤ 10
Index ranges	-15 ≤ <i>k</i> ≤ 16	-17 ≤ <i>k</i> ≤ 17
	-16 ≤ <i>l</i> ≤ 16	-12 ≤ <i>l</i> ≤ 15
Reflections collected	6468	9537

Independent reflections	2766	2796
R_{int}	0.0284	0.0769
Obs.refl. ($I > 2\sigma(I)$)	2178	1713
Completeness to 2 theta	93.5% / 27.45 °	96.20% / 27.87 °
Data/ restraints/ parameters	2766 / 0 / 180	2796 / 0 / 107
Goodness-of-fit on F^2	1.011	0.930
Final R indices ($I > 2\sigma(I)$)	$R_1^a = 0.0288$	$R_1^a = 0.0415$
	$wR_2^b = 0.0532$	$wR_2^b = 0.0765$
R indices (all data)	$R_1 = 0.0468$	$R_1 = 0.0928$
	$wR_2 = 0.0582$	$wR_2 = 0.0870$
$\rho_{\text{max}} / \rho_{\text{min}}$ ($\text{e} \cdot \text{A}^{-3}$)	0.574 / -0.414	0.673 / -1.509

$$^a R_1 = [(\Sigma \Delta F) / (\Sigma F_o)]$$

$$^b wR_2 = \Sigma [w(F_o^2 - F_c^2)^2] / \Sigma [w(F_o^2)^2]^{1/2}$$

3.3.2 The Crystal Structure of *trans*-[Pd(SCN)₂(PTAH)₂](SCN)₂

This crystal structure was done to: i) characterize the product isolated, ii) determine whether the PTA ligands are protonated at pH around 3, iii) what happens if substitution takes place (*cis* or *trans* configuration), and iv) whether the thiocyanate ligand coordinate *via* the sulfur or the nitrogen atom if substitution did take place. The molecular diagram showing the numbering scheme and thermal ellipsoids of *trans*-[Pd(SCN)₂(PTAH)₂](SCN)₂ is given in Fig. 3.1 and selected bond lengths and angles in Table 3.2.

Figure 3.1 Diamond drawing of *trans*-[Pd(SCN)₂(PTAH)₂](SCN)₂ showing the numbering scheme and thermal ellipsoids (30% probability). Only the H-atoms on the protonated N atom of the PTA ligands are included.

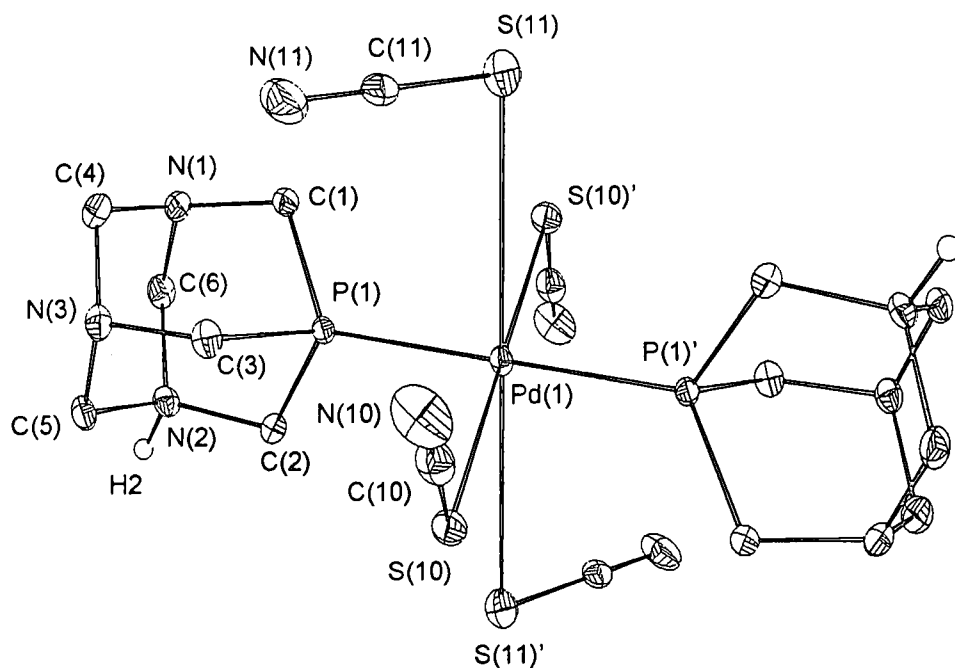


Table 3.2 Selected bond lengths (Å), angles (°), torsion angles (°) and effective cone angle (θ_E) of the PTA ligands (°), for *trans*-[Pd(SCN)₂(PTAH)₂](SCN)₂.

Pd(1)-P(1)	2.2940(8)	Pd(1)-S(11)	3.4284(8)
Pd(1)-S(10)	2.3509(8)	S(11)-C(11)	1.628(3)
S(10)-C(10)	1.676(3)	C(11)-N(11)	1.158(3)
C(10)-N(10)	1.155(3)	N(1)-C(1)	1.469(3)
P(1)-C(1)	1.837(3)	N(1)-C(4)	1.461(3)
P(1)-C(2)	1.835(2)	N(1)-C(6)	1.431(3)
P(1)-C(3)	1.839(2)	N(3)-C(3)	1.467(3)
N(2)-C(2)	1.498(3)	N(3)-C(4)	1.470(3)
N(2)-C(5)	1.522(3)	N(3)-C(5)	1.430(3)
N(2)-C(6)	1.526(3)		
P(1)-Pd(1)-P(1)'	180	S(10)-Pd(1)-S(10)'	180
P(1)-Pd(1)-S(10)	90.55(3)	P(1)-Pd(1)-S(10)'	89.45(3)

P(1)-Pd(1)-S(10)	89.45(3)	P(1)-Pd(1)-S(11)'	92.83(3)
C(10)-S(10)-Pd(1)	102.70(10)	C(11)-S(11)-Pd(1)	95.55(9)
S(10)-C(10)-N(10)	176.8(3)	S(11)-C(11)-N(11)	179.6(3)
C(1)-P(1)-Pd(1)	121.19(8)	C(1)-P(1)-C(2)	99.16(11)
C(2)-P(1)-Pd(1)	115.36(8)	C(1)-P(1)-C(3)	99.03(12)
C(3)-P(1)-Pd(1)	119.14(8)	C(2)-P(1)-C(3)	98.80(11)
P(1)-C(1)-N(1)	110.78(16)	N(1)-C(6)-N(2)	111.1(2)
P(1)-C(2)-N(2)	109.92(16)	N(1)-C(4)-N(3)	113.3(2)
P(1)-C(3)-N(3)	111.49(16)	N(2)-C(5)-N(3)	111.7(2)
C(1)-N(1)-C(4)	112.2(2)	C(3)-N(3)-C(4)	112.03(19)
C(1)-N(1)-C(6)	113.0(2)	C(3)-N(3)-C(5)	111.9(2)
C(4)-N(1)-C(6)	109.8(2)	C(4)-N(3)-C(5)	109.6(2)
C(2)-N(2)-C(5)	111.9(2)	C(5)-N(2)-C(6)	108.6(2)
C(2)-N(2)-C(6)	111.61(19)		
S(10)-Pd(1)-P(1)-C(1)	-162.90(10)	S(10)-Pd(1)-P(1)-C(3)	-39.70(10)
S(10)-Pd(1)-P(1)-C(2)	77.57(9)		
θ_E	117.77		

Results and Discussion

The *trans*-[Pd(SCN)₂(PTAH)₂](SCN)₂ complex was synthesized and crystals were obtained as reported in Par. 3.1.8. The complex crystallized in the monoclinic space group $P2_1/n$ with 2 molecules per unit cell and Pd atom situated on an inversion centre. The complex exhibit a square planar geometry around the Pd atom with the PTA ligands *trans* to each other (180°) and a Pd(1)-P(1) bond distance of 2.2940(8) Å. Both PTA ligands are protonated at one of the nitrogen atoms. Additionally the two coordinated thiocyanate ligands are *trans* (180°) with respect to each other in the equatorial plane, while two thiocyanate moieties, acting as counterions, occupy the axial positions (see Fig. 3.1). Both these thiocyanate anions interact with the Pd *via* the S atoms. The bond length of Pd(1)-S(10) is 2.3509(8) Å and the Pd(1)-S(11) bond interaction is 3.4384(8) Å.

The C(10)-N(10) and C(11)-N(11) bond lengths are virtually the same at 1.155(3) Å and 1.158(3) Å respectively, but the S(10)-C(10) bond is 1.676(3) Å versus the shorter S(11)-C(11) bond (1.628(3) Å). This is indicative of the resonance structure of the thiocyanate with approximate double bond character on the S(11)-C(11) moiety. Since Pd(1)-S(10) is a formal bond, the sulphur atom donates electron density to the metal centre, resulting in more single bond character in S(10)-C(10). The S(10)-C(10)-N(10) angle is 176.8(3)° compared to the virtually linear S(11)-C(11)-N(11) moiety (angle of 179.6(3)°). The C(10)-S(10)-Pd(1) angle is 102.70(10)°, characteristic of the thiocyanate bonded *via* the S atom (N-bonded thiocyanate usually exhibits a linear configuration).

Of interest is the fact that the bond distances P(1)-C(1), P(1)-C(2) and P(1)-C(3) do not differ significantly *i.e.*, 1.837(3) Å, 1.835(2) Å and 1.839(2) Å respectively, whereas the N(2)-C(2), N(2)-C(5) and N(2)-C(6) bond distances do differ significantly. The N(2)-C(2) bond is 1.498(3) Å *versus* the 1.522(3) Å and 1.526(3) Å of N(2)-C(5) and N(2)-C(6) respectively. The shorter N(2)-C(2) bond is due to the fact that the N(2) atom is protonated.

The effective cone angle of the PTA ligand was determined according to the Tolman model¹⁹ as $\theta_E = 117.77^\circ$.

Ambidentate bonding capability of thiocyanate

An interesting feature of the thiocyanate ion is the ambidentate bonding capability⁹ thereof, *i.e.*, the fact that the thiocyanate can coordinate *via* either the S- or the N atom. Thiocyanate will preferably coordinate *via* the S atom to soft metals and *via* the N atom to hard metal centres, and both electronic effects¹⁰ and steric effects^{11,12,13} or a combination thereof¹⁴ has been proposed to play a dominant role in determining the thiocyanate bonding mode. The thiocyanate bonding mode is finely balanced in Pd(II) complexes, and subtle changes in either one of the effects will tip the balance and determine both linkage and geometrical isomerism.

In many studies¹⁵ a bidentate neutral ligand (for example, bis(diphenylphosphino)methane, Ph₂PCH₂CCF₃CHPPh₂) was used to determine the bonding mode of the thiocyanate. Palenik and co-workers¹³ have reported examples of steric effects on the structure in the

series $[(\text{SCN})_2\text{Pd}(\text{Ph}_2\text{P}(\text{CH}_2)_n\text{PPh}_2)]$ with $n = 1, 2$, or 3 . As the angle of the bidentate ligand increase with increasing n , the bonding mode of the thiocyanates goes from N,N to N,S to S,S.

The bidentate ligand, however, prohibits geometrical isomerism and tends to give an incomplete picture of the various influences on the linkage isomerism in thiocyanate complexes. The $[\text{M}(\text{CNS})_2\text{L}_2]$ complexes (CNS – unspecified bonding mode), where L is a monodentate neutral ligand, have the capacity for geometrical isomerism, which can influence the thiocyanate bonding mode.

In Table 3.3 the bonding mode of thiocyanate in a series of palladium complexes containing monodentate ligands, are reported for comparative purposes.

Table 3.3 Selected bond lengths of monodentate Pd-SC- or Pd-NC- complexes^a and the bonding mode thereof

Complex ¹⁶	Pd-S	Pd-P	S-C	Ref.
<i>trans</i> -[Pd(SCN) ₂ (PTAH) ₂](SCN) ₂	2.3509(8)	2.2940(8)	1.676(3)	TW
<i>trans</i> -[Pd(SCN) ₂ {P(OPh) ₃ } ₂]	2.352(2)	2.312(2)	1.672(8)	17
<i>trans</i> -[Pd(SCN) ₂ (PCCBu ¹ Ph ₂) ₂]	2.336(3)	2.326(3)	1.635(14)	18
<i>cis</i> -[Pd(SCN) ₂ (TMP) ₂] ^b	2.382(2)	2.277(2)	1.677(8)	9
<i>trans</i> -[Pd(NCS) ₂ (PPh ₃) ₂] ^c	1.969(3)	2.340(9)	1.138(6)	17
<i>trans</i> -[Pd(C ₆ F ₅ P(CH ₃) ₂) ₂ (SCN) ₂]	2.351(1)	2.318(1)	-	13

^a CSD search, see Ref. 16

^c TMP: 1,3,4-trimethyl-phosphole

^b N-bonded

TW This work

The shorter Pd-P bonds in *trans*-[Pd(SCN)₂{P(OPh)₃}₂] (2.312(2) Å) compared to *trans*-[Pd(NCS)(PPh₃)₂] (2.340(9) Å) could be ascribed to one, or a combination of the following effects: (a) P(OPh)₃ has a smaller cone angle¹⁹ (128°) than PPh₃ (145°) and should therefore be sterically less demanding; (b) PPh₃ is more basic than P(OPh)₃ while the latter has a larger π -acceptor ability; (c) phosphines have a higher *trans*-influence than phosphites.

The Pd-P bond lengths in the four complexes *trans*-[Pd(NCS)(PPh₃)₂], *trans*-[Pd(SCN)₂Ph₂PC₂Bu¹]₂, *trans*-[Pd(SCN)₂{P(OPh)₃}₂] and *trans*-[Pd(SCN)₂(PTAH)₂](SCN)₂ (Table 3.3) show a gradual and significant decrease (2.340(9), 2.326(3), 2.312(2),

and 2.2940(8) Å) as the cone angles of the phosphorus ligands changes from 145° for PPh₃, 135° for Ph₂PC₂Bu^t, 121° for P(OPh)₃ and 118° for PTA²⁰ (see Par. 2.3.3). An increase in Pd-S bond lengths, 2.336(3) Å for *trans*-[Pd(SCN)₂Ph₂PC₂Bu^t]₂ to 2.352(2) Å in *trans*-[Pd(SCN)₂{P(OPh)₃}]₂, is observed, following the Pd-P distance decrease from 2.326(3) Å to 2.312(2) Å. This observation suggests a 'push-pull' mechanism for retaining the same electron-density on the metal and the same steric effects within the coordination sphere.

The relative ease with which two bent Pd-SCN moieties can be arranged within the environment created by two sterically, less demanding coordinated ligands (for example P(OPh)₃) is envisioned, in contrast to the incompatibility of the sterically more demanding framework (for example, Pd(PPh₃)₂) for two linear Pd-NCS moieties.

1-R-3,4-dimethylphospholes contains Pd-P bonds which are as strong, if not stronger, than those in structurally similar palladium-phosphine complexes. For *cis*-[Pd(SCN)₂(TMP)₂] the Pd-P bond length is 2.277(2) Å versus 2.2940(8) Å for *trans*-[Pd(SCN)₂(PTAH)₂](SCN)₂ and 2.340(9) Å for *trans*-[Pd(NCS)(PPh₃)₂]. Phospholes are sterically less demanding than phosphines and therefore probably also than PTA. The enhanced bonding properties of these phospholes is most likely a consequence of this and of intracyclic phosphorus electron delocalization. PTA²¹ is a strong σ-donor as well as a strong π-acceptor.

3.3.3 The Crystal Structure of *trans*-[PdBr₂(PTA)₂]

Introduction

This crystal structure was done to determine: i) if the complex is the [PdBr(PTA)₃]⁺ or the [PdBr₂(PTA)₂] complex, and ii) whether the PTA⁻ ligands are protonated. The molecular diagram showing the numbering scheme and thermal ellipsoids of *trans*-[PdBr₂(PTA)₂] is given in Fig. 3.2 and selected bond lengths and angles in Table 3.4.

Figure 3.2 Diamond drawing of *trans*-[PdBr₂(PTA)₂] showing the numbering scheme and thermal ellipsoids (30% probability). Hydrogen atoms are omitted for clarity.

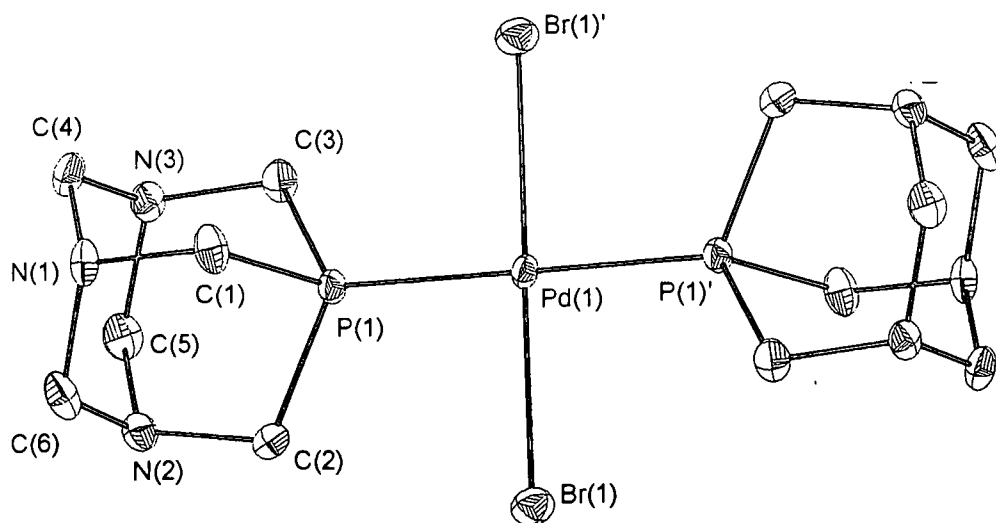


Table 3.4 Selected bond lengths (Å), angles (°), torsion angles (°) and effective cone angle (θ_E) of the PTA ligands (°), for *trans*-[PdBr₂(PTA)₂]

Pd(1)-P(1)	2.3199(10)	Pd(1)-Br(1)	2.4270(8)
P(1)-C(1)	1.839(5)	N(1)-C(1)	1.465(5)
P(1)-C(2)	1.846(4)	N(1)-C(4)	1.459(5)
P(1)-C(3)	1.837(4)	N(1)-C(6)	1.473(5)
N(2)-C(2)	1.474(5)	N(3)-C(3)	1.476(5)
N(2)-C(5)	1.466(5)	N(3)-C(4)	1.457(6)
N(2)-C(6)	1.457(6)	N(3)-C(5)	1.477(5)
P(1)-Pd(1)-P(1)'	180	Br(1)-Pd(1)-Br(1)'	180
P(1)-Pd(1)-Br(1)	90.6(3)	P(1)-Pd(1)-Br(1)'	89.4(3)
C(1)-P(1)-Pd(1)	113.74(13)	C(1)-P(1)-C(2)	98.5(2)
C(2)-P(1)-Pd(1)	121.12(14)	C(1)-P(1)-C(3)	98.1(2)
C(3)-P(1)-Pd(1)	122.37(14)	C(2)-P(1)-C(3)	98.2(2)
C(1)-N(1)-C(4)	110.9(3)	C(2)-N(2)-C(5)	110.7(3)
C(1)-N(1)-C(6)	110.9(3)	C(2)-N(2)-C(6)	111.0(3)
C(4)-N(1)-C(6)	107.7(3)	C(5)-N(2)-C(6)	108.8(3)
C(3)-N(3)-C(4)	111.8(3)	C(4)-N(3)-C(5)	108.8(3)

SYNTHESIS AND CHARACTERIZATION

C(3)-N(3)-C(5)	110.6(3)	N(1)-C(6)-N(2)	115.0(3)
N(1)-C(4)-N(3)	115.1(3)	N(3)-C(5)-N(2)	113.8(3)
Br(1)-Pd(1)-P(1)-C(1)	-100.19(17)	Br(1)-Pd(1)-P(1)-C(3)	142.35(19)
Br(1)-Pd(1)-P(1)-C(2)	16.8(2)		
θ_E	116.70		

Results

The *trans*-[PdBr₂(PTA)₂] complex was synthesized and crystals were obtained as reported in Par. 3.1.9. The complex crystallised in the monoclinic space group *P*2₁/*n* with 2 molecules per unit cell. The Pd atom is situated on an inversion centre, which implies a planar and *trans* arrangement. The Pd atom exhibits a square planar geometry and the PTA ligands lie *trans* to each other (180°). The PTA ligands are not protonated (see Fig. 3.2) and the Pd(1)-P(1) bond length is 2.3199(10) Å. The Pd(1)-Br(1) bond distance is 2.4270(8) Å.

The effective cone angle of the PTA ligand was determined according to the Tolman model¹⁹ as $\theta_E = 116.70^\circ$.

The complex is isostructural to both *trans*-[PdI₂(PTA)₂]²² and *trans*-[PtI₂(PTA)₂]²³.

Other palladium-bromide complexes

In Table 3.5 a representative number of [PdBr₂(L)₂] complexes (L = ligand with donor atom N, P, As or S) reported in the literature, are given.

Table 3.5 Selected bond lengths (Å) of some *trans*-[PdBr₂(L)₂] complexes (L = ligand with donor atom N, P, As or S).

Complex	Pd-Br	L	Pd-L	Ref.
<i>trans</i> -[PdBr ₂ (Ino) ₂]	2.430(1) _{av}	N	2.050(7) _{av}	24
<i>trans</i> -[PdBr ₂ (PPK) ₂]	2.414(2)	N	2.010(1)	25
<i>trans</i> -[PdBr ₂ (TP) ₂]	2.431(1)	N	2.020(6)	26
<i>trans</i> -[PdBr ₂ (2-dqmp) ₂]	2.435(1)	N	2.064(7)	27
<i>trans</i> -[PdBr ₂ (DTP) ₂]	2.420(1)	N	2.015(4)	28
<i>trans</i> -[PdBr ₂ (idaaH ₂) ₂]	2.412(1)	N	2.051(11)	29
<i>trans</i> -[PdBr ₂ (PTA) ₂]	2.427(1)	P	2.320(1)	TW
<i>trans</i> -[PdBr ₂ (DDEP) ₂]	2.412(1)	P	2.325(3)	30
<i>trans</i> -[PdBr ₂ (DPA) ₂]	2.447(1)	P	2.322(2)	31
<i>trans</i> -[PdBr ₂ (ppq) ₂]	2.435(1)	P	2.318(1)	32
<i>trans</i> -[PdBr ₂ (DMPP) ₂]	2.434(1) _{av}	P	2.316(2) _{av}	33
<i>trans</i> -[PdBr ₂ (H ₂ L) ₂]	2.442(1)	S	2.316(1)	34
<i>trans</i> -[PdBr ₂ (DAED) ₂]	2.414(1)	As	2.432(1)	35

av = average

Ino = inosine

PPK = phenyl-2-pyridyl ketone

TP = 2-(2'-thienyl)pyridine

2-dqmp = 2-quinolylmethylphosphonate

DTP = 5,7-dimethyl-8H-[1,2,4]triazolo[1,5-a]pyrimidine

idaaH₂ = iminodiacetamide

DDEP = 2-(diphenylphosphino)ethanephosphonate

DPA = diphenylphosphinoacetic acid

ppq = *p*-quinonyldiphenylphosphine

DMPP = 1-phenyl-3,4-dimethylphosphole

H₂L = N-alkyl-N'-aroylthiourea

DAED = 2-(2-{diphenylarsino}ethyl)-1,3-dioxane

It is clear from Table 3.5 that the Pd-Br bond lengths vary within the same range when changing the *cis* ligands, for example, from N to P to As. The shortest Pd-Br bond length is 2.412(1) Å (P or N as *cis* ligand) and the longest Pd-Br bond length is 2.447(1) Å (P as *cis* ligand). The Pd-L bond lengths lengthen when descending in group Va in the periodic table. The Pd-N bond lengths range from 2.010(1) Å to 2.064(7) Å, the Pd-P bond lengths from 2.316(2) Å to 2.325(3) Å and the only Pd-As bond length reported is 2.432(1) Å. When sulphur act as *cis* ligands the Pd-Br bond length is 2.442(1). *trans*-[PdBr₂(PTA)₂], having a Pd-Br bond length of 2.427(1) Å and a Pd-P bond length of 2.320(1) Å, fits well into the typical range where P act as *cis* ligands.

It is important to evaluate the σ -donor ability of phosphines and the labilizing effects they have when they occupy positions *trans* to one another in square planar complexes. In Table 3.6 typical bond lengths of Pd-Br, Pd-X (X = atom *trans* with respect of Br) and Pd-L (L =

phosphine/stibine) bonds in *trans*-[PdBr(X)(L)₂] complexes are shown. The *trans* Br-Pd-Br orientation of the title complex clearly illustrate the relative small *trans* influence of Br⁻ as ligand.

Table 3.6 Comparative table of bond lengths (Å) for *trans*-[PdBr(X)(L)₂] complexes.

Complex	Pd-Br	Pd-X	Pd-L _{av}	Ref.
<i>trans</i> -[PdBr ₂ (PTA) ₂]	2.427(1)		2.320(1)	TW
<i>trans</i> -[PdBr(PPh ₃) ₂ (C≡CSiMe ₃)]	2.481(2)	1.974(6)	2.300(2)	36
<i>trans</i> -[PdBr(PPh ₃) ₂ (3,4,5-C ₄ Br ₃ S)]	2.483(1)	2.004(8)	2.329(2)	40
<i>trans</i> -[PdBr(PPh ₃) ₂ (3,4-C ₄ HBr ₂ S)]	2.509(1)	1.998(3)	2.340(1)	40
<i>trans</i> -[PdBr(PMe ₃) ₂ [C(C≡C-CMe ₃)=C(C≡CCMe ₃)CMe ₃]]	2.512(2)	2.004(12)	2.309(4)	37
<i>trans</i> -[PdBr(PPh ₃) ₂ (<i>o</i> -CH ₃ C ₆ H ₄)]	2.517(2)	1.991(8)	2.321(2)	38
<i>trans</i> -[PdBr(PEt ₃) ₂ (C ₅ H ₄ N)]	2.522(1)	1.998(6)	2.323(2)	39
<i>trans</i> -[PdBr(PEt ₃) ₂ (C ₅ H ₄ N)]	2.524(1)	1.993(6)	2.313(3)	39
<i>trans</i> -[PdBr(PPh ₃) ₂ (C ₄ H ₃ S)]	2.526(1)	1.993(4)	2.351(1)	40
<i>trans</i> -[PdBr(PPh(Me) ₂) ₂ (PMQ)]	2.529(1)	1.996(6)	2.315(2)	41
<i>trans</i> -[PdBr(PPh ₃) ₂ (Ph)]	2.532(1)	1.995(6)	2.325(2)	42
<i>trans</i> -[PdBr(PPh(Me) ₂) ₂ (TQ)]	2.534(1)	1.987(5)	2.322(2)	41
<i>trans</i> -[PdBr(DPPD) ₂ (4- ¹ Bu-C ₆ H ₄)]	2.5378(7)	2.001(4)	2.349(1)	43
<i>trans</i> -[PdBr(PMe ₃) ₂ Et]	2.554(1)	2.063(5)	2.313(2)	44
<i>trans</i> -[PdBr(PEt ₃) ₂ (C ₅ H ₄ N)]	2.563(3)	2.030(17)	2.327(5)	39
<i>trans</i> -[PdBr(SbPh ₃) ₂ (Ph)]	2.491(2)	2.03(2)	2.542(1)	45

TW = This work

PMQ = 2,5,6,7,8-pentamethylquinoxalin-3-yl

TQ = terquinoxalinylyl

DPPD = 2-(2'-diphenylphosphinophenyl)-1,3-dioxolane

3.3.4 Structural parameter correlation in square planar and related palladium(II) and platinum(II) complexes containing PTA as ligand

In Table 3.7 below, selected geometrical parameters of the complexes investigated in this study are compared with those from other relevant square planar complexes found in literature.

Table 3.7 Comparative table of bond lengths (Å) of square planar complexes containing PTA as ligand (X = halide/pseudo-halide).

Complex	M-P	M-X	Ref.	
<i>cis</i> -[PdCl ₂ (PTA) ₂]	2.226(5)	2.363(5)	46	
	2.264(6)	2.360(5)		
{ <i>cis</i> -[PdCl ₂ (PTA) ₂]} ₂ .H ₂ O	2.2392(13)	2.3467(14)	47	
	2.2551(13)	2.3777(13)		
<i>cis</i> -[PtCl ₂ (PTAH) ₂]Cl ₂	2.219(5)	2.358(5)	46	
	2.218(5)	2.358(5)		
{ <i>cis</i> -[PtCl ₂ (PTA) ₂]} ₂ .H ₂ O	2.2240(12)	2.3490(1)	48	
	2.2284(12)	2.3712(13)		
<i>trans</i> -[PdBr ₂ (PTA) ₂]	2.320(1)	2.427(1)	TW	
<i>trans</i> -[PdI ₂ (PTA) ₂]	2.324(3)	2.592(1)	22	
<i>trans</i> -[PdI ₂ (PTAH) ₂] ^a	2.287(2)	2.622(1)	22	
[PdI ₃ (PTA)] ^a	2.238(1)	2.596(1)		
		2.633(1)		
		2.616(1)		
<i>trans</i> -[Pd(SCN) ₂ (PTAH) ₂](SCN) ₂	2.294(1)	2.351(1)	TW	
<i>trans</i> -[Pt(CN) ₂ (PTA) ₂]	2.305(2)	1.975(9)	49	
<i>trans</i> -[PtI ₂ (PTA) ₂]	2.313(1)	2.602(6)	23	
[PdCl(PTA) ₃]Cl	2.330(2) 2.238(3) 2.338(2)	2.375(3)	50	
[PtCl(PTA) ₃]Cl	2.326(2) 2.233(2) 2.320(2)	2.371(2)	51	
[Pt(NCS)(PTA) ₃](NCS)	2.3215(12) 2.2973(13) 2.2404(13)	2.036(4)	52	
[PtI ₂ (PTA) ₃]	2.313(1) 2.251(1) 2.321(1)	2.719(3) 3.327(3)	53	

TW This work

^a Crystallizes in the same crystal

U.O.V.S. BIBLIOTEK

115694513

In general, the M-P bond lengths are shorter in a *cis*-[PdCl₂(P)₂] than in the corresponding *trans*-[PdCl₂(P)₂] complex (P = PTA or PTAH⁺). The reason for this is that in the *trans* configuration the phosphine ligands compete for the same electron density and they labilize one another, whereas in the *cis* complexes the phosphine is *trans* to a halide. The *trans* influence of PTA, and in phosphines in general, is higher than that of the halide.

For the complexes *trans*-[Pd(SCN)₂(PTAH)₂](SCN)₂, *trans*-[PdBr₂(PTA)₂] and *trans*-[PdI₂(PTA)₂] the Pd-X bond lengths increases in the order 2.351(1) Å to 2.427(1) Å to 2.592(1) Å for SCN⁻ to Br⁻ to I⁻. Pd-P bond lengths for *trans*-[PdBr₂(PTA)₂] and *trans*-[PdI₂(PTA)₂] are the same at 2.320(1) Å and 2.324(3) Å, respectively. This nicely illustrates the *trans* influence of PTA ligands *trans* with respect to each other.

When the PTA ligand is protonated, a formal positive charge is present on an N atom thereof. Therefore, electron density will be drained from the P atom to neutralize the positive charge. As a result the P atom of the PTAH⁺ ligand has much less electron density for donation than the PTA and is therefore a weaker σ -donor. The labilizing effect of PTAH is thus correspondingly restricted and it has a weak *trans* influence. The Pd-P bond lengths for the PTAH ligands *trans* to one another in the complexes *trans*-[Pd(SCN)₂(PTAH)₂](SCN)₂ and *trans*-[PdI₂(PTAH)₂][PdI₃(PTA)] are 2.294(1) Å and 2.287(2) Å respectively. This is much shorter than the Pd-P bond lengths reported in related complexes for unprotonated PTA ligands, e.g., Pd-P bond lengths are 2.320(1) Å and 2.324(3) Å respectively for the complexes *trans*-[PdBr₂(PTA)₂] and *trans*-[PdI₂(PTA)₂]. Consequently the Pd-P bond lengths will be shorter and Pd-X bond lengths will be correspondingly longer in PTAH⁺ complexes than those containing the neutral PTA.

The M-P bond (M = Pt or Pd) in general is shorter for the Pt-P bond than the Pd-P bond. Although Pt lies below Pd in the same group on the periodic table, the ionic radius⁵⁴ of Pt²⁺ is 0.74 Å and it is less than that of Pd²⁺, which is 0.78 Å. It is illustrated by the following examples: The Pd-P bond lengths in the *cis*-[PdCl₂(PTA)₂] complex are 2.2392(13) Å and 2.2551(13) Å, and in the *cis*-[PtCl₂(PTA)₂] complex it is 2.2240(12) Å and 2.2284(12) Å, whereas in the complexes *trans*-[PdI₂(PTA)₂] and *trans*-[PtI₂(PTA)₂] it is 2.324(3) Å and 2.313(1) Å respectively.

The Pd-P bond lengths for the PTA ligands *trans* to each other in $[\text{Pd}(\text{X})(\text{PTA})_3]\text{Cl}$ are 2.330(2) and 2.338(2) Å, respectively and this is longer than the corresponding Pt-P bond lengths, *i.e.*, 2.326(2) and 2.320(2) Å in the $[\text{PtCl}(\text{PTA})_3]\text{Cl}$ complex. The M-P bond for the PTA ligand that lies *trans* to the Cl atom is 2.238(3) and 2.233(2) Å respectively for the complexes $[\text{PdCl}(\text{PTA})_3]\text{Cl}$ and $[\text{PtCl}(\text{PTA})_3]\text{Cl}$. The M-Cl bond lengths are 2.375(3) Å (Pd-Cl) and 2.371(2) Å (Pt-Cl) respectively.

NCS^- has a larger *trans* influence⁵⁵ than Cl^- and evidence hereof, for Table 3.7, is the following: The Pt-N bond length in the complex $[\text{Pt}(\text{NCS})(\text{PTA})_3](\text{NCS})$ is 2.036(4) Å, whereas in $[\text{PtCl}(\text{PTA})_3]\text{Cl}$ the Pt-Cl bond is 2.371(2) Å. The Pt-P bond lengths for the complexes $[\text{Pt}(\text{NCS})(\text{PTA})_3](\text{NCS})$ and $[\text{PtCl}(\text{PTA})_3]\text{Cl}$, where the PTA ligand lie *trans* to the halide/pseudo-halide ligand X, are 2.2404(13) Å and 2.233(2) Å respectively.

The five-coordinated $[\text{PtI}_2(\text{PTA})_3]$ complex have interesting features. Although the Pt-P bond length, 2.251(1) Å (PTA virtually *trans* to I) is longer than in the four-coordinated $[\text{PtCl}(\text{PTA})_3]\text{Cl}$ complex (2.238(3) Å), the bond lengths Pd-P of the PTA ligands *trans* to each other, is much shorter at 2.313(1) Å and 2.312(1) Å *versus* 2.330(2) Å and 2.338(2) Å. The five coordinated complex, $[\text{PtI}_2(\text{PTA})_3]$, have a trigonal bipyramidal geometry whereas the $[\text{PtCl}(\text{PTA})_3]\text{Cl}$ is square planar.

Both the complexes investigated structurally in this study and as confirmed to literature have shown interesting characteristics of the PTA ligand. For example, i) the small cone angle, ii) the relative electron density manipulation by protonation and the consequences thereof on other ligand interactions in the metal complexes, iii) the crystallisation mode and iv) conformation that simple halides/pseudo-halides can actually substitute the PTA ligand.

All the above have significant consequences from the construction of a reaction scheme, as well as the general solution behaviour of these PTA metal systems. These aspects will be discussed and utilised in more detail in the following chapter.

- ¹ D. J. Daigle, *Inorg. Synth.*, 1998, **32**, 40.
- ² D. J. Darensbourg, T. Decuir, N. Stafford, J. Robertson, J. Draper, J. Reibenspies, *Inorg. Chem.*, 1997, **36**, 19.
- ³ D. Drew, J. R. Doyle, *Inorg. Synth.*, 1990, **28**, 346.
- ⁴ M. J. Buerger, *Contemporary Crystallography*, McGraw-Hill, Inc, 1970, 11.
- ⁵ C. Hammond, *The Basics of Crystallography and Diffraction*, Oxford Science Publications, 1997, Chapter 9.
- ⁶ H. S. Lipson, *Crystals and X-rays*, Wykeham Publications (London), Chapter 8,9.
- ⁷ M. F. C. Ladd, R. A. Palmer, *Structure Determination by X-ray Crystallography*, Plenum Press, New York, 1993.
- ⁸ G. M. Sheldrick, SHELXS 97 and SHELXL 97, *Program for Refinement of Crystal Structures*, 1997, University of Göttingen, Germany.
- ⁹ J. J. MacDougall, E. M. Holt, P. de Meester, N. W. Alcock, F. Mathey, J.H. Nelson, *Inorg. Chem.*, 1980, **19**, 1439.
- ¹⁰ D. A. Redfield, J. H. Nelson, *J. Am. Chem. Soc.*, 1974, **96**, 6219.
- ¹¹ G. Beran, G. J. Palenik, *J. Chem. Commun.*, 1970, 1354.
- ¹² D. A. Redfield, J. H. Nelson, R. H. Henry, D. W. Moore, H. B. Jonasson, *J. Am. Chem. Soc.*, 1974, **96**, 6298.
- ¹³ G. J. Palenik, M. Mathew, W. L. Stefen, G. Beran, *J. Am. Chem. Soc.*, 1975, **97**, 1059 and references therein.
- ¹⁴ J. L. Burmeister, F. Basolo, *Inorg. Chem.*, 1964, **3**, 1587.
- ¹⁵ J. J. MacDougall, A. W. Verstuyft, L. W. Cary, J. H. Nelson, *Inorg. Chem.*, 1980, **19**, 1036, and references therein.
- ¹⁶ Cambridge Structural Database, Version 5.22, Cambridge Crystallographic Centre, Cambridge, UK, Oct. 2001.
- ¹⁷ A. J. Carty, P. C. Chieh, N. J. Taylor, Y. S. Wong, *J. Chem. Soc., Dalton Trans.*, 1976, 572.
- ¹⁸ G. Beran, A. J. Carty, P. C. Chieh, H. A. Patel, *J. Chem. Soc., Dalton Trans.*, 1973, 488
- ¹⁹ C. A. Tolman, *Chem. Rev.*, 1977, **77**, 313.
- ²⁰ S. Otto, A. Roodt, *Inorg. Chem. Commun.*, 2001, **4**, 49.
- ²¹ E. C. Alyea, K. J. Fisher, S. Foo, B. Philip, *Polyhedron*, 1993, **12**, 489.
- ²² A. Meijj, S. Otto, A. Roodt, Unpublished results.
- ²³ S. Otto, A. Roodt, *Acta Cryst.*, 2001, **C57**, 540.

- ²⁴ M. Quiros, J. M. Salas, M. P. Sanchez, A. L. Beauchamp, X. Solans, *Inorg. Chim. Acta*, 1993, **240**, 213.
- ²⁵ D. Kovala-Demertzi, A. Michealides, A. Aubry, *Inorg. Chim. Acta*, 1992, 189.
- ²⁶ T. J. Giordana, W. M. Butler, P. G. Rasmussen, *Inorg. Chem.*, 1978, **17**, 1917.
- ²⁷ L. Tusek-Bozi, I. Matijasic, G. Bocelli, G. Calestani, A. Furlani, V. Scarcia, A. Papaioannou, *J. Chem. Soc., Dalton Trans.*, 1991, 195.
- ²⁸ R. Hage, R. A. G. de Graaff, J. G. Haasnoot, K. Kieler, J. Reedijk, *Acta Cryst.*, 1990, **C46**, 2349.
- ²⁹ M. Sekizaki, *Bull. Chem. Soc. Jpn.*, 1981, **54**, 3861.
- ³⁰ S. Ganguly, J. T. Mague, D. M. Roundhill, *Inorg. Chem.*, 1992, **31**, 3500.
- ³¹ J. Podlahova, J. Loub, J. Jecny, *Acta Cryst.*, 1979, **B35**, 328.
- ³² B. B. Sembiring, S. B. Colbran, D. C. Craig, *Inorg. Chem.*, 1995, **34**, 761.
- ³³ W. Wilson, J. Fischer, R. Wasylishen, K. Eichele, V. Catalano, J. Frederick, J. H. Nelson, *Inorg. Chem.*, 1996, **35**, 1486.
- ³⁴ K. Koch, Y. Wang, A. Coetzee, *J. Chem. Soc., Dalton Trans.*, 1999, 1013.
- ³⁵ A. K. Singh, C. Amburose, T. Kraemer, J. P. Jasinski, *J. Organomet. Chem.*, 1999, **592**, 240.
- ³⁶ E. van der Voort, A. L. Spek, W. de Graaf, *Acta Cryst.*, 1987, **C43**, 2311.
- ³⁷ H. F. Klein, B. Zettel, U. Florke, H. J. Haupt, *Chem. Ber.*, 1992, **125**, 9.
- ³⁸ R. J. Cross, A. R. Kennedy, K. W. Muir, *Acta Cryst.*, 1995, **C51**, 208.
- ³⁹ K. Isobe, E. Kai, Y. Nakamura, K. Nishimoto, T. Miwa, S. Kawaguchi, *J. Am. Chem. Soc.*, 1980, **102**, 2475.
- ⁴⁰ Y. Xie, B. Wu, F. Xue, S. Ng, T. Mak, T. Hor, *Organomet.*, 1998, **17**, 3988.
- ⁴¹ Y. Ito, E. Ihara, M. Murakami, *J. Am. Chem. Soc.*, 1990, **112**, 6447.
- ⁴² J. P. Flemming, M. C. Pilon, O. Borbulevitch, M. Antipin, V. Grushin, *Inorg. Chim. Acta*, 1998, **280**, 87.
- ⁴³ X. Bei, T. Uno, J. Norris, H. Turner, W. Weinberg, A. Guram, J. Petersen, *Organomet.*, 1999, **18**, 1840.
- ⁴⁴ K. Osakada, Y. Ozawa, A. Yamamoto, *J. Chem. Soc., Dalton Trans.*, 1991, 759.
- ⁴⁵ A. Mentès, R. Kemmit, J. Fawcett, D. Russel, *J. Organomet. Chem.*, 1997, **528**, 59.
- ⁴⁶ D. J. Darensbourg, T. J. Decuir, N. W. Stafford, J. B. Robertson, J. D. Draper, J. H. Reibenspies, A. Kathó, F. Joó, *Inorg. Chem.*, 1997, **36**, 4218.
- ⁴⁷ E. C. Alyea, G. Ferguson, S. Kannan, *Chem. Commun.*, 1998, 345.

- ⁴⁸ S. Otto, A. Roodt, W. Purcell, *Inorg. Chem. Commun.*, 1998, 415.
- ⁴⁹ Z. Assefa, B. G. McBurnett, R. J. Staples, J. P. Fackler, *Acta Cryst.*, 1995, **C51**, 1742.
- ⁵⁰ D. Darensbourg, J. B. Robertson, D. L. Larkins, J. H. Reibenspies, *Inorg. Chem.*, 1999, **38**, 2473.
- ⁵¹ M. M. Muir, J. A. Muir, E. C. Alyea, K. J. Fisher, *J. Cryst. Spectr. Res.*, 1993, **23**, 745.
- ⁵² Z. Sam, S. Otto, A. Roodt, Unpublished results.
- ⁵³ S. Otto, A. Roodt, *Inorg. Chem. Commun.*, 2001, **4**, 49.
- ⁵⁴ F. Cotton, G. Wilkinson, *Advanced Inorganic Chemistry*, 5th Edition, John Wiley and Sons Inc, 1988, p. 1395.
- ⁵⁵ Reference 54: Chapter 29.

4 Solution Behaviour and Kinetics Studies

4.1 Introduction

In the previous chapter the complexes studied in this work were synthesized and characterized. The following will be discussed in this chapter: theoretical overview of reaction kinetics, square planar substitution reactions and NMR kinetics. Thereafter a reaction scheme/mechanism of the complete system investigated will be presented.

4.2 Reaction Kinetics – Theoretical Overview ^{1,2,3}

4.2.1 Introduction

Chemical reactions are processes in which a substance or substances (reactants) are transformed into other substances (products). In some processes the change occurs directly and the complete description of the mechanism of the reaction presents few difficulties. However, complex processes in which the substances undergo a series of stepwise changes, each constituting a reaction in its own right, are much more common. The overall mechanism is then made up of contributions from all such reactions and is far too complex to determine from the knowledge of the reactants and products alone. In these complex cases chemical kinetics can often provide the only feasible approach toward the unravelling of the reaction mechanism.

Chemical kinetics is concerned with the processes involved when a system shifts from one state to another, that is, the mechanism of the reaction and the time in which it takes place. It involves the measurements of rates of reactions, and the aim is to explain these rates in terms of a complete reaction mechanism. Complex mechanisms can be explained by sequences of elementary reactions which combine together to give the overall reaction. Chemical kinetics provides no information on the energetic or stereochemical state of

individual molecules, since a measured rate reflects a statistical average state of the molecules taking part in the reaction.

Reaction kineticists seek to answer some of the following questions:

- (i) why some reactions are fast and others slow;
- (ii) why the rates of some reactions show a temperature dependence and others do not;
- (iii) how can a particular reaction be promoted most efficiently;
- (iv) can the transition state be studied;
- (v) how is the energy liberated in a reaction distributed among products.

4.2.2 Rate and Order of a Reaction

The single most important factor that determines the rate of a reaction is concentration. The rate of a reaction (R) is defined as the change of concentration of one of the reactants or one of the products with any given unit of time, t . The relationship is given in Eq. 4.1:

$$\text{Rate} = R = \frac{-d[\text{reactant}]}{dt} = \frac{d[\text{product}]}{dt} \quad 4.1$$

Since reactants disappear in reactions, their rate expressions are given a negative sign. The amounts of products increase and their rates of change are therefore positive. The rates are written as differentials as they are seldom constant.

The proportionality factor, or constant, k , relating rate to concentration is defined as:

$$\text{Rate} = \text{constant} \times \text{function of concentration}$$

$$R = k \times f(\text{conc})$$

$$k = \text{rate constant of the reaction}$$

Consider the reaction $aA + bB \rightarrow cC + dD$. The function of concentration in the rate law is given in Eq. 4.2:

$$R = k[A]^a[B]^b \quad 4.2$$

$[A]$ and $[B]$ is the concentrations of A and B, at any time t , while a and b is the order of the reaction with respect to the reagents A and B respectively. The overall order of the reaction

is given as $n = a + b$ and the order of the reaction for each reaction compound must be determined experimentally. If $a = 1$, the reaction is first-order, and if $a = 2$ the reaction is second-order in A. If the rate is independent of the concentration of A, $a = 0$, and the reaction is zero-order in A.

For multi-step reactions the slow step, or the rate-determining step, governs the overall rate of the reaction. The molecularity of a reaction is determined by the number of species involved in forming the collision complex during the rate-determining step. The terms uni- and bimolecular refer respectively to reactions with molecularity of one and two.

The half-life ($t_{1/2}$) of a reaction is the time required for one-half of the initial concentration of a given reactant to be consumed. The half-life depends on the order of the reaction and therefore its determination at various initial concentrations can be used to evaluate the order. The relationship between half-life and the respective reaction orders are given in Table 4.1.

Table 4.1 Relationship between the order and half-life of a reaction

Order of reaction	Half-life $t_{1/2}$	Experimental straight line plots
0	$[A]_0/2k$	$[A]$ vs. time
1	$\ln 2/k$	$\ln[A]$ vs. time
2	$1/(k[A]_0)$	$1/[A]$ vs. time
3	$3/(2k[A]_0)^2$	$1/[A]^2$ vs. time
n	$2^{n-1} - 1 / (n-1)k[A]_0^{n-1}$	$1/[A]^{n-1}$ vs. time

Chemical reactions approach completion gradually therefore the end time of the reaction can not be determined precisely. Sometimes it is necessary to determine the final concentrations of the reactants accurately. For all practical considerations the time it takes for a reaction to be completed (that is 99.9 % conversion) is referred to as the infinite time and for first-order reactions it is reached after ten half-lives.

4.2.3 Pseudo-Order Reactions

If the rate of a reaction is dependent on the concentration of various reactants, the complex rate law can be simplified by manipulating the experimental conditions.

A reaction that proceeds to completion in which the concentration of only one of the reactants changes appreciably during the reaction may arise because:

- (i) there is only one reactant – for example in a stereochemical change
- (ii) all the other possible reactants are in much larger (\geq tenfold) concentration
- (iii) the concentration of one of the other reactants may be held constant by buffering, or be constantly replenished, as it would be if it was acting in a catalytic role.

The order of the reaction is then lowered to the order of the reactant with the lowest concentration.

Consider, as shown in Eq. 4.3, a unidirectional reaction, that is a reaction where the reagents are converted irreversibly to the product.



The rate law is given by: Eq. 4.4:

$$R = - \frac{d[A]}{dt} = k_1[A][B] \quad 4.4$$

If B is present in a large excess with respect to A, the rate law simplifies to $R = k_{\text{obs}}[A]$, with $k_{\text{obs}} = k_1[B]$

k_{obs} = observed pseudo-first-order rate constant

k_1 = second-order rate constant

A graph of the observed rate constant (k_{obs}) at different concentrations of B will give a straight line with slope k_1 . The intercept will be equal to zero.

If an equilibrium is present between the reagents and the products, it can be illustrated as in Eq. 4.5:



where, k_1 = rate constant of forward reaction, k_{-1} = rate constant of reverse reaction and K_1 = equilibrium constant. The rate law is given by Eq. 4.6:

$$R = k_1[A][B] - k_{-1}[P]$$

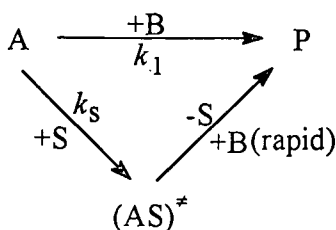
$$\text{with } k_{\text{obs}} = k_1[B] + k_{-1} \quad 4.6$$

$$\text{and } K_1 = \frac{k_1}{k_{-1}} = \frac{\text{slope}}{\text{intercept}} \quad 4.7$$

A graph of the observed rate constant (k_{obs}) at different concentrations of B will give a straight line with slope k_1 and intercept of k_{-1} see Eq. 4.6.

In the case where two non-reversible parallel reaction routes take place that gives the same product, k_{obs} can be derived from Scheme 4.1.

Scheme 4.1 Two parallel reaction routes



In the k_s route the formation of the transition state, $(AS)^\ddagger$, is rate determining, and the rate law is given by Eq. 4.7:

$$R = k_1[A][B] + k_s[A]$$

$$= (k_1[B] + k_s)[A]$$

$$= k_{\text{obs}}[A] \quad 4.8$$

$$\text{with } k_{\text{obs}} = k_1[B] + k_s$$

The k_s pathway is common in square planar substitution reactions where a contribution to the total reaction is often made by the solvent species 'S'. The rate constant, k_s , also contains the

concentration of the solvent. A graph of the observed rate constant, k_{obs} , at different concentrations of B will give a straight line with slope k_1 and intercept of k_s .

4.2.4 Activation Parameters

The rates of chemical reactions do not only depend on concentration. It is found experimentally that the rate and hence the rate coefficient both depend on the temperature T and this dependence is often very strong. The rate of a chemical reaction may be affected by temperature in several ways, but the most common behaviour is given by the Arrhenius equation, as given in Eq. 4.8:

$$k = Ae^{-E_a/(RT)} \quad 4.9$$

where k = rate constant

A = pre-exponential factor

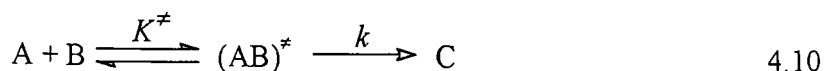
T = absolute temperature

R = universal gas constant

E_a = energy of activation

The empirical expression, which relates the rate constant k to the absolute temperature T (in K), describes the behaviour of a vast number of chemical reactions, particularly over a fairly small temperature range, but in some instances, over as large as 100 K. The pre-exponential factor, A , and the energy of activation, E_a , are often constant over a moderate temperature range for a reaction. A plot of $\log k$ vs. $1/T$ is linear, with slope $-E_a/2.3R$ and intercept $\log A$.

In Eq. 4.9 only the activated complex is considered, that is, the complex in the transition state that is reached by reactants in the initial state as the highest point of the most favourable reaction path on the potential energy surface. This is also the fundamental difference between the activated complex and an intermediate. Although the intermediate only exists for a short time it still corresponds to a minimum on the potential energy profile. The activated complex is considered as a thermodynamic entity in equilibrium with the reactants and is going in the direction of the products. The reaction that is observed is the rate of decomposition of the activated complex to the product. A general bimolecular reaction is given in Eq. 4.9:



The rate of the reaction is

$$R = \frac{k_B T [AB^\ddagger]}{h} = \frac{k_B T K^\ddagger [A][B]}{h} \quad 4.10$$

where k_B = Boltzmann's constant, h = Planck's constant and K^\ddagger = equilibrium constant of the activated state. The experimental second-order rate constant k , at a specific temperature, T , is given by Eq. 4.11:

$$k = \frac{k_B T K^\ddagger}{h} \quad 4.12$$

The free energy of activation, ΔG^\ddagger , can be determined according to normal thermodynamics, as shown in Eq. 4.12:

$$\Delta G^\ddagger = -RT \ln K^\ddagger = \Delta H^\ddagger - T\Delta S^\ddagger \quad 4.13$$

The combination of Eq. 4.12 and Eq. 4.13 leads to Eq. 4.13:

$$k = \frac{k_B T}{h} \exp\left(\frac{-\Delta G^\ddagger}{RT}\right) = \frac{k_B T}{h} \left[\exp\left(\frac{-\Delta H^\ddagger}{RT} + \frac{\Delta S^\ddagger}{R}\right)\right] \quad 4.14$$

where ΔH^\ddagger = enthalpy of activation, ΔS^\ddagger = entropy of activation and T = absolute temperature. After rearrangement of Eq. 4.14 it gives the Eyring relationship in Eq. 4.14:

$$\ln\left(\frac{k}{T}\right) = \ln\left(\frac{k_B}{h}\right) + \left(\frac{\Delta S^\ddagger}{R}\right) - \left(\frac{\Delta H^\ddagger}{RT}\right) \quad 4.15$$

A graph of $\ln(k/T)$ vs. $(1/T)$ gives a linear relationship with the slope $[-\Delta H^\ddagger/R]$ and the intercept $[\ln(k_B/h) + (\Delta S^\ddagger/R)]$.

The enthalpy of activation, ΔH^\ddagger , provides little information regarding the mechanism of the reaction. The entropy of activation, on the other hand, gives more information regarding the specific mechanism that has been followed. Negative values for ΔS^\ddagger show that there is a

decrease in entropy during the formation of the transition state (rate limiting step) and therefore a decrease in disorder if it is associated with bond formation. This is a good indication of an associative mechanism. Positive values for ΔS^\ddagger is usually an indication of bond breaking and is therefore indicative of a dissociative activation.

The effect of pressure, P , on the rate of a reaction is given in Eq. 4.15

$$\ln k = -\left[\frac{\Delta V^\ddagger}{RT}\right]P \quad 4.16$$

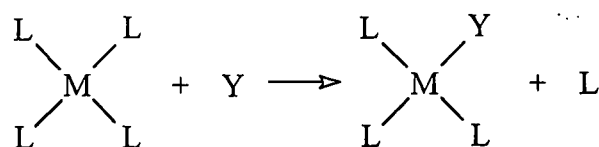
The slope of a graph of $\ln k$ against P will give the volume of activation, ΔV^\ddagger , of the reaction. This is one of the parameters that give the best indication of the specific mechanism that has been followed. Positive values for ΔV^\ddagger are usually an indication of a dissociative mechanism of activation and negative values indicate an associative mechanism.

4.3 Square Planar Substitution Reactions^{4,5,6}

4.3.1 Introduction

A substitution reaction is a reaction wherein ligand-metal bonds are broken and new ones formed in their place. Sometimes all the ligands of a homoleptic compound (all the ligands attached to the central metal atom or ion are identical) are replaced at once by a different ligand, but more often only a fraction of the original ligands are replaced. The substitution of ligands occurs without any change in the coordination number or the oxidation state of the metal.

A general substitution reaction of square planar complexes is given in Eq. 4.16, where M is a metal ion and L and Y any two monodentate ligands:



4.17

Transition metal ions with d^8 electron configurations that form square planar complexes are Rh(I), Ir(I), Pd(II), Pt(II), Ni(II), Cu(II) and Au(III).

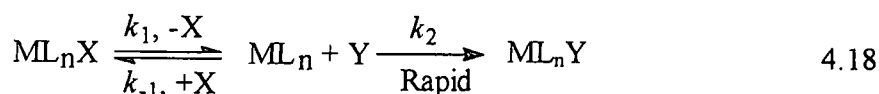
4.3.2 General Reaction Mechanism

The mechanism of a reaction is an indication of the various steps that the reaction consists of. In the industry where maximum yield with time is important, the mechanistic steps are investigated so that conditions that influence the course of the reaction can be optimised. By mechanism is meant all the individual collisional or other elementary processes involving molecules that take place simultaneously or consecutively in producing the observed overall reaction. Also, the mechanism should give information on the geometry, such as interatomic distances and angles, of the molecules.

Three main reaction mechanisms is considered:

The dissociative mechanism

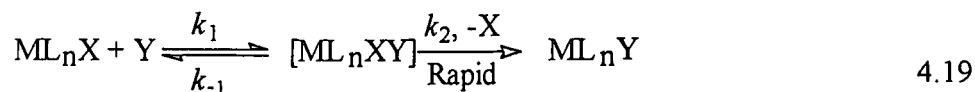
A dissociative mechanism (D) is when the labile ligand is leaving the complex in the first rate-determining step to produce an intermediate with a lowered coordination number. In the second, faster reaction the intermediate and the entering ligand join together to yield the product. The dissociative mechanism is illustrated by Eq. 4.17:



The dissociative mechanism is seldom found in square planar complexes, but is common in octahedral substitution reactions.

The associative mechanism

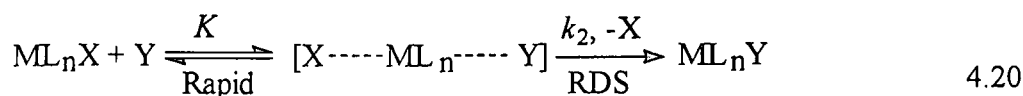
An associative mechanism (A) is when the entering ligand is added in the first rate-determining step to the metal complex to produce an intermediate with a higher coordination number. The second, faster step is the dissociation of the leaving ligand to produce the desired product, and the initial coordination number is restored. It can be illustrated by Eq. 4.18:



The associative mechanism is commonly found with square planar substitution reactions.

The interchange mechanism

An interchange mechanism is where the entering ligand, Y, is found just outside the coordination sphere of the metal complex, ML_nX , and, as the M-X bond starts to break and the X starts to move away, the M-Y bond simultaneously starts to form and Y moves into the coordination sphere. In this case, the entering (Y) and leaving (X) ligands gradually interchange places in the coordination sphere of the metal and no distinct intermediate would be formed (or, therefore, be available to be isolated). It can be illustrated by Eq. 4.19:



RDS = Rate-determining step

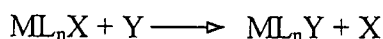
For square planar complexes, wherein that the metal p_z and s orbitals are not primarily involved in metal-ligand σ -bonding in the equatorial plane; they are available for the initiation of the addition of a fifth ligand to the square planar substrate, and an associative mechanism is easily envisioned. The existence of numerous d^8 compounds that are five-coordinate, especially compounds of Fe(0), Ru(0), Os(0), Rh(I), Ir(I), and Ni(II), are proof for the formation of these compounds.

Substitution reactions of square planar complexes should, according to electronic structural considerations, primarily proceed *via* an associative mechanism.

4.3.3 General Rate Law for Square Planar Substitution Reactions

The general substitution reaction in square planar complexes is illustrated in Scheme 4.1.

For the general reaction



The rate law is given by Eq. 4.20:

$$R = \frac{-d[\text{ML}_n\text{X}]}{dt} = (k_s + k_1[\text{Y}])[\text{ML}_n\text{X}] \quad 4.21$$

It is clear from Scheme 4.1 that there are two parallel pathways for the associative mechanism. The nucleophile Y attacks the metal complex and the reaction passes through a five-coordinate transition state and intermediate in the k_1 pathway (direct path). This complex presumably has a trigonal bipyramidal structure. The geometry of the original complex is invariably maintained, that is the ligand *cis* and *trans* to the substituted ligand remain in that arrangement. It implies that the entering and leaving groups as well as the ligand originally *trans* to the leaving group are in the trigonal plane. In the k_s pathway (solvent path) the solvent molecule acts as the entering group, and it also involves the formation of a trigonal bipyramidal transition state.

Electronic considerations show that both the trigonal bipyramidal geometry and square pyramidal geometries are possible for the five-coordinated intermediate that forms during an associative mechanism. There is evidence that the trigonal bipyramidal transition state is electronically more favourable for low spin d^8 complexes that have good acceptor ligands.

4.3.4 Factors Influencing the Reactivity of Square Planar Complexes

The factors influencing the reactivity of Pd(II) and other d^8 metal square planar complexes are the following:

- (i) The nature of the ligand entering the complex;
- (ii) The nature of the leaving ligand;
- (iii) The nature of the central metal ion;
- (iv) The effect of non-labile ligands in the complex
– ligands *trans* to the leaving group

- ligands *cis* to the leaving group;
- (v) Steric influence of non-labile ligands.

Influence of the Entering Ligand

A parameter often used as a measure of the coordination ability of ligands to a metal centre is the nucleophilicity thereof. The nucleophilicity is a concept that refers to the ability of the Lewis base to act as the entering group and influence the reaction rate in a nucleophilic substitution. One of the earliest successful equations relating reactivity and nucleophilicity is the Swain-Scott equation, as given by Eq. 4.21:

$$\log \frac{k_1}{k_s} = sn \quad 4.22$$

where k_1 = rate constant of direct substitution route

k_s = rate constant of solvent dependent route

s = discrimination constant, a number that "measures" the sensitivity of the substrate to various nucleophiles ($s = 1.0$ per definition for CH_3Br)

n = nucleophilic constant, a number characteristic of a given nucleophile ($n = 0.0$ per definition for H_2O)

Knowledge of the s and n parameters for various electrophiles and nucleophiles, can be used to predict reaction rates. Also, values of n for various nucleophiles toward a common electrophile can be examined to understand the factors determining relative nucleophilicities. For the reaction of a given Pt(II) complex with a given nucleophile, k_1 is the rate constant, while k_s is the rate constant for the reaction of the same Pt(II) complex with a specific solvent.

In general, the following can be concluded:

- (i) The nucleophilicity of the halide ions decreases in the order $\text{I}^- > \text{Br}^- > \text{Cl}^- \gg \text{F}^-$;
- (ii) The group VA bases, except amines, are all excellent nucleophiles for Pt(II), but their nucleophilicity declines in the order: phosphines > arsines > stibines \gg amines;
- (iii) Sulphur donors are better nucleophiles than oxygen donors.

The Central Metal

The general tendency for the central metal ions Ni(II), Pd(II) and Pt(II) to undergo substitution is in the order of Ni(II) > Pd(II) >> Pt(II). This order of reactivity is in the same order as the tendency to form five-coordinate complexes. More readily formation of a five-coordinate intermediate complex leads to stabilization of the transition state and to an increase in the reaction rate. This tendency can be explained by the better electronic screening of the metal centre from the top to the bottom of a group in the periodic table. Ni has, in the axial position, only one filled d -orbital ($3d_z^2$), whereas Pt has three filled d -orbitals ($3d_z^2$, $4d_z^2$ and $5d_z^2$). Nucleophilic attack of the entering ligand will decrease from the top to the bottom of the group because of unfavourable electronic interactions.

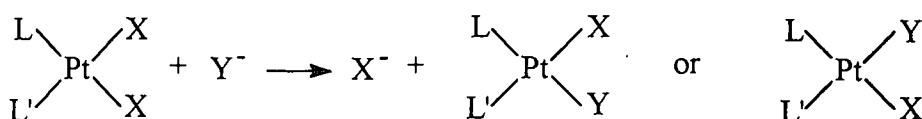
The charge of the metal ion can also give information about the specific mechanism that is been followed during substitution reactions. A larger positive charge on the metal centre will enhance the rate of substitution for an associative (greater electrostatic attraction between the positively charged metal ion and the entering ligand), while the rate will decrease for a dissociative mechanism.

The effect of non-labile ligands in the complex

Both the *cis* and the *trans* ligands have an effect on the rate of substitution. The effect of the *cis* ligand is mainly sterically in nature, whereas the *trans* ligand influence the rate electronically. It occurs *via* the labilization of the leaving group in the ground state, or *via* the electronic stabilization of the transition state.

The ligand trans to the leaving group

Ligand exchange reactions in square planar complexes show distinct preferences for the site *trans* to one ligand rather than another. For example, consider a reaction where two isomeric products are possible.



The *trans* effect is defined as the effect of a coordinated ligand (L') on the rate of substitution of the ligand opposite of L'. It is important to differentiate between the *trans* effect (a kinetic phenomenon) and the *trans* influence (a thermodynamic phenomenon) which involves weakening of the bond *trans* to L' in the ground state.

Trans influence can be attributed to the fact that two *trans* ligands will both depend on the participation of one metal orbital, and the more one ligand pre-occupies this orbital, the weaker will the bond to the other ligand be. Thus, ligands can influence the ground state properties of groups to which they are *trans*, such as the *trans* metal-to-ligand bond distance, the vibrational frequency and force constant, the NMR coupling constant between the metal and the *trans* ligand donor atom (example ^{195}Pt and ^{31}P) and other parameters.

The *trans* influence order⁶, based on extensive data, has been given as: $\sigma\text{-R} \sim \text{H} \geq \text{carbenes} \sim \text{PR}_3 \geq \text{AsR}_3 > \text{SCN}^- > \text{I}^- \sim \text{CH}_3^- \sim \text{CO} \sim \text{RNC} \sim \text{C}=\text{C} > \text{Br}^- > \text{Cl}^- > \text{NH}_3 > \text{OH}^-$.

The approximate ordering of ligands for the *trans* effect⁶ on the other hand is $\text{CO} \sim \text{CN}^- \sim \text{C}=\text{C} > \text{PR}_3 \sim \text{AsR}_3 \sim \text{H}^- > \text{CH}_3^- \sim \text{S}=\text{C}(\text{NH}_2)_2 > \text{C}_6\text{H}_5^- \sim \text{NO}_2^- \sim \text{I}^- \sim \text{SCN}^- > \text{Br}^- \sim \text{Cl}^- > \text{amines} \sim \text{NH}_3 \sim \text{OH}^- \sim \text{H}_2\text{O}$.

The sequences are generally the same, except for certain striking exceptions, such as the positions of CN^- , CO and $\text{C}=\text{C}$. This can be traced to the ability of these, and some other ligands, to produce a *trans* effect by significant participating in π -bonding in the transition state. The π -bonding ligand withdraws electron density from the trigonal plane formed by the entering and leaving ligands must be in the transition state.

Steric influence of non-labile ligands

For large, space occupying ligands in the *trans* or the *cis* positions with respect to the leaving group, the positions where the entering ligand can coordinate (perpendicular to the plane) in an associative mechanism, can be blocked. This can in turn have a significant effect on the rate of square planar substitution reactions. Moreover, steric hindrance from a ligand in the *cis* position has an even larger effect on the rate of the reaction than it does in the *trans* position. These results are in agreement with a trigonal bipyramidal transition state, since such a transition state is significantly hindered by *cis*-interaction. In general, *cis* ligands

have little electronic effect on reaction rates, but can be important sterically because of their proximity to the site of replacement.

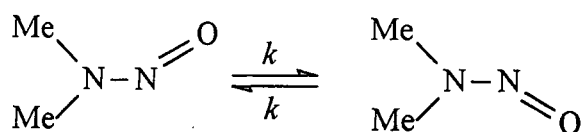
4.3.5 Coordination Number Four: Square Planar vs. Tetrahedral⁷

Square planar geometries were considered in the preceding paragraphs for complexes with coordination number four. This coordination number is important, since it gives either the square planar or tetrahedral geometry. Square planar hybridization (dsp^2) forms when a $d_{x^2-y^2}$ orbital, an s orbital, and p_x and p_y orbitals combine to give a set of equivalent hybrid molecular orbitals with lobes directed to the corners of a square in the xy plane. Tetrahedral hybridization (sd^3) forms when an s orbital and the set d_{xy} , d_{yz} , d_{zx} combine to give a set of tetrahedral orbitals.

The d^8 electron configuration characteristically in general leads to square planar geometry, and is common for complexes of the ions Ni(II), Pd(II), Pt(II), Rh(I), Ir(I) and Au(III). This geometry is also common for complexes of the d^9 ion, Cu(II). The special preference of the d^8 metal ions for the square planar geometry occurs because this requires only one d orbital to be used in forming the four metal-ligand σ bonds (the $d_{x^2-y^2}$). This orbital has lobes pointing towards the non-halide ligands. The remaining four d orbitals are then occupied by the four electron pairs of the metal ion without being repelled by the electron pairs that form the metal-ligand bonds. For the d^9 case, only one electron has to be placed in the high energy $d_{x^2-y^2}$ orbital.

4.4 NMR Kinetic Studies⁸

The simplest case of dynamic equilibrium is when a molecule converts between two conformations of equal energy with identical forward and backward first-order rate constants, k . Dimethylnitrosamine is a good example of such a dynamic equilibrium.



Due to the partial double bond character of the N-N bond the skeleton of the molecule is planar. The two conformations of the molecule have identical energy and interconvert by 180° rotation of the nitroso group around the N-N bond. Two equally intense resonances from the methyl groups *cis* and *trans* to the oxygen is observed from the ^1H spectrum due to the slow internal rotation at low temperatures. At higher temperatures, the nitroso group flips at an appreciable rate and with every rotation the chemical shift of the two sets of methyl protons interchange. The resonance frequency of each group of protons hops between the *cis* and *trans* frequencies. The average time between these jumps is equal to $\tau = 1/k$ (τ = mean life-time). These processes are known as chemical exchange even though the dynamic equilibrium may not necessarily involve the formation or breaking of a bond. Chemical exchange is divided into two groups, namely symmetrical two-site exchange and unsymmetrical exchange.

Symmetrical two-site exchange

Consider the simple two-site exchange $A \rightleftharpoons B$ with equal forward and backward rates. When the exchange is very slow, the NMR spectra shows two equally intense, narrow peaks at the resonance frequencies of the two sites, ν_A and ν_B . The two lines first broaden as the rate constant increases and then shifts towards one another, broadening further until the two lines merge into a single, wide flat-topped resonance. This merging of the two lines happens when the rate constant, k is similar in magnitude to the difference in the resonance frequencies $|\nu_A - \nu_B|$ of the two exchanging sites. A sharp resonance at the mean frequency $\frac{1}{2}(\nu_A + \nu_B)$ is produced due to further increase in the exchange rate. Thus, if the exchange is fast enough, the difference in resonance frequencies of the two sites collapses to zero.

Slow exchange

Slow exchange is the regime in which the separate resonances are exchange-broadened but is still found to be at frequencies ν_A and ν_B . The increase in line width as a result of exchange is given by Eq. 4.22:

$$\Delta\nu = k/\pi = (\pi\tau)^{-1} \quad 4.23$$

where k = observed rate constant and τ = mean life-time. The consequence is that the line width increases with increased exchange rate.

Fast exchange

Fast exchange is the other extreme, in which the two lines have merged to form a single, broadened resonance at the mean resonance frequency. The extra line width due to chemical exchange is given by Eq. 4.23:

$$\Delta\nu = [\pi(\delta\nu)^2]/2k = \frac{1}{2}(\delta\nu)^2\tau \quad 4.24$$

where $\delta\nu = \nu_A - \nu_B$ (difference in frequency of sites) and $\Delta\nu$ = line-broadening.

The single line observed in the fast exchange regime becomes narrower as the rate increases, reflecting the more effective averaging of the two environments A and B. This is in contrast with slow exchange where the separate resonances are broadened. Fast exchange causes the spins to experience an effective local field that is the average of the two sites between which they hop.

Intermediate exchange

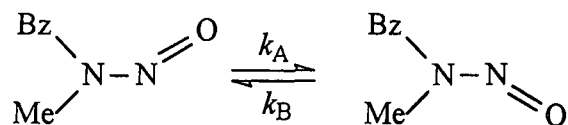
Between the fast and slow exchange there is a so-called intermediate exchange and is here that the separate resonances coalesce. The condition for the two resonances to just merge into a single broad line and the point at which the valley between the peaks is smoothed out is given by Eq. 4.24:

$$k = (\pi\delta\nu)/2^{1/2} \approx 2.2 \delta\nu \quad 4.25$$

A single line is expected when k is larger than the right-hand side of this expression and when k is smaller, the two separate resonances should be seen.

Unsymmetrical two-site exchange

Two-site exchange with equal populations is clearly a special case of the more general situation in which the two sites can have arbitrary concentrations. Benzylmethylnitrosamine is an example of unsymmetrical two-site exchange. The two conformers are no longer degenerate, the populations differ as well as the forward and backward rates.



If the fractional populations of the two sites are p_A and p_B (i.e., $p_A + p_B = 1$) and the two first-order rate constants are k_A and k_B , then at equilibrium $p_A k_A = p_B k_B$ for the reaction is given in Eq. 4.25:



The average lifetimes of the two sites are then $\tau_A = 1/k_A$ and $\tau_B = 1/k_B$.

In the slow exchange regime the lifetime broadenings are given in Eq. 4.26:

$$\begin{aligned}
 \Delta\nu_A &= k_A/\pi = (\pi\tau_A)^{-1} \quad \text{and} \\
 \Delta\nu_B &= k_B/\pi = (\pi\tau_B)^{-1}
 \end{aligned} \tag{4.27}$$

The two resonances are unequally affected because of their different lifetimes (the less concentrated species has the shorter lifetime and the larger broadening). For fast exchange, a single resonance is observed at the weighted average frequency

$$\nu_{AV} = p_A \nu_A + p_B \nu_B \tag{4.28}$$

Eq. 4.27 is not surprising because each nucleus spends a proportion p_A of its time in site A, and p_B in site B, giving an average resonance frequency weighted in favour of the more stable site. The result is that the exchange-averaged resonance moves around as the relative

amounts of A and B are changed. The line-broadening of the unsymmetrical two-exchange site is given by Eq. 4.28:

$$\Delta \nu = (4\pi p_A p_B (\delta \nu)^2) / (k_A + k_B) \quad 4.29$$

These expressions can be reduced to the formulae for symmetrical exchange when $p_A = p_B = 1/2$, and $k_A = k_B = k$.

Spin Relaxation

The relaxation processes allow nuclear spins to return to equilibrium following some disturbance.

In the slow-exchange limit⁹ the transverse relaxation rate ($1/T_2^b$) is given Eq. 4.29 where τ is the mean life-time of a species existing in a specific site and T_{2Q}^b is the quadrupolar relaxation time:

$$1/T_2^b = 1/\tau + 1/T_{2Q}^b \quad 4.30$$

The temperature dependence of τ and its relation to k_{ex} , the pseudo-first-order rate constant for the exchange of a particular molecule, is described from the transition-state theory by the Eq. 4.30:

$$1/\tau = k_{ex} = \frac{k_B T}{h} e^{(\Delta S^*/R - \Delta H^*/RT)} \quad 4.31$$

For the quadrupolar relaxation rate an Arrhenius temperature-dependence can be given, where $(T_{2Q}^b)^{298}$ is the contribution at 298.15 K and E_Q^b is the corresponding activation energy, given in Eq. 4.31:

$$1/T_{2Q}^b = (T_{2Q}^b)^{298} e^{[E_Q^b/R (1/T - 1/298.15)]} \quad 4.32$$

4.5 Experimental Procedures

The preparation and characterization of complexes were described in Chapter 3. All common laboratory reagents were of analytical grade and double-distilled water was used in all the experiments unless stated otherwise. All the reagents were used without further purification.

4.5.1 Multinuclear NMR

Kinetic measurements were done on a 300 MHz Bruker spectrometer operating at 300 MHz, 121.497 MHz and 29.408 MHz for ^1H , ^{31}P and ^{35}Cl respectively. The NMR spectra were recorded in $\text{H}_2\text{O}/\text{D}_2\text{O}$ solutions. ^{31}P spectra were calibrated relative to 85 % H_3PO_4 in a capillary at 0 ppm and the free Cl^- peak in ^{35}Cl NMR is observed at δ -43.783 ppm. The ^{35}Cl NMR experiments were performed in 2, 3, 4 and 5 M chloride, respectively, with four different $[\text{PdCl}(\text{PTA})_3]^+$ concentrations, namely 1.28, 2.57, 3.85 and 5.14 mM, respectively. All experiments were done at 22 °C, unless stated otherwise.

4.5.2 General UV-Vis Measurements

UV-Vis spectra were recorded in the range 200–500 nm using 1.00 cm³ quartz cells with a Varian Cary (model 50 conc) spectrophotometer at 25 °C. The spectrophotometer was equipped with constant temperature cell holders (accurate within 0.1 °C). Experiments for the stability checks, the determination of the equilibrium constants and the influence of chloride concentration and pH were performed using freshly prepared Pd(II) and halide solutions.

4.5.3 Equilibrium Constant Determination

For the equilibrium constant determination all the experiments were studied in aqueous media at 25 °C. Absorbance spectra were recorded for a range of solutions containing the same total metal concentration but with varying amounts of the appropriate halide. Absorbance values at a fixed wavelength were fitted to the appropriate equations (Par. 4.7.1), using the least-squares program Scientist¹⁰ from which the equilibrium constants were

obtained. Final concentrations of approximately 0.05–0.13 mM *cis*-[PdCl₂(PTA)₂] and [PdCl(PTA)₃]Cl were used to obtain appropriate UV-Vis spectra in 1 M NaCl. Halide/pseudo-halide concentrations varied between 0.5 mM and 1.0 M.

4.6 Reaction Scheme/Mechanism and Rate Law

In order to construct a complete mechanistic scheme, the following arguments were utilized as obtained from preliminary measurements, characterization studies and literature:

4.6.1 Characterization of the Starting Complexes

The structures^{11,12,13} of the starting complexes, [PdCl(PTA)₃]Cl (I) and *cis*-[PdCl₂(PTA)₂] (II), have been done and characterized by crystallography (see Par. 2.3.5, 3.1.5 and 3.1.7). The complexes were therefore successfully synthesized according to literature¹¹. The ³¹P spectrum of the [PdCl(PTA)₃]Cl (I) complex consisted of two broad peaks, at δ -26.0 ppm due to [PdCl₂(PTA)₂] and the other at δ -42.7 ppm assigned to [PdCl(PTA)₃]Cl (I), see Fig. 4.9. The ³¹P spectrum of the *cis*-[PdCl₂(PTA)₂] (II) complex showed a peak at δ -20.7 ppm, see Fig. 4.10. ¹H NMR analysis of these complexes were not very successful due to the quadrupolar moment of ¹⁰³Pd and a lack of any characteristic spin system.

4.6.2 Stability of [PdCl(PTA)₃]⁺ (I) in Aqueous Media

In order to study the [PdCl(PTA)₃]⁺ (I) complex, the stability of the complex in aqueous media had to be evaluated. The following UV-Vis spectrophotometric experiments were performed with [PdCl(PTA)₃]⁺ (I):

- (i) When dissolved in water (pH = 6.5) the complex showed significant decomposition over a two hour period, see Fig. 4.1.
- (ii) When the complex was dissolved in aqueous HCl (pH = 3.2), a spectral change immediately occurred (will be discussed in Par. 4.6.6). Slow decomposition over a time of two hours was observed thereafter, see Fig. 4.2.
- (iii) When the complex was dissolved in aqueous NaCl (1.0 M, pH = 6.5), virtually identical spectra were obtained over a time of two hours, see Fig. 4.3, indicating good stability under these conditions.

(iv) When the complex was dissolved in aqueous HClO_4 ($\text{pH} = 5.0$), significant decomposition occurred over a two hour period, see Fig. 4.4.

Figure 4.1 UV-Vis spectral changes of $[\text{PdCl}(\text{PTA})_3]^+$ dissolved in pure H_2O . Scans were recorded at 20 minute intervals over a period of 2 hours; an isobestic point is observed at 361 nm. $[\text{Pd}] = 0.08 \text{ mM}$, $\text{pH} = 6.5$, $T = 25 \text{ }^\circ\text{C}$.

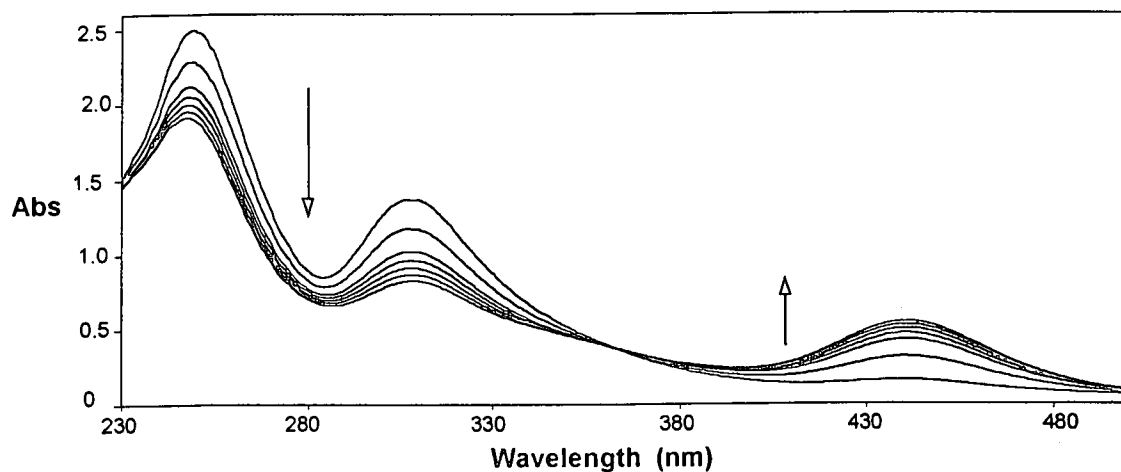


Figure 4.2 UV-Vis spectral changes of $[\text{PdCl}(\text{PTA})_3]^+$ dissolved in aqueous HCl . Scans were recorded at 40 minute intervals over a period of 2 hours. The first scan was performed without the addition of HCl . $[\text{Pd}] = 0.06 \text{ mM}$, $\text{pH} = 3.2$, $T = 25 \text{ }^\circ\text{C}$.

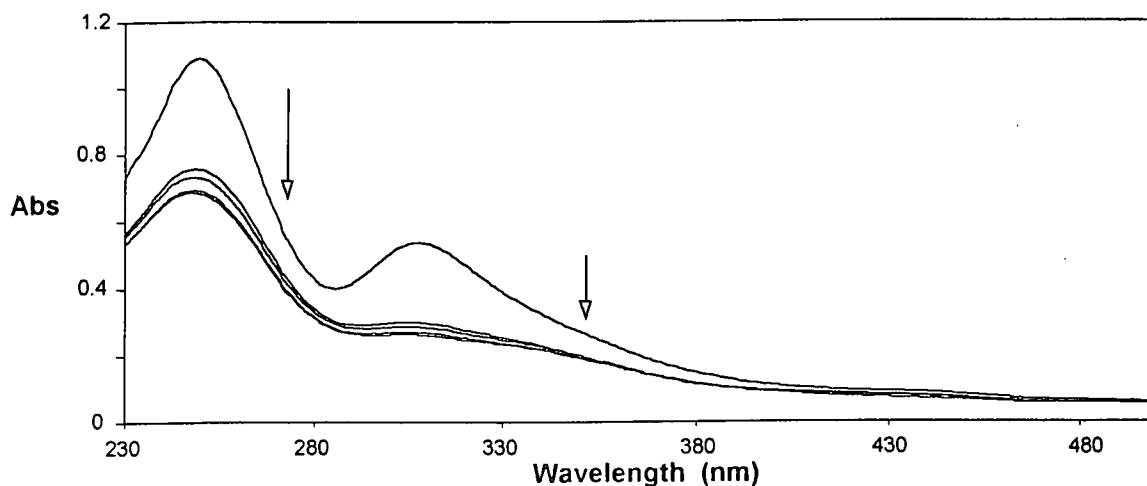


Figure 4.3 UV-Vis spectral changes of $[\text{PdCl}(\text{PTA})_3]^+$ dissolved in aqueous NaCl. Repeated scans in the overlay mode were obtained at 40 minute intervals over a period of 2 hours. $[\text{Pd}] = 0.06 \text{ mM}$, $[\text{Cl}^-] = 1 \text{ M}$, $\text{pH} = 6.5$, $T = 25 \text{ }^\circ\text{C}$.

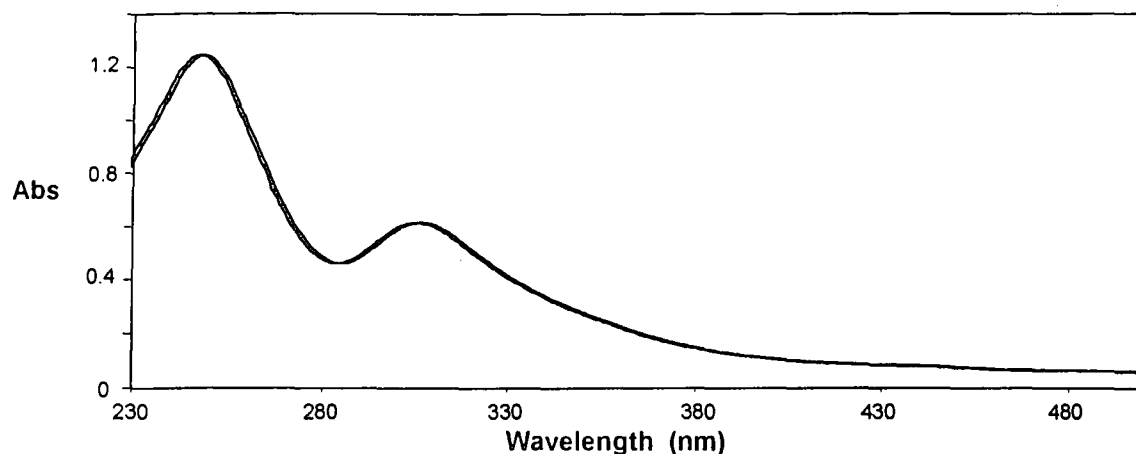
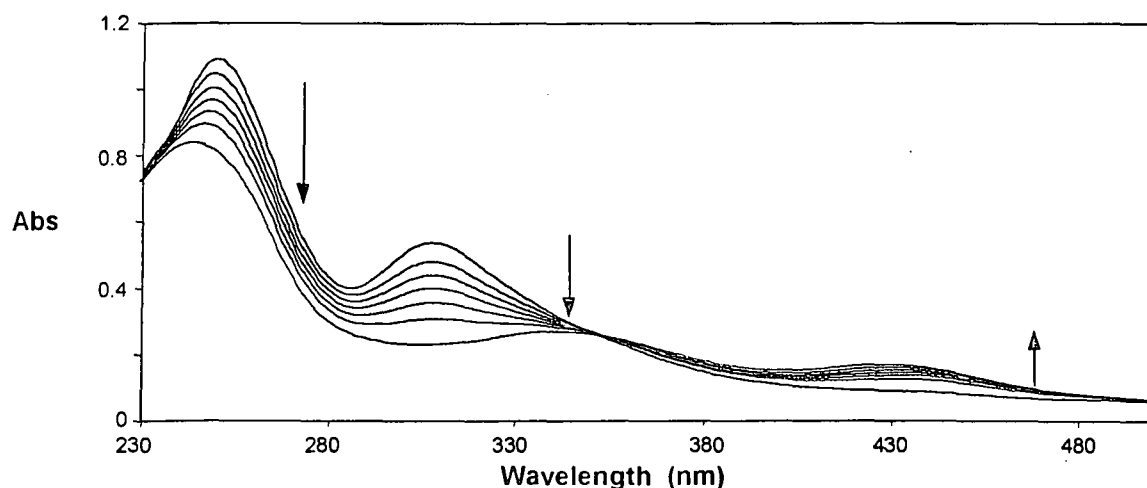
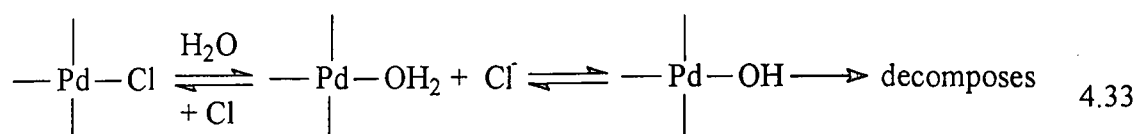


Figure 4.4 UV-Vis spectral changes of $[\text{PdCl}(\text{PTA})_3]^+$ dissolved in aqueous HClO_4 . Scans were recorded at 20 minute intervals over a period of 2 hours; an isobestic point is observed at 351 nm. $[\text{Pd}] = 0.06 \text{ mM}$, $\text{pH} = 5.0$, $T = 25 \text{ }^\circ\text{C}$.



In solution an equilibrium exists between the palladium-chloro species and the palladium-aqua species. The palladium-aqua species can also lose a proton to form the hydroxo-palladium species, which decomposes, as illustrated in Eq. 4.32.



The repeated scans in the overlay mode of a $[\text{PdCl}(\text{PTA})_3]^+$ solution in 1 M NaCl, as shown in Fig. 4.3, were obtained over a period of two hours, indicating good stability under these conditions. Therefore, for the purpose of this study it was assumed that the complex is stable in a excess of Cl^- solution (see Fig. 4.3) and all the UV-Vis experiments, equilibrium constant determination and the influence of pH on the complexes, were done in 1 M NaCl to prevent hydrolysis and consequent decomposition of the $[\text{PdCl}(\text{PTA})_3]^+$ (I) complex.

4.6.3 Stability of *cis*- $[\text{PdCl}_2(\text{PTA})_2]$ (II) in Aqueous Media

In order to study *cis*- $[\text{PdCl}_2(\text{PTA})_2]$ (II), the stability of the complex in aqueous media had to be evaluated. The following UV-Vis spectrophotometric experiments were performed with *cis*- $[\text{PdCl}_2(\text{PTA})_2]$ (II):

- (i) When dissolved only in water (pH = 6.0), the complex showed significant decomposition over a two hour period, see Fig. 4.5.
- (ii) When the complex was dissolved in aqueous HCl (pH = 2.3), a spectral change occurred immediately; however, thereafter repeated spectra were obtained over a period of two hours, see Fig. 4.6.
- (iii) When the complex was dissolved in aqueous NaCl (1.0 M, pH = 6.5), a spectral change immediately occurred and thereafter repeatable spectra were obtained over a time of two hours, see Fig. 4.7.
- (iv) When the complex was dissolved in aqueous HClO_4 (pH = 2.3), significant decomposition over a two hour period occurred, see Fig. 4.8.

Figure 4.5 UV-Vis spectral changes of *cis*- $[\text{PdCl}_2(\text{PTA})_2]$ only dissolved in H_2O . Scans were recorded at 15 minute intervals over a period of 2 hours. $[\text{Pd}] = 0.13 \text{ mM}$, pH = 6.0, $T = 25 \text{ }^\circ\text{C}$.

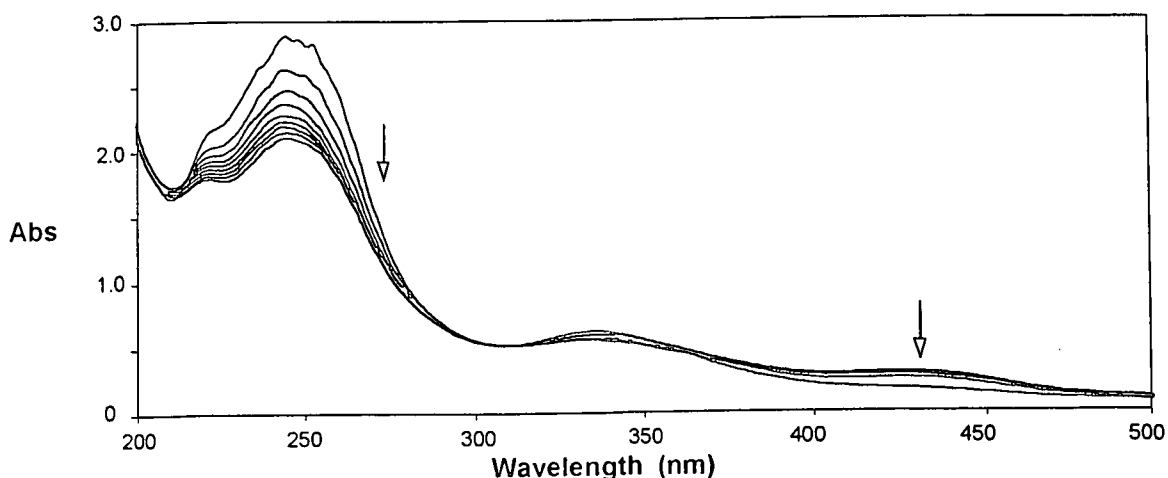


Figure 4.6 UV-Vis spectral changes of *cis*-[PdCl₂(PTA)₂] dissolved in aqueous HCl. Scans were recorded at 15 minute intervals over a period of 2 hours. The first scan was performed without the addition of HCl. [Pd] = 0.13 mM, pH = 2.3, T = 25 °C.

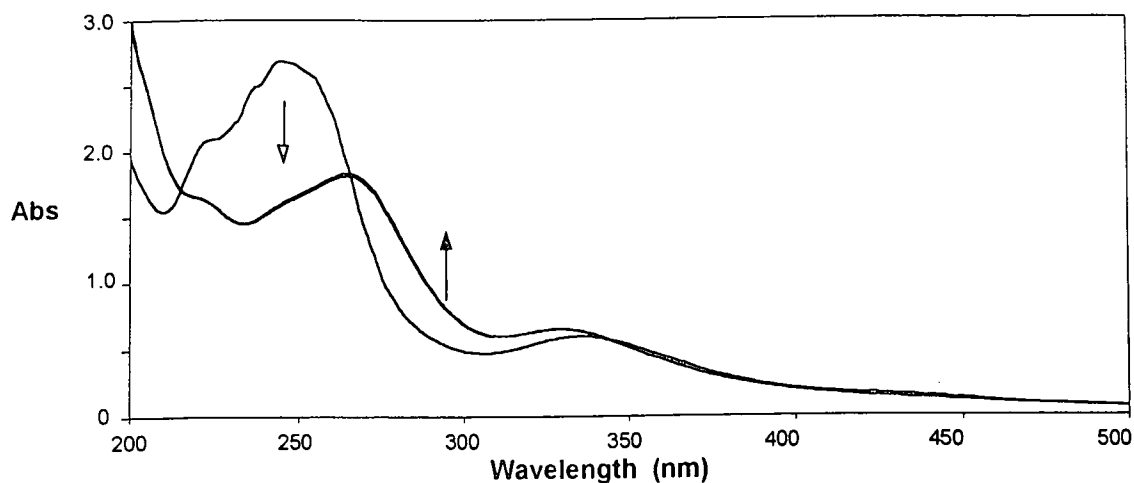


Figure 4.7 UV-Vis spectral changes of *cis*-[PdCl₂(PTA)₂] dissolved in aqueous NaCl. Scans were recorded at 15 minute intervals over a period of 2 hours. The first scan was performed without the addition of NaCl. [Pd] = 0.13 mM, [Cl⁻] = 1M, pH = 6.5, T = 25 °C.

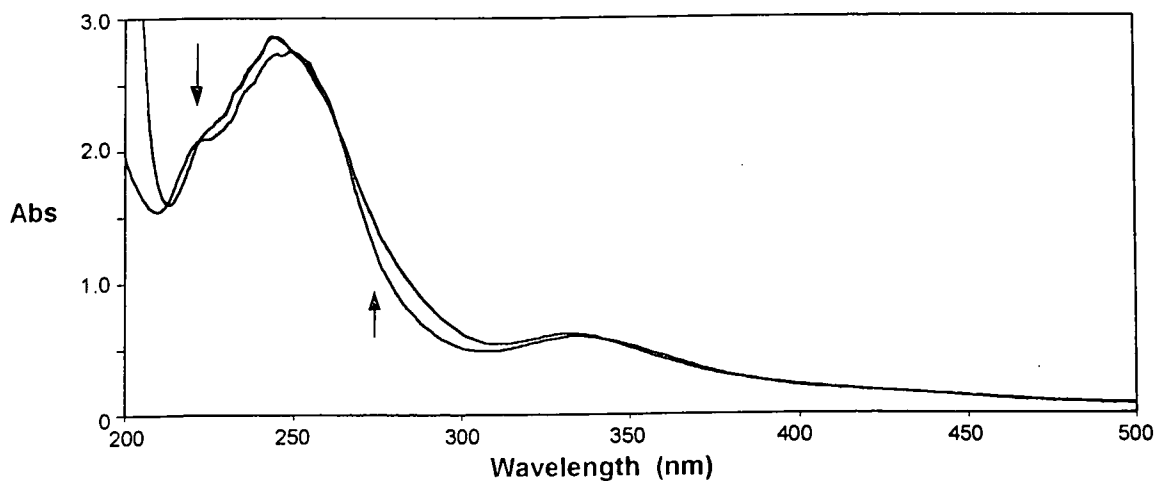
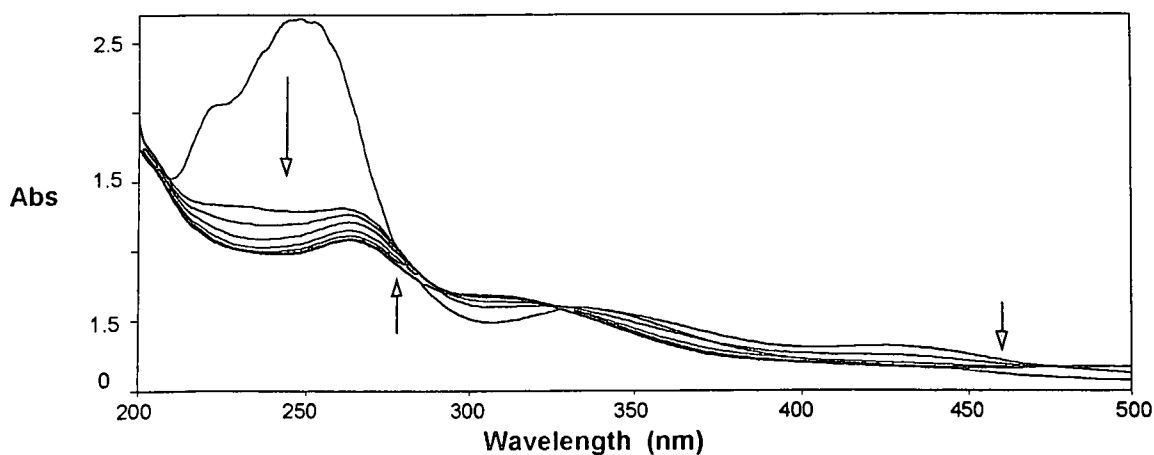


Figure 4.8 UV-Vis spectra of *cis*-[PdCl₂(PTA)₂] dissolved in aqueous HClO₄. Scans were recorded at 15 minute intervals over a period of 2 hours. The first scan was performed without the addition of HClO₄. [Pd] = 0.13 mM, pH = 2.5, T = 25 °C.



In solution an equilibrium exists between the palladium-chloro species and the palladium-aqua species, see Eq. 4.33.

UV-Vis experiments for *cis*-[PdCl₂(PTA)₂] (II) to determine equilibrium constants and the influence of pH, were done in 1 M NaCl to prevent hydrolysis and consequent decomposition. It was thus concluded that whenever an excess of free Cl⁻ ions are present, the hydrolysis is prevented to a large extent.

4.6.4 Multinuclear NMR

¹H NMR

¹H NMR analysis of these complexes were not very informative due to the quadrupolar moment of ¹⁰³Pd and a lack of any characteristic spin system.

³¹P NMR

³¹P NMR analysis of the complexes were reasonable/useful and confirmed the existence of [PdCl(PTA)₃]⁺ (I) and *cis*-[PdCl₂(PTA)₂] (II), see Fig. 4.9 and Fig. 4.10.

Fast exchange of $[\text{PdCl}(\text{PTA})_3]^+$ (I) with PTA and/or halide/pseudo-halide was observed whenever an excess of PTA and/or halide/pseudo-halide was present. In Fig. 4.12 the fast exchange is seen for the reaction of $[\text{PdCl}(\text{PTA})_3]^+$ and HClO_4 , where one PTA ligand is liberated from the $[\text{PdCl}(\text{PTA})_3]^+$ complex and the fast exchange occurs between the $[\text{PdCl}_2(\text{PTA})_2]$ complex and free PTA at δ -44.53 ppm under these conditions. No free PTA peak (δ -94.095 ppm) could be observed – see Fig. 4.11. In Fig. 4.13 and Fig. 4.14 the ^{31}P spectra for the reaction of $[\text{PdCl}(\text{PTA})_3]^+$ with Cl^- and N_3^- , respectively, are given.

Figure 4.9 ^{31}P NMR spectrum of the complex $[\text{PdCl}(\text{PTA})_3]^+$ (I). Two broad peaks are observed at δ -26.0 ppm, due to *cis*- $[\text{PdCl}_2(\text{PTA})_2]$ (II), and δ -42.7 ppm, due to $[\text{PdCl}(\text{PTA})_3]^+$ (I). $[\text{Pd}] = 0.028 \text{ M}$, $\text{pH} = 6.0$, $T = 22 \text{ }^\circ\text{C}$.

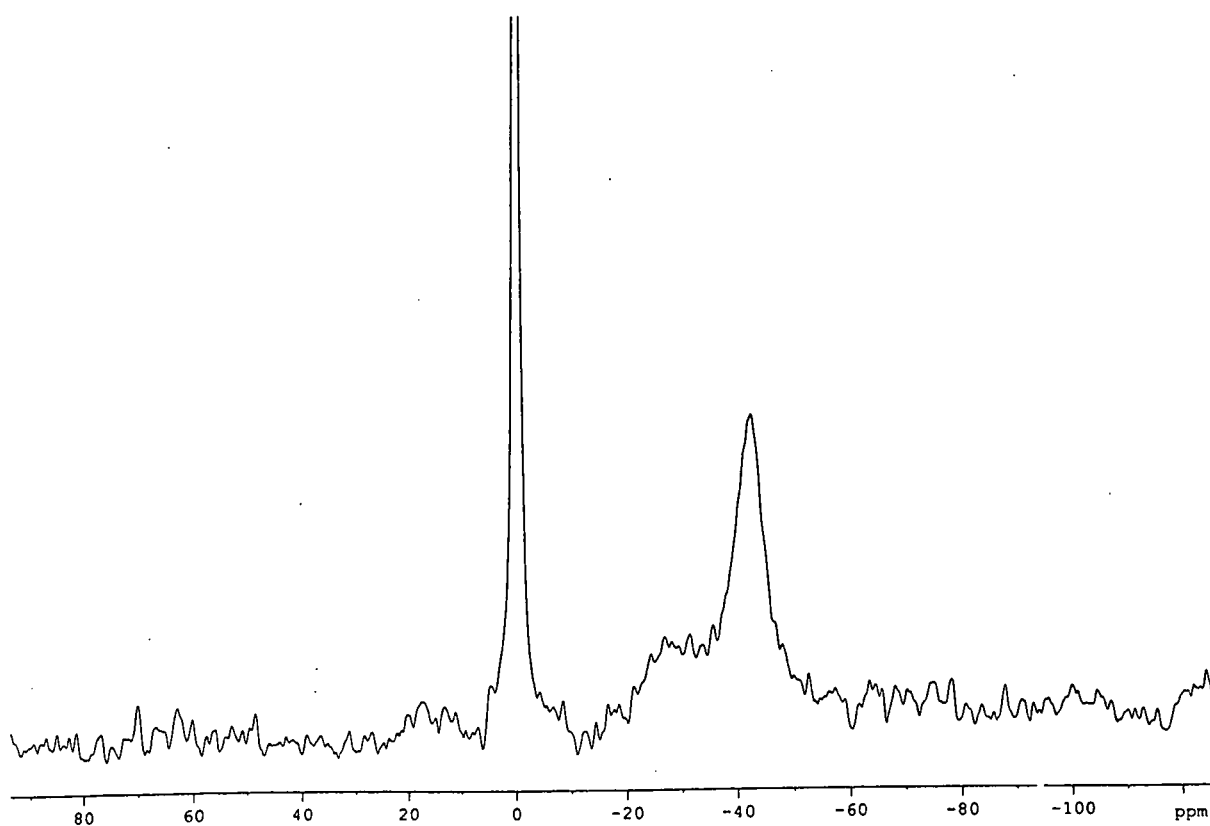


Figure 4.10 ^{31}P NMR spectrum of the complex $\text{cis}[\text{PdCl}_2(\text{PTA})_2]$ (II). A peak is observed at δ -20.7 ppm. $[\text{Pd}] = 0.037 \text{ M}$, $\text{pH} = 6.0$, $T = 22 \text{ }^\circ\text{C}$.

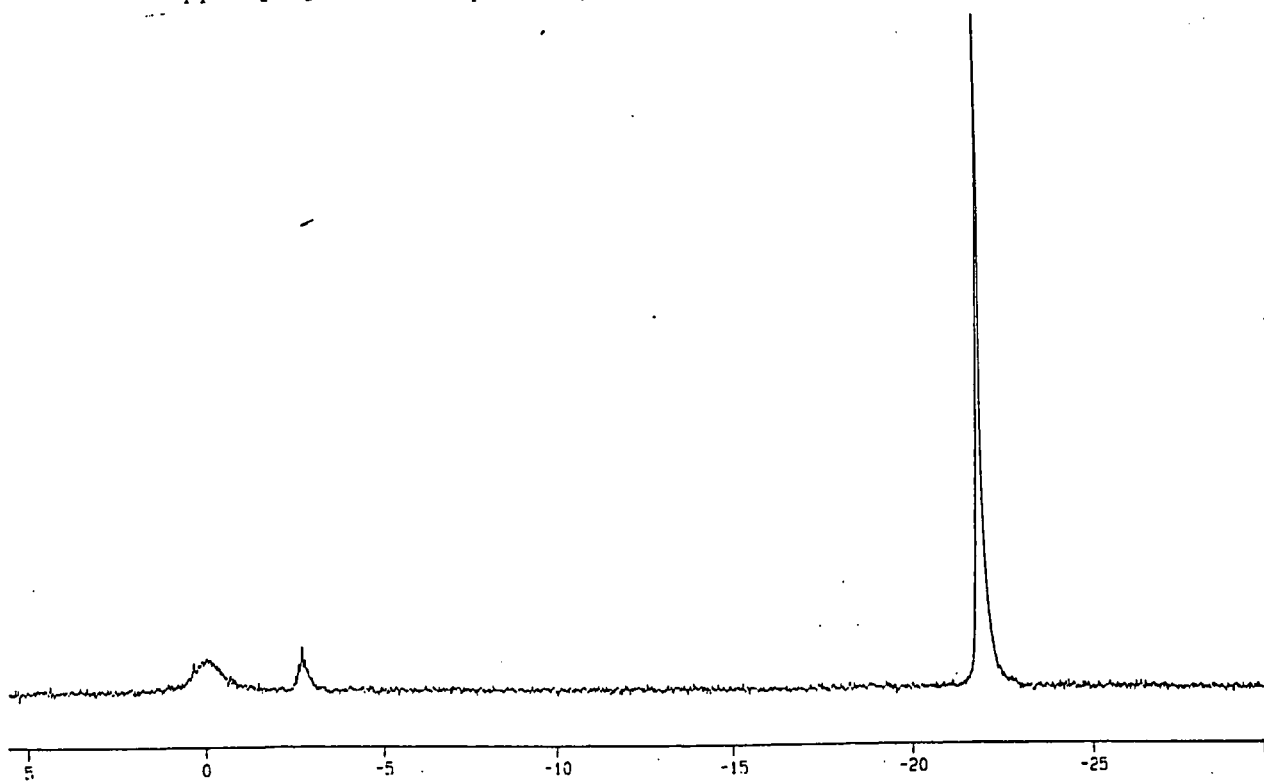


Figure 4.11 ^{31}P NMR spectrum of PTA. A sharp peak is observed at δ -94.1 ppm. $[\text{PTA}] = 0.13 \text{ M}$, $\text{pH} = 6.1$, $T = 22 \text{ }^\circ\text{C}$.

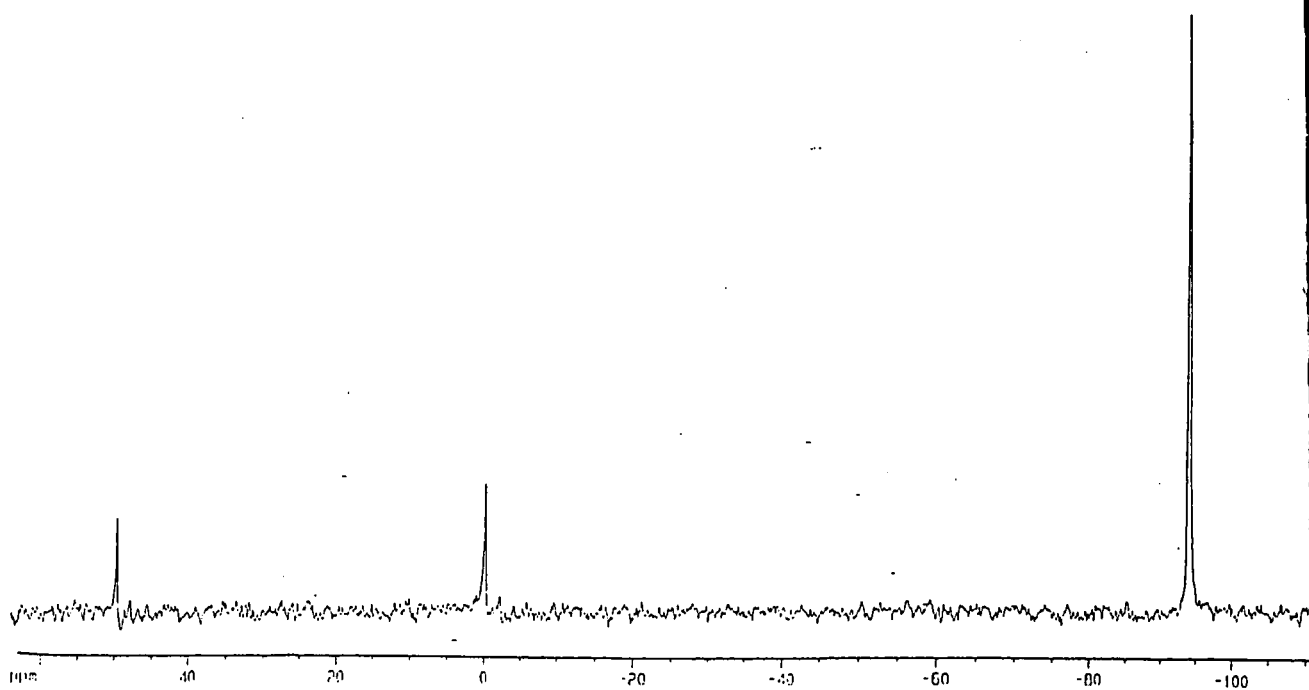


Figure 4.12 ^{31}P NMR spectrum for the reaction between $[\text{PdCl}(\text{PTA})_3]^+$ and HClO_4 . Fast exchange occurs between the liberated PTA and the $[\text{PdCl}_2(\text{PTA})_2]$ complex; a peak is observed at δ -44.5 ppm. $[\text{Pd}] = 0.028 \text{ M}$, $\text{pH} = 6.0$, $T = 22 \text{ }^\circ\text{C}$.

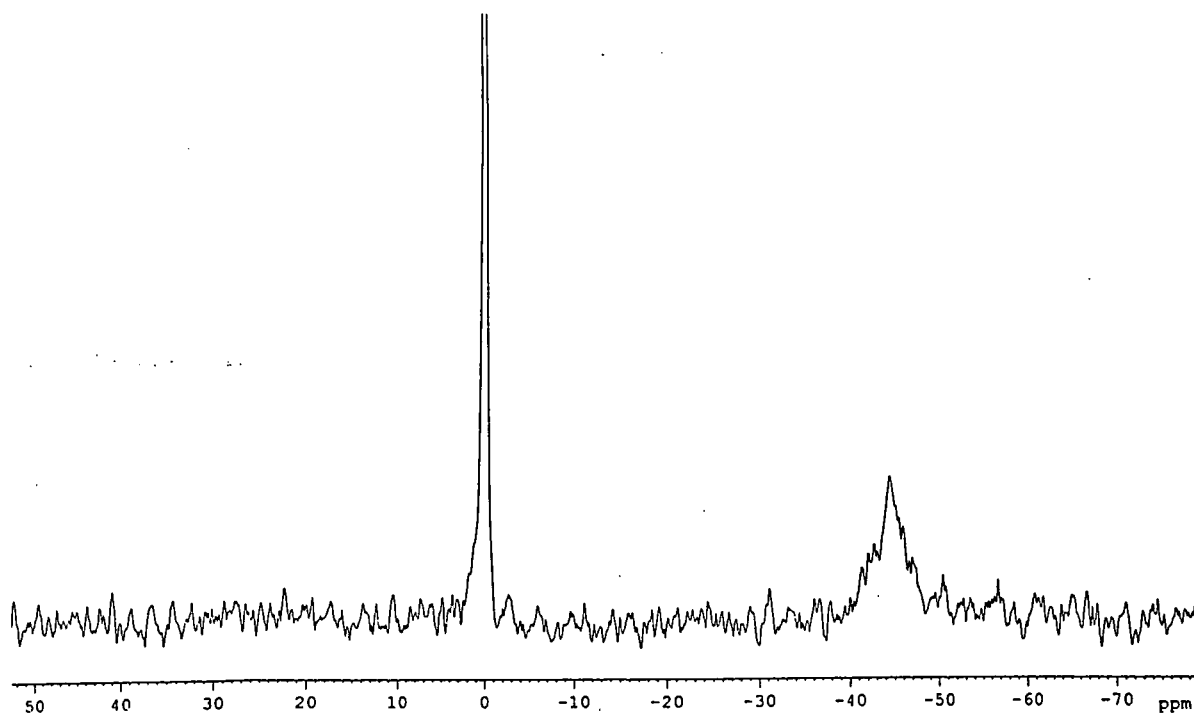


Figure 4.13 ^{31}P NMR spectrum for the fast exchange observed for the reaction of $[\text{PdCl}(\text{PTA})_3]^+$ and an excess of Cl^- (as NaCl). A peak is observed at δ -38.0 ppm. $[\text{Pd}] = 0.028 \text{ M}$, $\text{pH} = 6.0$, $T = 22 \text{ }^\circ\text{C}$.

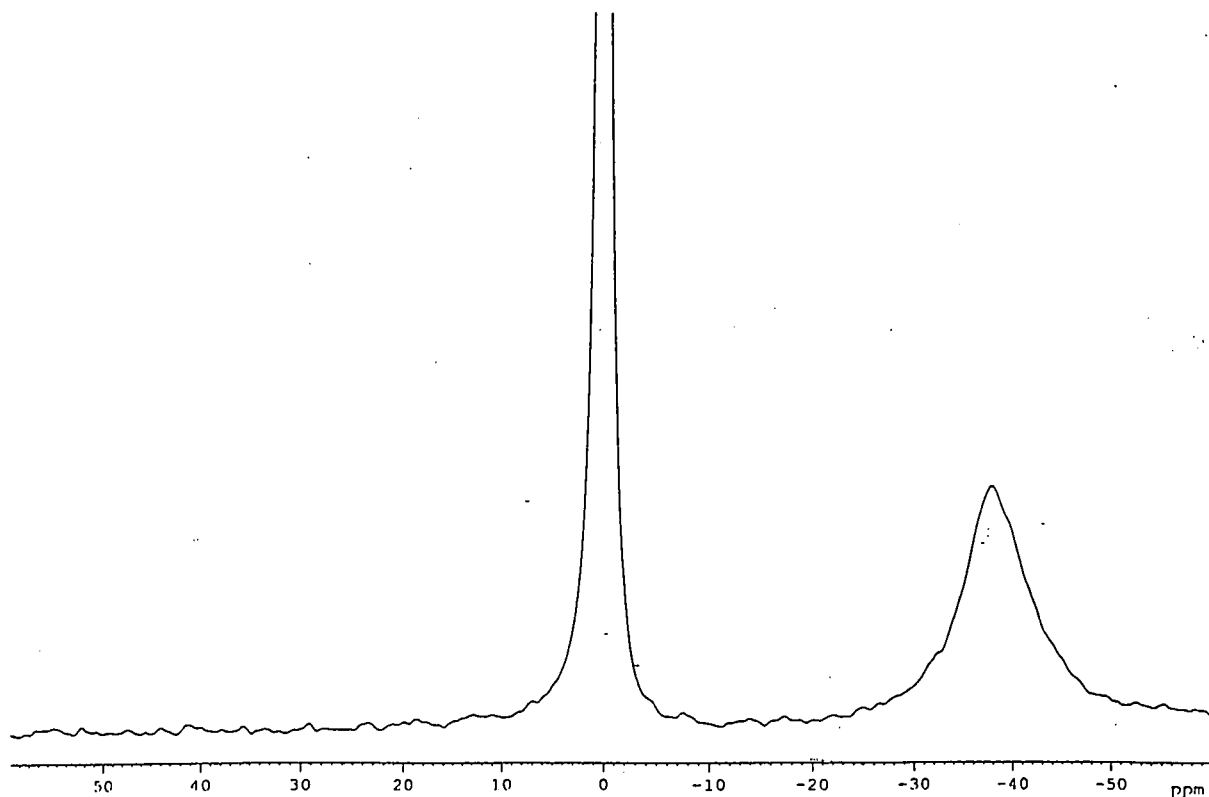
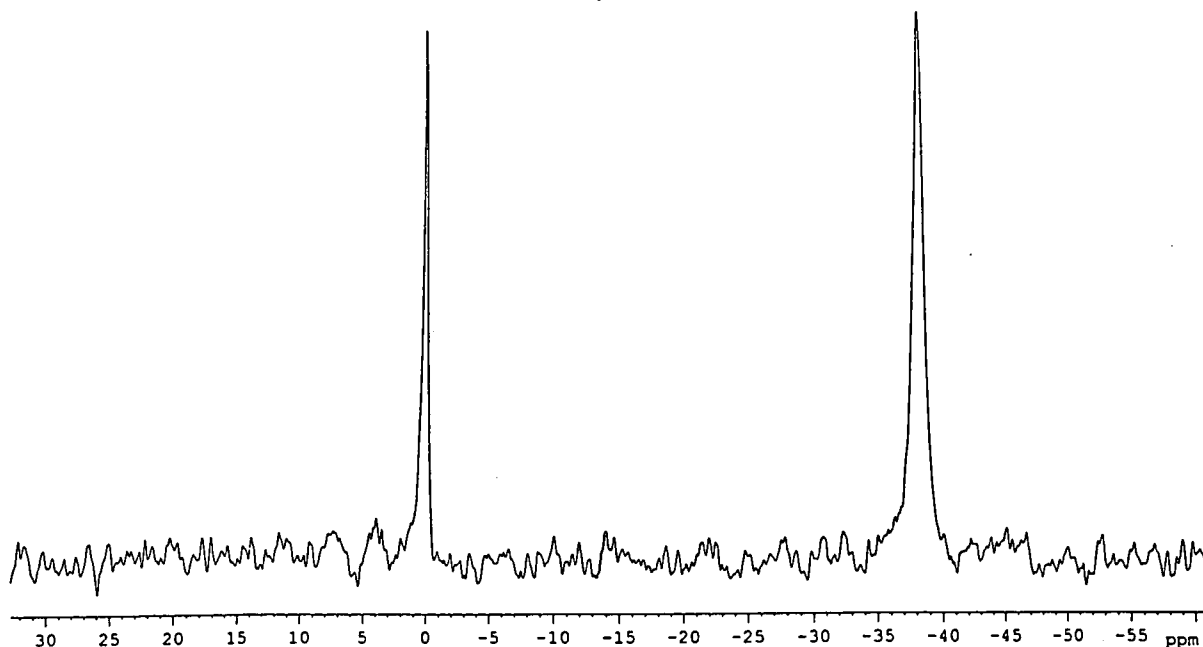


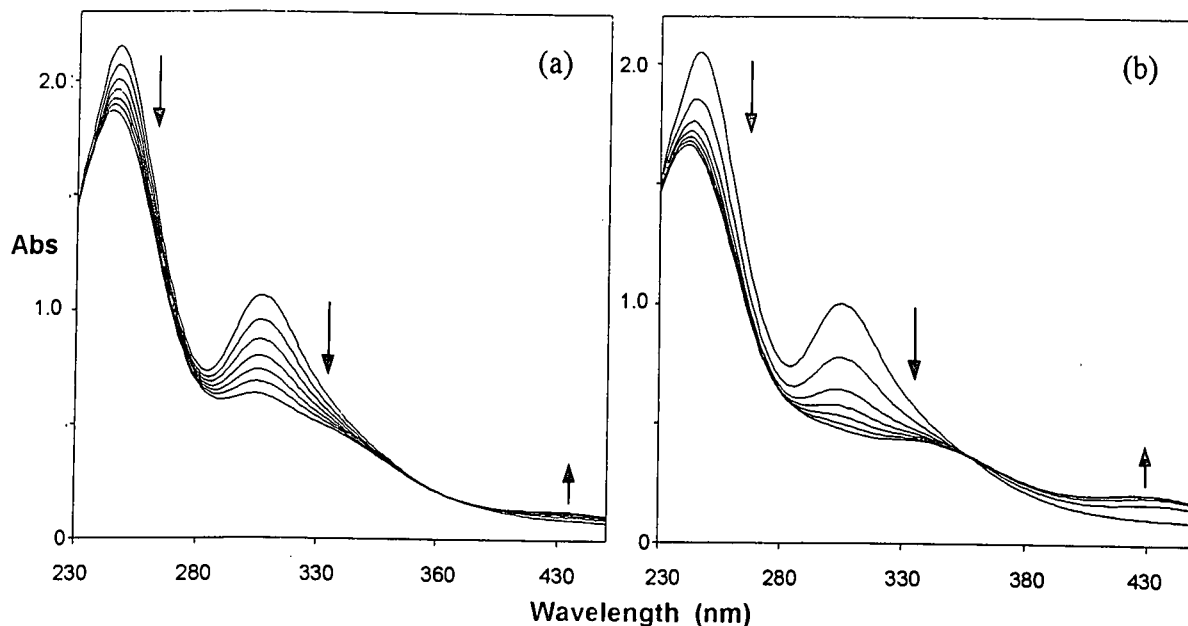
Figure 4.14 ^{31}P NMR spectrum for the fast exchange observed for the reaction of $[\text{PdCl}(\text{PTA})_3]^-$ and an excess of N_3^- (as NaN_3). A peak is observed at δ -38.1 ppm. $[\text{Pd}] = 0.028 \text{ M}$, $\text{pH} = 6.0$, $T = 22 \text{ }^\circ\text{C}$.



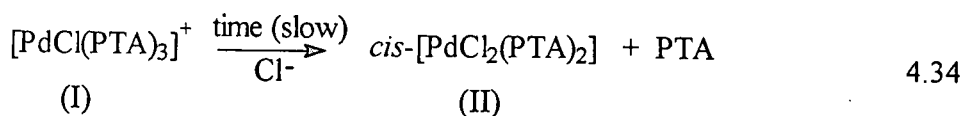
4.6.5 Conversion of $[\text{PdCl}(\text{PTA})_3]^+$ (I) to *cis*- $[\text{PdCl}_2(\text{PTA})_2]$ (II) as a function of chloride

The stability evaluation (see Par. 4.6.2) clearly showed that a chloride dependence exists for the $[\text{PdCl}(\text{PTA})_3]^+$ (I) when the complex was dissolved in water. The extent of the latter was determined by the following experiment: $[\text{PdCl}(\text{PTA})_3]^+$ (I) (0.07 mM) was dissolved in an aqueous solution of 0.2, 0.5, 1.0, 1.5 and 2.0 M NaCl respectively (pH 6.0–6.5). Repeated scans in the overlay mode for the individual solutions were obtained over 50 hours at 30 minute intervals. The spectral changes of the individual solutions of 0.5 and 2 M NaCl are shown in Fig. 4.15 (only selected scans of the individual solutions are shown for clarity).

Figure 4.15 UV-Vis spectral changes for the slow conversion of $[\text{PdCl}(\text{PTA})_3]^+$ (I) (0.07 mM) to $[\text{PdCl}_2(\text{PTA})_2]$ (II) (pH = 6.0-6.7), at 25 °C, in the presence of (a) $[\text{Cl}^-] = 0.5 \text{ M}$ with an 8 hour time interval between each scan and a total time of 48 hours; an isobestic point is observed at 363 nm, and (b) $[\text{Cl}^-] = 2.0 \text{ M}$ with a 6 hour time interval between each scan and a total time of 36 hours; an isobestic point is observed at 356 nm.



From the spectral changes in Fig. 4.15 it is clear that in the presence of different Cl^- concentrations, slow conversion over extended time of $[\text{PdCl}(\text{PTA})_3]^+$ (I) to *cis*- $[\text{PdCl}_2(\text{PTA})_2]$ (II) occurs as illustrated in Eq. 4.33.

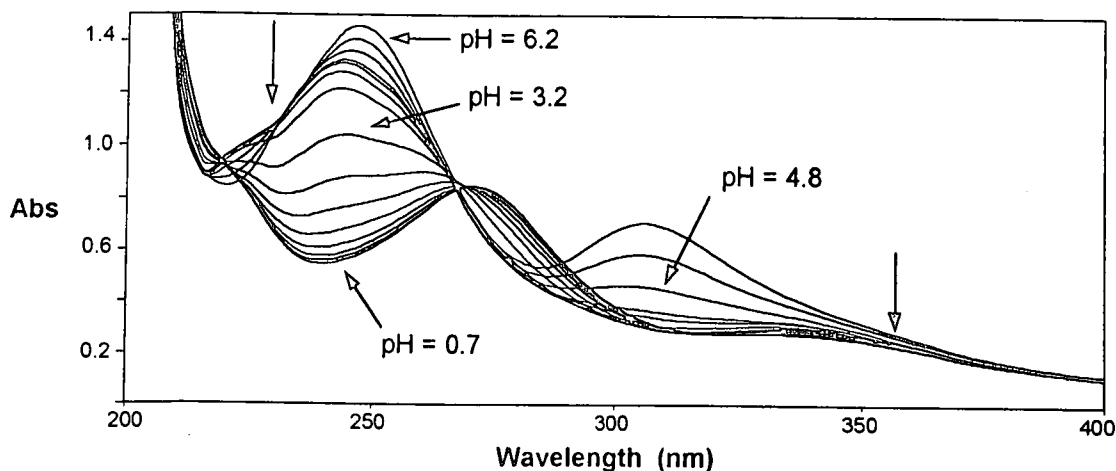


4.6.6 Protonation Behaviour of $[\text{PdCl}(\text{PTA})_3]^+$ (I)

In addition to a chloride dependence, a pH dependence also exists for $[\text{PdCl}(\text{PTA})_3]^+$ (I). Perchloric acid was added to a solution of $[\text{PdCl}(\text{PTA})_3]^+$ (I) (in 1 M NaCl) and after each addition the absorbance spectra were recorded and the pH measured. At a specific pH repeated scans in the overlay mode were obtained and the absorbance changes, once the pH has been adjusted, were negligible. The pH ranged from pH = 6.2 (no perchloric acid added) to pH = 1 (after several additions of perchloric acid). To improve the stability of the complex the $[\text{Cl}^-] = 1 \text{ M}$ and the experiment was performed quickly to eliminate external

effects that can have an influence on the complex. The spectral changes are illustrated in Fig. 4.16.

Figure 4.16 UV-Vis spectral changes to illustrate the protonation behaviour of $[\text{PdCl}(\text{PTA})_3]^+$ (I) in excess of Cl^- . $[\text{Pd}] = 0.06 \text{ mM}$, $[\text{Cl}^-] = 1 \text{ M}$ (as NaCl), $\text{pH} = 6.2\text{--}0.7$ (with HClO_4), $T = 25^\circ\text{C}$.



It is concluded from Fig. 4.16 that there is a rapid decomposition of the complex $[\text{PdCl}(\text{PTA})_3]^+$ (I) to form the *cis*- $[\text{PdCl}_2(\text{PTA})_2]$ (II) complex and thus there is an enhancement of the reaction illustrated in Eq. 4.34.

Furthermore, a protonated PTA palladium species is formed upon further addition of perchloric acid to the solution containing the *cis*- $[\text{PdCl}_2(\text{PTA})_2]$ (II) complex. The conversion of the $[\text{PdCl}(\text{PTA})_3]^+$ (I) complex to the *cis*- $[\text{PdCl}_2(\text{PTA})_2]$ (II) complex is therefore catalyzed by the addition of acid, see Fig 4.15 and Fig 4.16, respectively. A plot of absorbance vs. pH is given in Fig. 4.17, Fig. 4.18 and Fig. 4.19 for the wavelengths 245, 275 and 315 nm, respectively and in Appendix A, Table C1, is given the absorbance values obtained vs. pH. These were fitted to the general equation and the values are reported in Table 4.2.

Figure 4.17 Absorbance change upon variation of pH (with HClO_4) in an aqueous solution of $[\text{PdCl}(\text{PTA})_3]^+$. A value for $\text{p}K_{\text{a}2} = 3.12(2)$ was obtained. $[\text{Pd}] = 0.06 \text{ mM}$, $[\text{Cl}^-] = 1 \text{ M}$, pH varied from 5.5–0.7, $\lambda = 275 \text{ nm}$, $T = 25 \text{ }^\circ\text{C}$.

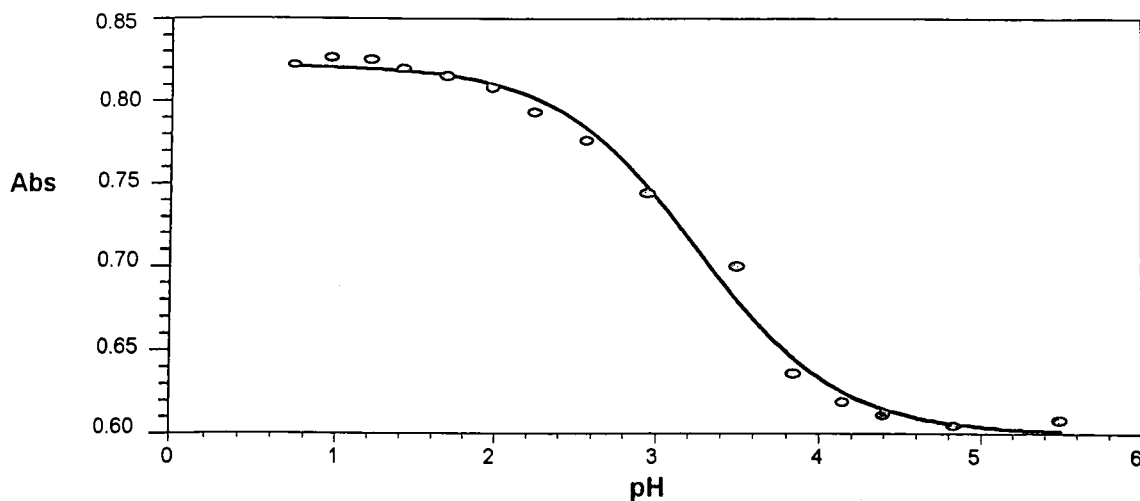


Figure 4.18 Absorbance change upon variation of pH (with HClO_4) in an aqueous solution of $[\text{PdCl}(\text{PTA})_3]^+$. A value for $\text{p}K_{\text{a}2} = 2.72(2)$ was obtained. $[\text{Pd}] = 0.06 \text{ mM}$, $[\text{Cl}^-] = 1 \text{ M}$, pH varied from 6.2–0.7, $\lambda = 245 \text{ nm}$, $T = 25 \text{ }^\circ\text{C}$.

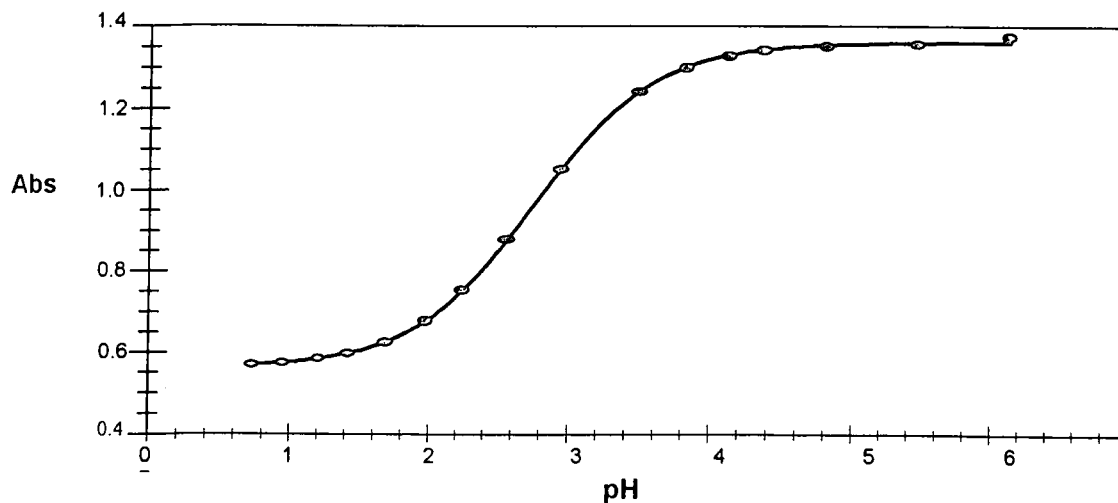
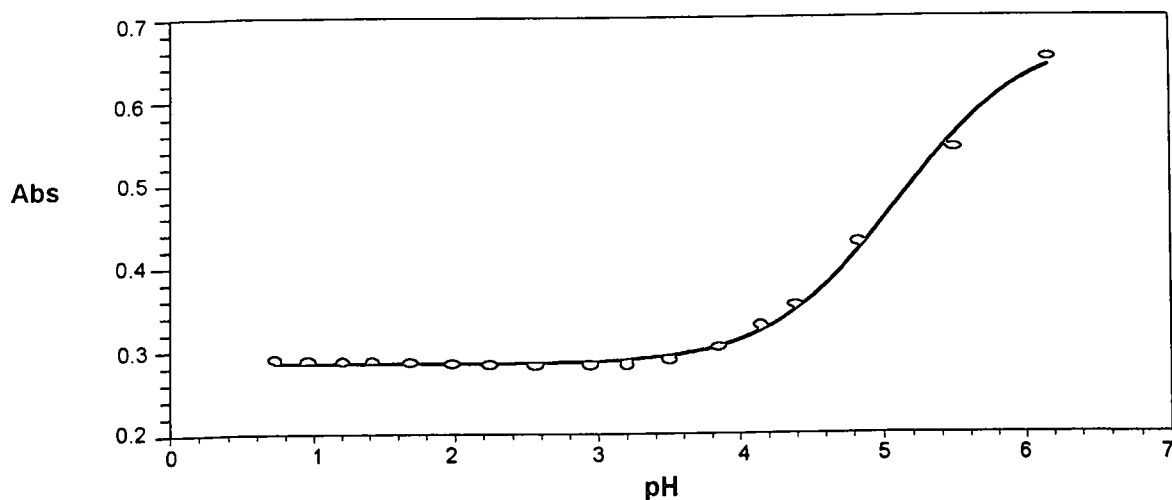


Figure 4.19 Absorbance change upon variation of pH (with HClO₄) in an aqueous solution of [PdCl(PTA)₃]⁺. A value for pK_{a1} = 5.11(4) was obtained. [Pd] = 0.06 mM, [Cl⁻] = 1 M, pH varied from 6.2–0.7, λ = 315 nm, T = 25 °C.



Two pH dependences were thus observed which are attributed to protonations occurring at the [PdCl(PTA)₃]⁺ and [PdCl₂(PTA)₂] complexes, respectively. The first is pK_{a1} = 5.11 and at this stage it assumed to represent a PTA ligand that protonates, and consequently dissociates upon substitution by Cl⁻ from [PdCl(PTA)₃]⁺ as the pH is lowered. The second is pK_{a2} = 2.92 (average pK_a) and it represents the protonation of a PTA ligand of [PdCl₂(PTA)₂]. Isolation¹¹ of the protonated species *cis*-[PtCl₂(PTAH)₂]²⁺ is evidence of protonation occurring at the [PdCl₂(PTA)₂] complex. The reactions from which pK_{a1} and pK_{a2} were calculated are illustrated in Eq. 4.34 and Eq. 4.35, respectively, and the results are summarized in Table 4.2.

Table 4.2 pK_a-values for [PdCl(PTA)₃]⁺ and [PdCl₂(PTA)₂], [Pd] = 0.06 mM, [Cl⁻] = 1 M (as NaCl), T = 25 °C.

pK _a -value	
pK _{a2} ^a	2.72(2) ^c
	3.12(2) ^d
pK _{a1} ^b	5.11(4) ^e

Fitted to the following equation (see Ref. 14):

$$A_{\text{obs}} = \frac{A_{\text{AH}} + A_{\text{A}}(K_{\text{a}}/[\text{H}^+])}{1 + (K_{\text{a}}/[\text{H}^+])}$$

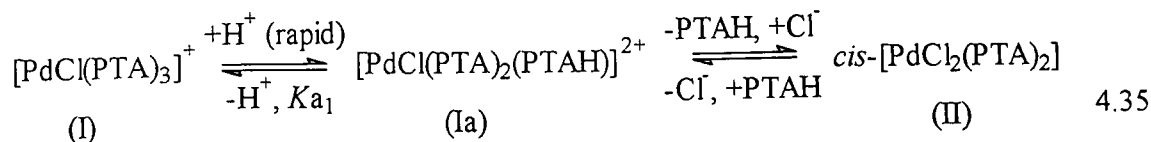
^a Defined by Eq. 4.36

^b Defined by Eq. 4.35

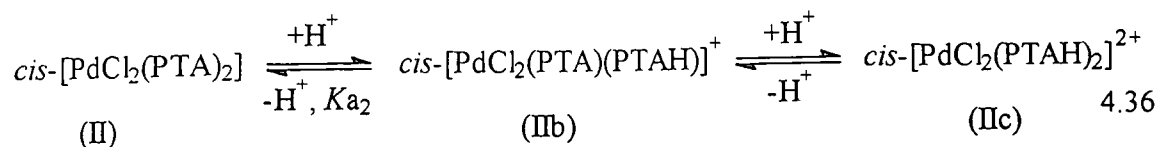
^c At 245 nm

^d At 275 nm

^e At 315 nm



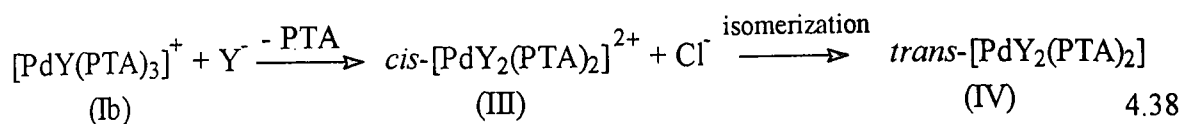
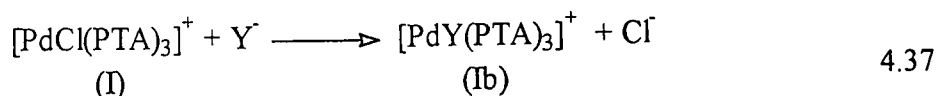
PTAH = protonated PTA



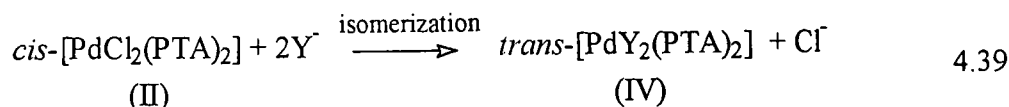
Experiments were also done at a fixed pH values for the different concentrations of NaCl. $[\text{PdCl}(\text{PTA})_3]^+$ (I) were added respectively to 1.0, 2.0, 3.0 and 4.0 M NaCl solutions buffered at pH 5.5 and pH 6.5, respectively. 1 mM NaOAc, 1 mM HOAc and 2 mM MES solutions were prepared and used as the buffer solution. From the spectra obtained of $[\text{PdCl}(\text{PTA})_3]^+$ (I) in buffered solutions of the different NaCl concentrations, it was concluded that the complex is much more stable in the buffered solutions than in the non-buffered ones. Therefore, the pH and protonation of the PTA ligand definitely plays a mayor role in the conversion of $[\text{PdCl}(\text{PTA})_3]^+$ (I) to *cis*- $[\text{PdCl}_2(\text{PTA})_2]$ (II). The buffered solutions of the complex however was not investigated further, since some buffers showed definite tendencies for coordination.

4.6.7 Addition of Halides or Pseudo-halides

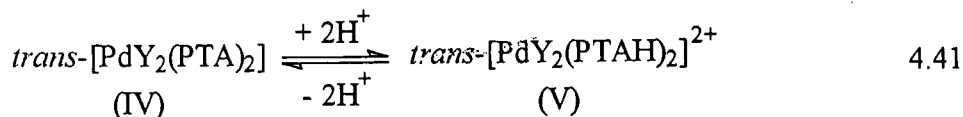
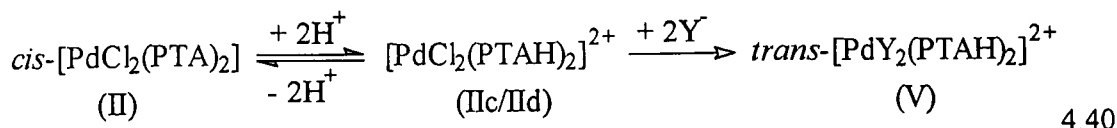
The addition of a halide or pseudo-halide (Y^-) to $[\text{PdCl}(\text{PTA})_3]^+$ (I), in neutral solution (pH = 5.0–6.5), results in the rapid substitution of the chloride in $[\text{PdCl}(\text{PTA})_3]^+$ (I) to form $[\text{PdY}(\text{PTA})_3]^+$ (Ib), Eq. 4.36, which subsequently, upon substitution of a PTA ligand, rapidly converts to *trans*- $[\text{Pd}(\text{PTA})_2\text{Y}_2]$ (IV) (*cis-trans* equilibrium), Eq. 4.37. The *trans*- $[\text{PdBr}_2(\text{PTA})_2]$ characterized in Par. 3.3.3 and *trans*- $[\text{PdI}_2(\text{PTA})_2]$ complexes (also characterized, but not reported in this work) provide evidence for this reasoning.



Upon addition of a halide or pseudo-halide (Y) to *cis*-[PdCl₂(PTA)₂] (II), the chloride ligands are also rapidly substituted to form *trans*-[PdY₂(PTA)₂] (IV), as the final product, see Eq. 4.38. Subsequently, a *cis-trans* isomerization reaction also occurs. A *trans*-[PdCl₂(PTA)₂] complex may even exist, although it has not been isolated to date.



Similarly, in more acidic solution, *cis*-[PdCl₂(PTA)₂] (II) and [PdY₂(PTA)₂] (IV) is further converted to the protonated PTA complex, [PdY₂(PTAH)₂]²⁺ (V), see Eq. 4.39 and Eq. 4.40, respectively. The crystal structures of the *trans*-[Pd(SCN)₂(PTAH)](SCN)₂ in Par. 3.3.2 and the *trans*-[PdI₂(PTAH)₂][PdI₃(PTA)]¹⁵ complexes reported, are evidence for this statement.



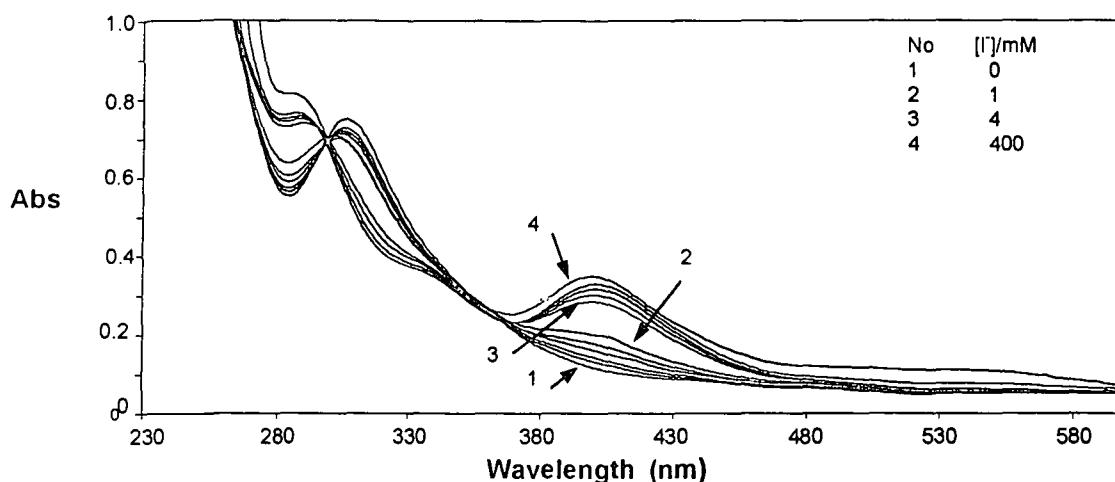
4.6.8 *Cis-Trans* Isomerization of [PdY₂(PTA)₂]

The isolation of the *trans*-[PdY₂(PTA)₂] complexes (IV) implies that isomerization of *cis*-[PdY₂(PTA)₂] to *trans*-[PdY₂(PTA)₂] has to take place, which yielded both *trans*-[PdBr₂(PTA)₂] (see Par. 3.3.3) and *trans*-[PdI₂(PTA)₂]¹⁵ that have been characterized. Furthermore, the protonated analogues of the complexes also exhibit the *trans* configuration and examples hereof are *trans*-[Pd(SCN)₂(PTAH)](SCN)₂ (see Par. 3.3.2) and *trans*-[PdI₂(PTAH)₂][PdI₃(PTA)]¹⁵.

4.6.9 Equilibrium Studies

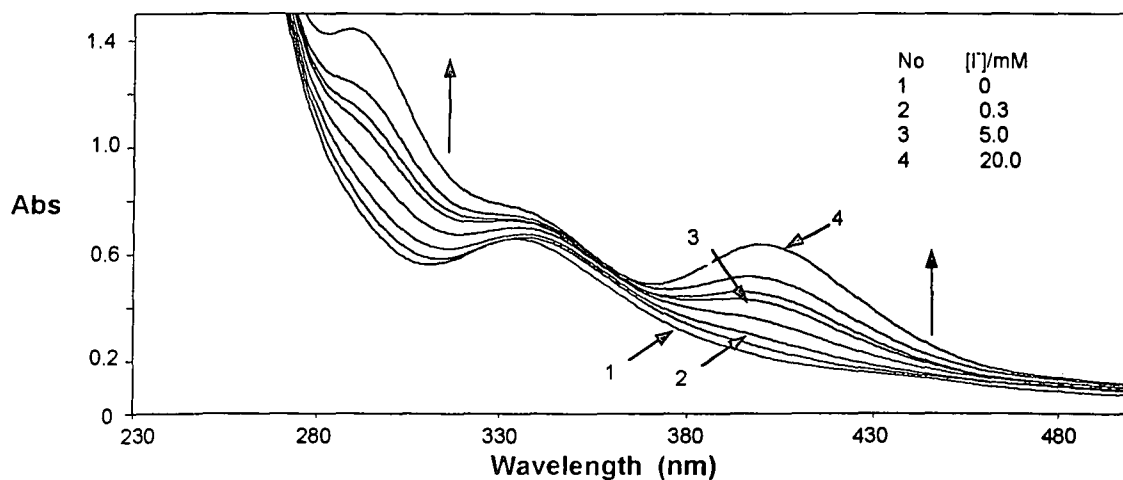
Upon reaction of [PdCl(PTA)₃]⁺ (I), with a halide or pseudo-halide, well-defined equilibria were observed, forming the final products, see Eq. 4.37 and the spectrum of the reaction of [Pd(PTA)₃Cl]⁺ and I⁻, illustrated in Fig. 4.20.

Figure 4.20 UV-Vis spectral changes upon variation of $[I^-]$ (as NaI) of an aqueous solution of $[PdCl(PTA)_3]^+$ in an excess of Cl^- . The spectrum numbers and $[I^-]$ are indicated in the legend. $[Pd] = 0.057 \text{ mM}$, $[Cl^-] = 1 \text{ M}$ (as NaCl), $[I^-] = 0-0.6 \text{ M}$, $pH = 6.2$, $T = 25 \text{ }^\circ\text{C}$.



Similar, well-defined equilibria exists when reacting a halide/pseudo-halide with the complex *cis*- $[PdCl_2(PTA)_2]$ (II), see Eq. 4.39 and Fig. 4.21.

Figure 4.21 UV-Vis spectral changes upon variation of $[I^-]$ (as NaI) of an aqueous solution of $[PdCl_2(PTA)_2]$ in an excess of Cl^- . The spectrum numbers and $[I^-]$ are indicated in the legend. $[Pd] = 0.057 \text{ mM}$, $[Cl^-] = 1 \text{ M}$ (as NaCl), $[I^-] = 0-0.02 \text{ M}$, $pH = 4.0$, $T = 25 \text{ }^\circ\text{C}$.

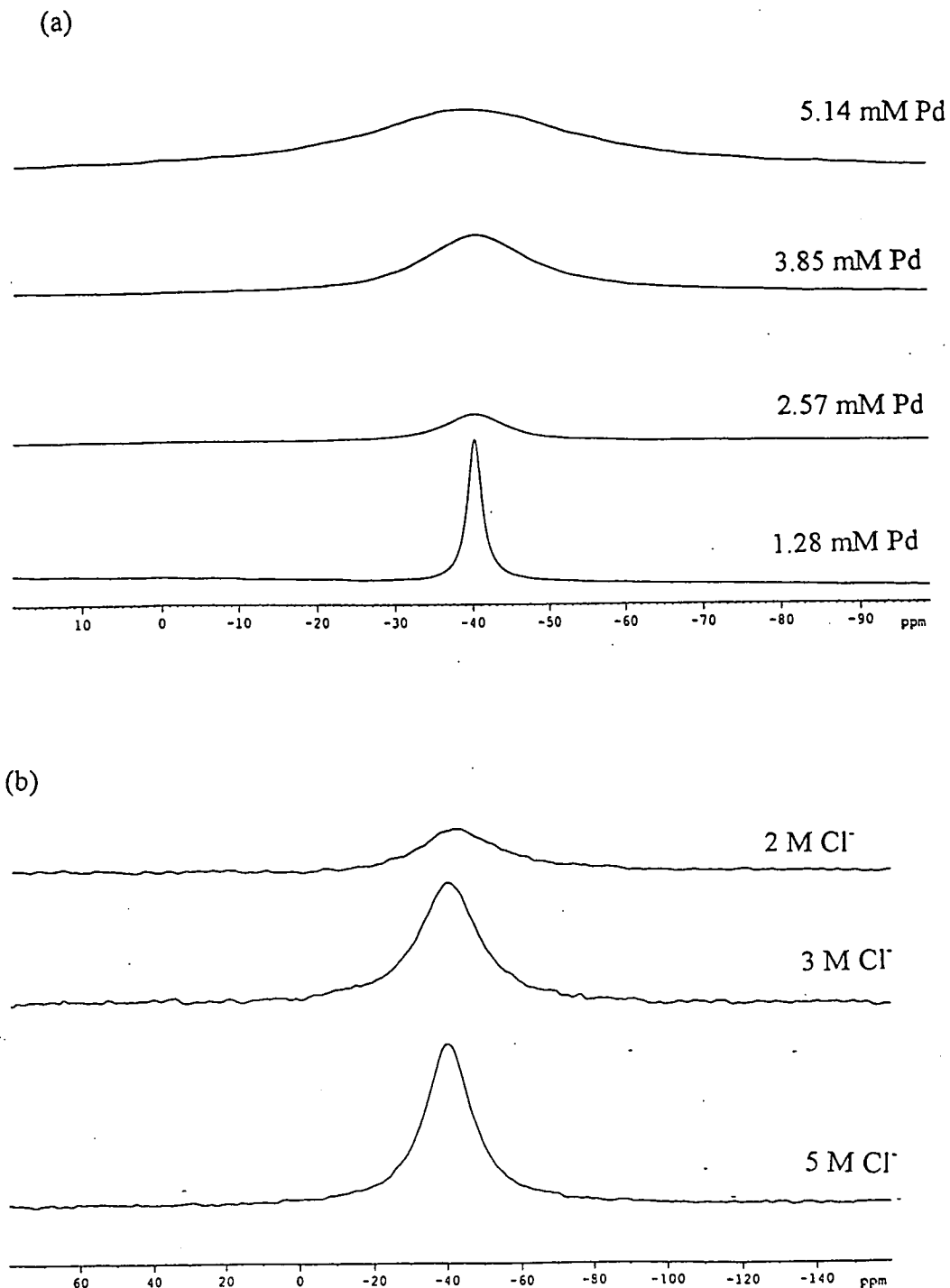


4.6.10 Reactivity of Complexes

All the complexes investigated showed a very high reactivity towards substitution reactions. It was thus not possible to study these complexes by time resolved spectroscopy. However, significant line-broadening on ^{35}Cl NMR was observed, see Fig. 4.22, which enabled the

study of the rapid chloride exchange process. Only the free ^{35}Cl peak was observed and the line-width in the absence of exchange is 18 Hz.

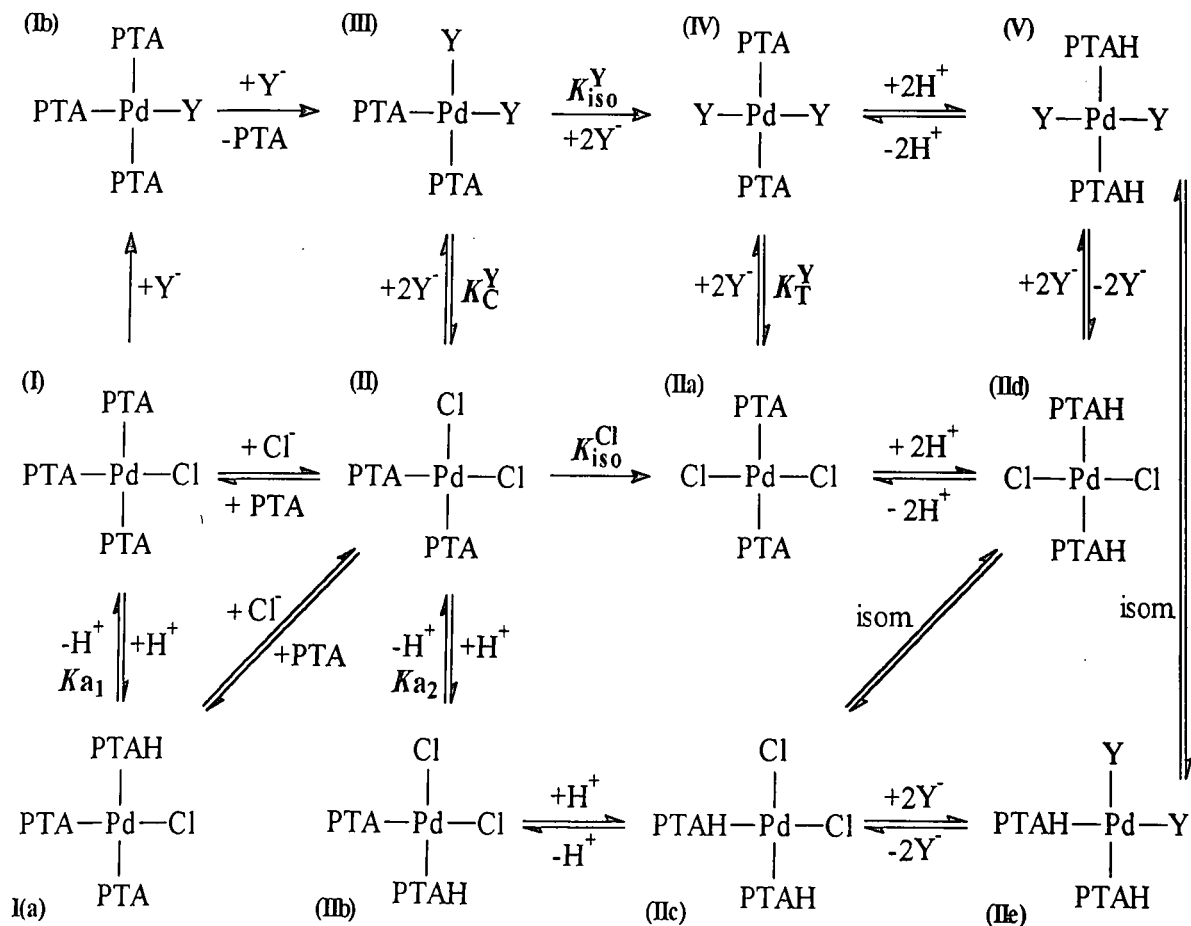
Figure 4.22 ^{35}Cl NMR spectra for the exchange of (a) 1.28, 2.57, 3.85 and 5.14 mM $[\text{PdCl}(\text{PTA})_3]^+$, respectively, in $[\text{Cl}^-] = 4 \text{ M}$ (as NaCl) and $T = 22 \text{ }^\circ\text{C}$, and (b) 1.28 mM $[\text{PdCl}(\text{PTA})_3]^+$ in $[\text{Cl}^-] = 2, 3$ and 5 M (as NaCl), respectively, at $T = 22 \text{ }^\circ\text{C}$, $\text{pH} = 6.5$.



4.6.11 Reaction Scheme

With the above mentioned arguments (Par 4.6.1 – 4.6.10) in mind the following reaction scheme as shown in Scheme 4.2 is postulated.

Scheme 4.2 Postulated reaction scheme*. Note numbering scheme of complexes that corresponds to Eq. 4.34–4.41.

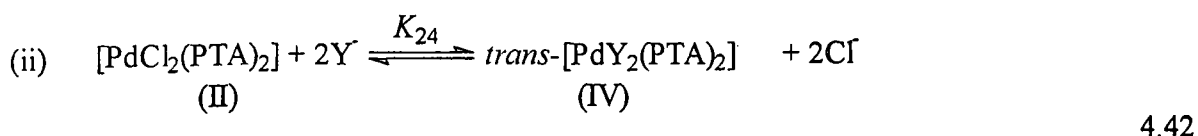
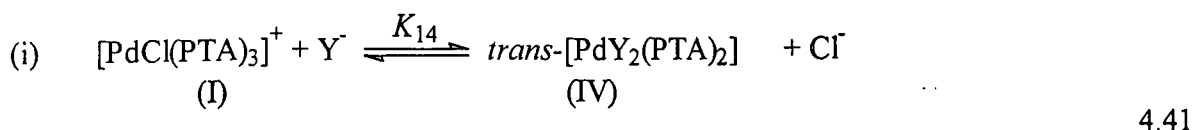


*Aqua species and charges of complex ions omitted for simplicity, PTAH = protonated PTA, isom. = isomerization.

4.7 Results

4.7.1 Equilibrium Studies

Since the *cis-trans* isomerization process could not be quantified at this stage, only the overall equilibria could be studied. Combined equilibrium constants were thus determined for the following reactions:



In Eq. 4.42 and 4.43 K_{14} is the equilibrium constant determined when starting with complex (I) and forming complex (IV), and K_{24} is the equilibrium constant determined when starting with complex (II) and forming complex (IV), see Scheme 4.2, and $\text{Y}^- = \text{halide/pseudo-halide}$, *i.e.*, I^- , Br^- , SCN^- and N_3^- .

Eq. 4.43 is derived from mass balance and Beer's Law as given in Appendix A.

$$\text{Abs} = \frac{(A_B[\text{Cl}^-] + KA_F[\text{Y}^-])}{([\text{Cl}^-] + K[\text{Y}^-])} \quad 4.44$$

where Abs = absorbance measured

A_B = absorbance of reactant

A_F = absorbance of product

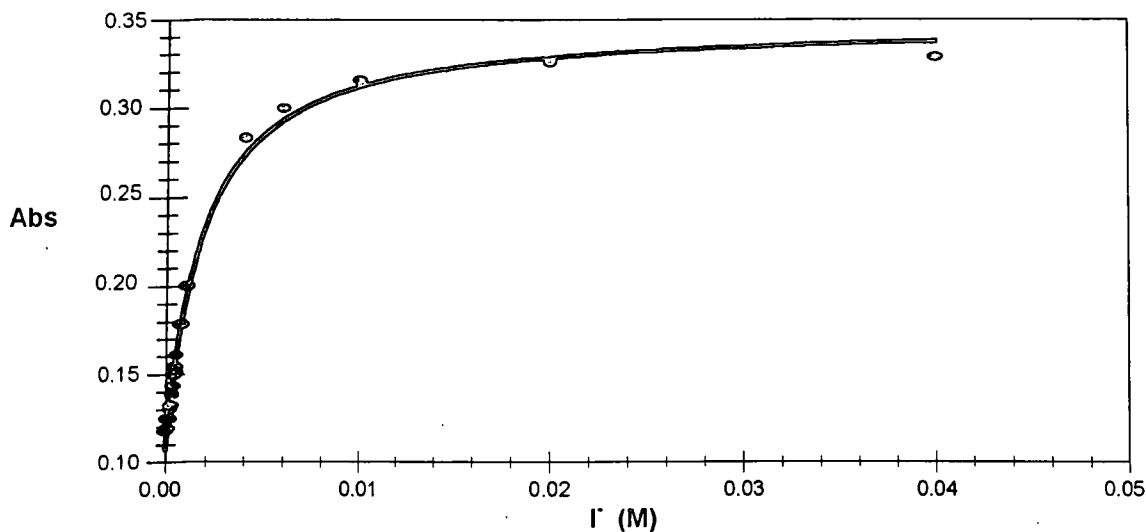
K = equilibrium constant

$[\text{Y}^-]$ = concentration of incoming ligand (halide/pseudo-halide)

$[\text{Cl}^-]$ = concentration of Cl^- – held constant at 1 M (see Par. 4.6.2)

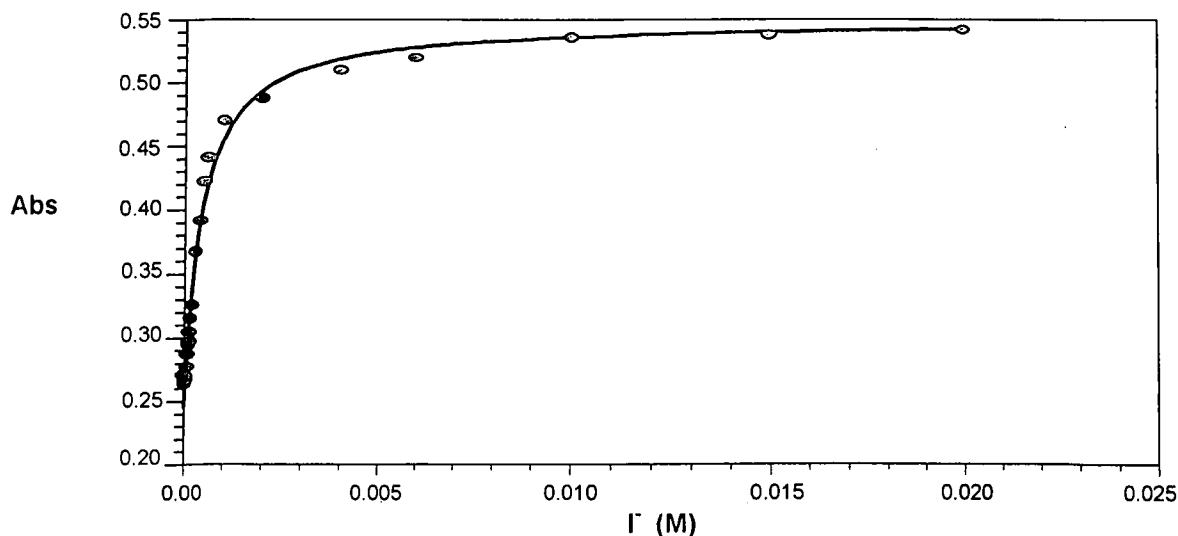
To determine the equilibrium constant for the reactions shown in Eq. 4.42 and Eq. 4.43, data points of absorbance vs. $[Y]$ were fitted to Eq. 4.43, and as an example the reaction of $[\text{PdCl}(\text{PTA})_3]^+$ with I^- is illustrated in Fig. 4.23.

Figure 4.23 Absorbance change upon variation of $[\text{I}^-]$ (as NaI) in an aqueous solution of $[\text{PdCl}(\text{PTA})_3]^+$ in Cl^- . $[\text{Pd}] = 0.062 \text{ mM}$, $[\text{Cl}^-] = 1 \text{ M}$ (as NaCl), $[\text{I}^-] = 0\text{--}0.04 \text{ M}$, $\text{pH} = 6.2$, $\lambda = 400 \text{ nm}$, $T = 25 \text{ }^\circ\text{C}$.



As an example for determining the equilibrium constant for the reaction between *cis*- $[\text{PdCl}_2(\text{PTA})_2]$ and Y^- , the plot of absorbance vs. $[\text{I}^-]$ changes for the reaction of *cis*- $[\text{PdCl}_2(\text{PTA})_2]$ with I^- is illustrated in Fig. 4.24.

Figure 4.24 Absorbance change upon variation of $[\text{I}^-]$ (as NaI) in an aqueous solution of $[\text{PdCl}_2(\text{PTA})_2]$ in Cl^- . $[\text{Pd}] = 0.062 \text{ mM}$, $[\text{Cl}^-] = 1 \text{ M}$ (as NaCl), $[\text{I}^-] = 0\text{--}0.02$, $\text{pH} = 4.0$, $\lambda = 400 \text{ nm}$, $T = 25 \text{ }^\circ\text{C}$.



DISCUSSION

The equilibrium constants determined for the reactions between: i) $[\text{PdCl}(\text{PTA})_3]^+$ and a range of entering ligands Y^- (K_{14}), and ii) *cis*- $[\text{PdCl}_2(\text{PTA})_2]$ and Y^- (K_{24}) are given in Table 4.3 (see also Scheme 4.2). Appendix A, Table C2 and Table C3 reports a complete list of absorbance as a function of ligand concentration for the various ligands used in the determination of the equilibrium constants for the reactions given in Eq. 4.42 and Eq. 4.43, respectively.

Table 4.3 Equilibrium constants determined for the reactions between $[\text{PdCl}(\text{PTA})_3]^+$ and Y^- (K_{14}) (see Eq. 4.42), and $[\text{PdCl}_2(\text{PTA})_2]$ and Y^- (K_{24}) (see Eq. 4.43). $[\text{Cl}^-] = 1 \text{ M}$ (as NaCl), $T = 25 \text{ }^\circ\text{C}$

Y	K_{14}	K_{24}
Br^-	3.0(3)	4.1(3)
N_3^-	-	$6.0(4) \times 10$
SCN^-	$1.9(4) \times 10$	$1.1(6) \times 10^2$
I^-	$5.8(4) \times 10^2$	$3.0(3) \times 10^3$

K_{14} could not be determined for N_3^-

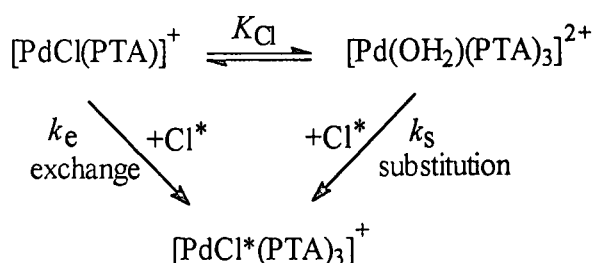
It is clear from Table 4.3 that K_{14} is consistently larger than K_{24} . For the reaction of $[\text{PdCl}(\text{PTA})_3]^+$ with Y^- (K_{14}) a Cl^- ligand needs to be replaced by the halide/pseudo-halide and a five-coordinated intermediate species might then even be present (see for example Ref. 20). This intermediate species probably has a trigonal bipyramidal configuration, and with a large amount of electron density present on the metal complex, then results in the dissociation of one of the PTA ligands. A square planar geometry for the complex $[\text{PdY}_2(\text{PTA})_2]$ is assumed again after rearrangement of the complex.

In these type of reactions the probability that more than one reaction are present resulting in the fact that only overall reactions could be studied, are not excluded, since extremely complex solution behaviour exists (see Scheme 4.2). For this study the equilibrium constants, K_{14} and K_{24} , determined can indeed be considered as overall equilibrium constants for the reactions in Eq. 4.42 and Eq. 4.43.

4.7.2 Chloride Exchange

The rapid chloride exchange process was studied on ^{35}Cl NMR and significant line-broadening was observed (see Fig 4.22). The chloride exchange process, which includes two steps, *i.e.*, the hydrolysis to an aqua species which can undergo rapid nucleophilic substitution by the Cl^- , and the direct exchange pathway, as illustrated in Scheme 4.3, could be investigated.

Scheme 4.3 Solvent and direct pathway for chloride exchange of $[\text{PdCl}(\text{PTA})_3]^+$.



where K_{Cl} = hydrolysis equilibrium constant

k_e = rate constant for the exchange (direct path)

k_s = rate constant for the substitution (solvent path)

Cl^* = free chloride

An expression for the observed rate constant, $(k_{\text{obs}})_{\text{Cl}}$, and $[\text{Cl}^-]$ at a specific $[\text{Pd}]$ can be derived from the mechanism presented in Scheme 4.3. (See also complete derivation in Appendix A).

The rate of formation of $[\text{PdCl}^*(\text{PTA})_3]$ is given by

$$R = (k_e[\text{PdCl}(\text{PTA})_3] + k_s[\text{Pd}(\text{OH}_2)(\text{PTA})_3])[\text{Cl}^-] \quad 4.44$$

Similarly, the equilibrium constant is given by

$$K_{\text{Cl}} = [\text{Pd}(\text{OH}_2)(\text{PTA})_3] [\text{Cl}^-] / [\text{PdCl}(\text{PTA})_3] \quad 4.45$$

Upon inclusion of the hydrolysis equilibrium, as given in Eq. 4.46, and by definition, the rate constant observed (as a function of line-width) on the free Cl^- peak, is given by:

$$d[\text{PdCl}]/dt[\text{Cl}^-] = (k_{\text{obs}})_{\text{Cl}} = ((k_e + k_s (K_{\text{Cl}}/[\text{Cl}^-])) / (1 + K_{\text{Cl}}/[\text{Cl}^-])) [\text{Pd}]_{\text{T}} \quad 4.46$$

If $[\text{Cl}^-] \gg K_{\text{Cl}}$ then

$$(k_{\text{obs}})_{\text{Cl}} = ((k_e + k_s (K_{\text{Cl}}/[\text{Cl}^-])))[\text{Pd}] \quad 4.47$$

$$\text{and } (k_{\text{obs}})_{\text{Cl}} / [\text{Pd}] = (k_{\text{obs}})' = k_e + k_s (K_{\text{Cl}}/[\text{Cl}^-]) \quad 4.48$$

It is clear from Eq. 4.49 that k_e , and therefore the direct route, contributes more to $(k_{\text{obs}})_{\text{Cl}}$ if the $[\text{Cl}^-]$ is high. In Table 4.4 the observed rate constants, $(k_{\text{obs}})_{\text{Cl}}$ calculated for specific $[\text{Cl}^-]$ with different $[\text{PdCl}(\text{PTA})_3]^+$ concentrations, at 22 °C, are reported.

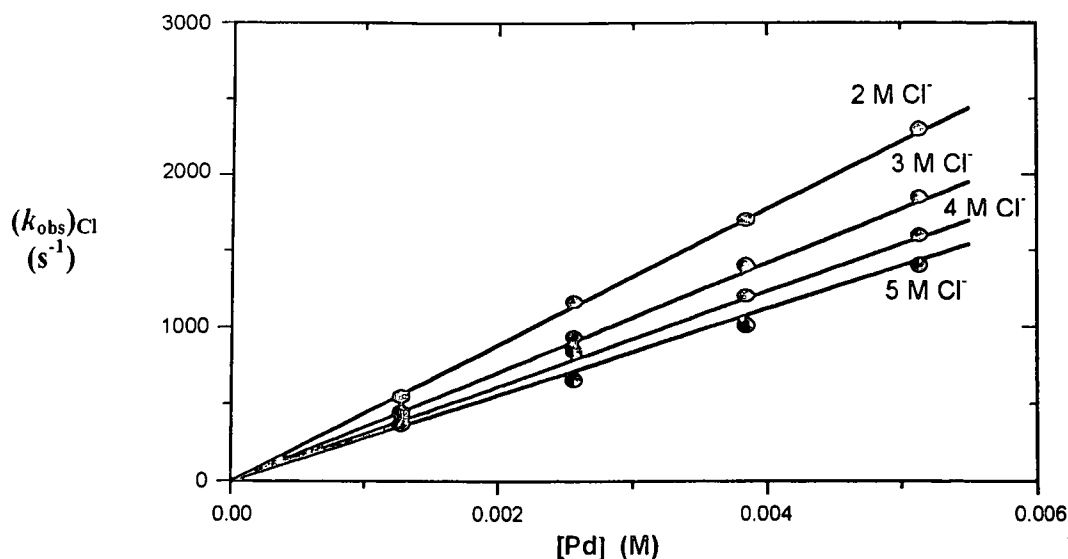
Table 4.4 $^{35}\text{Cl}^-$ NMR: Observed rate constants, $(k_{\text{obs}})_{\text{Cl}}$, calculated for the rapid chloride exchange observed for $[\text{PdCl}(\text{PTA})_3]^+$ and Cl^- ; pH = 6.0, T = 22 °C.

[PdCl(PTA) ₃] ⁺ (mM)	(k _{obs}) _{Cl} (s ⁻¹) for specific [Cl] ^a			
	2 M	3 M	4 M	5 M
1.28	652	450	445	372
2.57	1164	937	848	660
3.85	1702	1539	1203	1013
5.14	2156	1920	1600	1282

^a Determined with Eq. 4.27

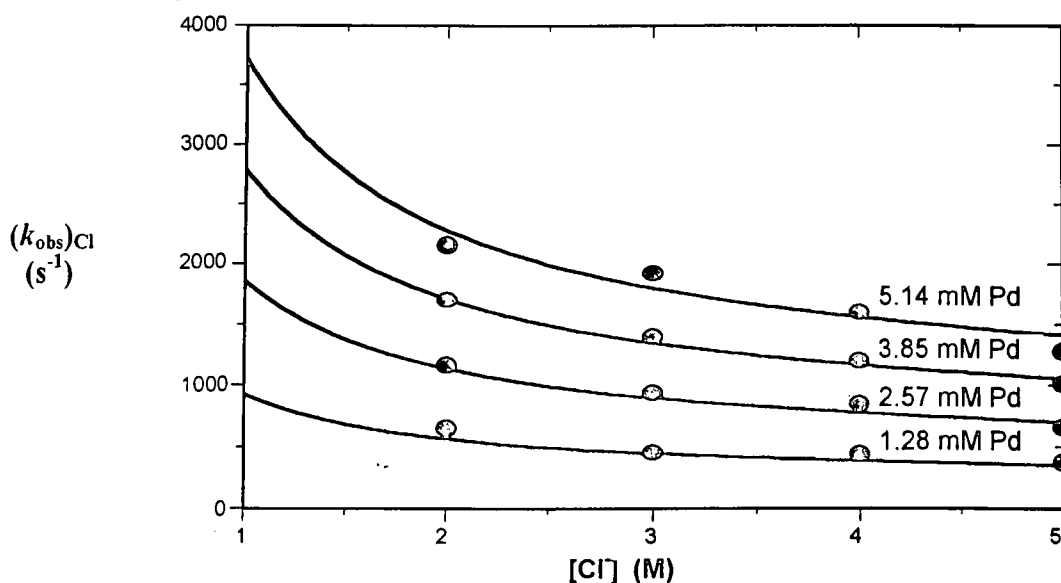
The data in Table 4.4 are graphically illustrated in different ways as shown in Fig 4.25–4.28. First, a plot of $(k_{\text{obs}})_{\text{Cl}}$ vs. $[\text{Pd}]$, as shown in Fig 4.25, clearly indicates the direct relationship, given in Eq. 4.48.

Figure 4.25 Plot of exchange rate, $(k_{\text{obs}})_{\text{Cl}}$, vs. $[\text{Pd}]$ (with a specific $[\text{Cl}^-]$ as is indicated on the figure) for the exchange of free Cl^- with $[\text{PdCl}(\text{PTA})_3]^+$, see Table 4.4. $T = 22^\circ\text{C}$. A linear relationship is obtained with an intercept = 0.



Next, in Fig. 4.26, the plot of $(k_{\text{obs}})_{\text{Cl}}$ vs. $[\text{Cl}^-]$, see Eq. 4.48, is shown. The inverse relationship of $(k_{\text{obs}})_{\text{Cl}}$ on $[\text{Cl}^-]$ is clear.

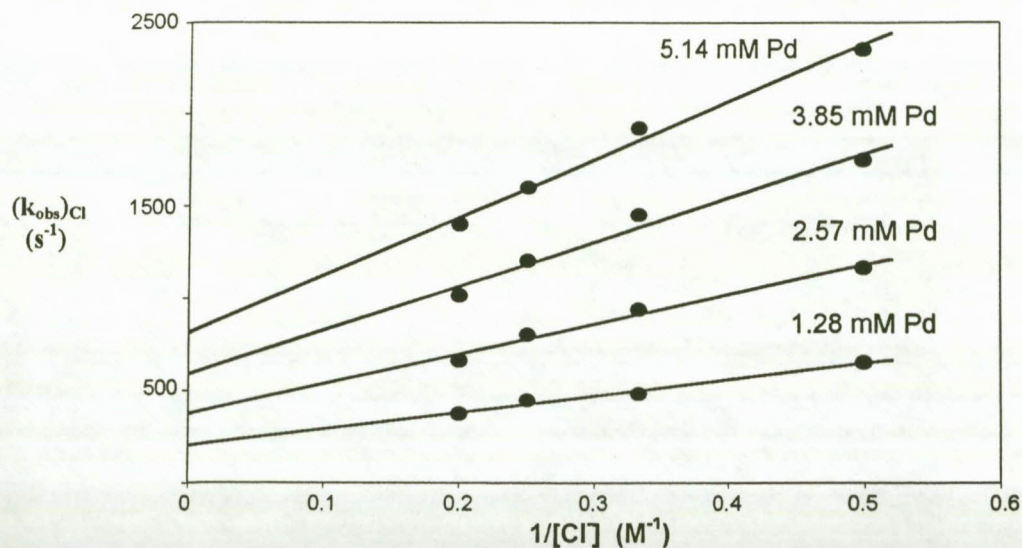
Figure 4.26 Plot of exchange rate, $(k_{\text{obs}})_{\text{Cl}}$, vs. $[\text{Cl}^-]$ (with a specific $[\text{Pd}]$ as is indicated on the figure) for the exchange of free Cl^- with $[\text{PdCl}(\text{PTA})_3]^+$, see Table 4.4. $T = 22^\circ\text{C}$. A non-linear (exponential) relationship is obtained. The lines represent the least-squares fit of the data to Eq. 4.48.



To further illustrate the inverse relationship of the observed rate constant on $[\text{Cl}^-]$, a plot of $(k_{\text{obs}})_{\text{Cl}}$ vs. $1/[\text{Cl}^-]$ is shown in Fig 4.27. According to Eq. 4.49 the slope is given by $k_s K_{\text{Cl}} [\text{Pd}]$

and the intercept by $k_e[\text{Pd}]$. It is clear that the rate of Cl^- exchange, k_e , at the Pd centre is quite high. The values of k_e and $k_e K_{\text{Cl}}$ thus obtained are reported in Table 4.5.

Figure 4.27 Plot of exchange rate, $(k_{\text{obs}})_{\text{Cl}}$, vs. $1/[\text{Cl}^-]$ for a specific $[\text{Pd}]$, as is indicated on the figure (see Eq. 4.49 and Table 4.4). $T = 22^\circ\text{C}$.



Finally, the data in Table 4.4 were fitted to a complete model, given in Eq. 4.48, both as a function of $[\text{Pd}]$ and $[\text{Cl}^-]$, and a three dimensional representation of the system is illustrated in Fig. 4.28. The results obtained are reported in Table 4.5. Unfortunately, $k_e K_{\text{Cl}}$ is only obtained as a combined constant (see Eq. 4.48).

Figure 4.28 3D presentation of $(k_{\text{obs}})_{\text{Cl}}$ vs. $[\text{Cl}^-]$ vs. $[\text{Pd}]$ for the reaction of $[\text{PdCl}(\text{PTA})_3]^+$ and Cl^- .

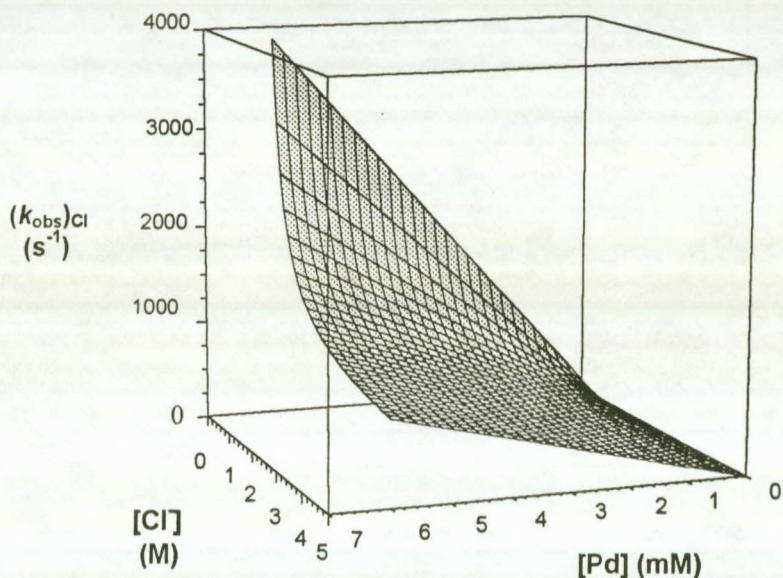


Table 4.5 Rate constants for the Cl⁻ exchange on [MCl(PTA)₃]⁺, pH = 6.0, T = 22°C.

M	k_e (M ⁻¹ s ⁻¹)	$k_s K_{Cl}$ (s ⁻¹)
Pd ^a	1.5(4) × 10 ⁵	6.4(4) × 10 ⁵
Pd ^b	1.64(8) × 10 ⁵	5.7(2) × 10 ⁵
Pt ^c	9.2(3) × 10 ³	2.9(4) × 10 ⁴

^aFrom Fig. 4.26 ^bFrom Fig 4.28 ^cSee Ref. 16

From Figs. 4.25 – 4.28 it is observed that the higher the [Cl⁻], the smaller (k_{obs})_{Cl} becomes. Thus, two species contribute to the kinetic process in solution, *i.e.*, the Pd-Cl and the Pd-OH₂/Pd-OH species. The Pd-OH₂ is the more reactive species towards chloride substitution and as the [Cl⁻] increases the equilibrium is shifted towards the Pd-Cl species, the less reactive one. The chloride exchange between the Pd-Cl species and free chloride is therefore slower than the substitution of H₂O, from Pd-H₂O, with free chloride. However, it is clear that the reactivity of these processes are very high, typically of Pd(II) metal centres, and explains why the typical substitution reactions could not be studied by, *e.g.*, stopped flow methods.

There is an intricate interaction¹⁷ between the metal centre and the *trans* and entering ligands for associative substitution reactions. These are mainly responsible for the overall rate of the reaction. The interplay between the Pd metal centre and the respective ligands are of importance in the reactions studied. It has been shown¹⁸ that the exchange rates of a series of square-planar palladium(II) solvates with amide, nitrile, isonitrile and sulfide ligands span almost 8 orders of magnitude as a result of the large changes in nucleophilicity of entering ligands, *trans* effects and different steric hindrance of ligands and complexes. For complexes of the type [PdL₄]²⁺ (L = ligand), ligands with hard donor atoms such as H₂O, MeCN and amides have similar exchange rates ($k = 10.2, 48.8$ and 34.8 M⁻¹s⁻¹). The much softer Me₂S and MeNC ligands undergo substitution more rapidly, indicating that in the absence of steric effects, ligand nucleophilicity and *trans* effect determine reactivity. The enhanced reactivity of MeNC complexes (approximately 10³ times more rapid than Me₂S) may be due to a stabilization of a five-coordinate intermediate by π back-bonding from the metal to the ligand. A five-coordinate intermediate has been isolated in the substitution of coordinated methyl isocyanate by iodide in [Pt(PPh₃)₂(MeNC)₂](BF₄)₂¹⁹.

It is interesting to compare the rate of Cl-exchange^{17,18} for Pd²⁺ with the Pt²⁺ metal centre. With a relative hard ligand such as H₂O, [Pd(H₂O)₄]²⁺ undergoes exchange 10⁶ times more rapidly than [Pt(H₂O)₄]²⁺. In contrast, with soft ligands such as CN⁻ or MeNC the rates of exchange are virtually the same ([M(CN)₄]²⁻: $k_{\text{Pd}} = 120 \text{ M}^{-1}\text{s}^{-1}$, $k_{\text{Pt}} = 26 \text{ M}^{-1}\text{s}^{-1}$). It is clear that the Cl-exchange on the Pd centre in [PdCl(PTA)₃]⁺ is also only 20 times more reactive than the corresponding Pt in [PtCl(PTA)₃]⁺. A reason for this behaviour could be as explained above – stabilization of a five-coordinate transition state or intermediate by π back-bonding from the metal to the ligand. A five-coordinate intermediate has indeed been isolated for substitution of chloride by iodide in [PtCl(PTA)₃]Cl to form the [PtI₂(PTA)₃] complex²⁰.

Two factors can mainly contribute to the line-broadening of the spectra obtained from the experiments: chemical exchange of the chloride bonded to the Pd centre with free chloride and the quadrupolar relaxation of the Pd metal centre, as is given in Eq. 4.30. To determine whether the line-broadening observed is due to chloride exchange or a result of the quadrupolar relaxation, many more complex experiments have to be done at various temperatures. For the purpose of this study it is assumed that the line-broadening observed was primarily due to the exchange process. This, however, needs to be investigated in the future.

For the purpose of this study the interesting (and complex) reactivity and thermodynamics of the [PdCl(PTA)₃]⁺ aqueous system has been adequately studied. It provides a base for future study, and to indeed evaluate the combined Pd(II)/Pt(II) systems for application in *e.g.*, catalysis.

¹ C. Capellos, B. Bielski, *Kinetic Systems – Mathematical Description of Chemical Kinetics in Solution*, John Wiley and Sons Inc, New York, 1972, Chapter 1.

² J. H. Espenson, *Chemical Kinetics and Reaction Mechanisms*, Second Edition, McGraw-Hill, Inc, 1995, Chapter 1, 2.

- ³ Michael J. Pilling, Paul W. Seakins, *Reaction Kinetics*, Oxford Science Publications, 1999, Chapter 1.
- ⁴ F. Cotton, G. Wilkinson, *Advanced Inorganic Chemistry (Fifth Edition)*, John Wiley and Sons, New York, 1988, Chapter 29.
- ⁵ G. Rodgers, *Introduction to Coordination, Solid State, and Descriptive Inorganic Chemistry*, McGraw-Hill, Inc, 1994, Chapter 5.
- ⁶ K. Purcell, J. Kotz, *Inorganic Chemistry*, Holt-Saunders International Editions, 1977, Chapter 13.
- ⁷ F. Cotton, G. Wilkinson, P. L. Gaus, *Basic Inorganic Chemistry*, Third Edition, John Wiley and Sons, New York, 1995, p 83 and 167.
- ⁸ P. J. Hore, *Nuclear Magnetic Resonance*, Oxford University Press, 1996, Chapters 4 and 5.
- ⁹ D. Hugi-Clearly, L. Helm, A. E. Merbach, *Helv. Chim. Acta*, 1985, **68**, 545.
- ¹⁰ Scientist for Windows, Least-squares Parameter Estimation, Version 4.00.950, MicroMath, 1990.
- ¹¹ D. J. Darensbourg, T. J. Decuir, N. W. Stafford, J. B. Robertson, J. D. Draper, J. H. Reibenspies, A. Kathó, F. Joó, *Inorg. Chem.*, 1997, **36**, 19.
- ¹² D. J. Darensbourg, J. B. Robertson, D. L. Larkins, J. H. Reibenspies, *Inorg. Chem.*, 1999, **38**, 2473.
- ¹³ E. C. Alyea, G. Ferguson, S. Kannan, *Chem. Commun.*, 1998, 345.
- ¹⁴ A. Roodt, J. G. Leipoldt, L. Helm, A. E. Merbach, *Inorg. Chem.*, 1992, **31**, 2864.
- ¹⁵ A. Meij, S. Otto, A. Roodt, Unpublished results.
- ¹⁶ Z. Sam, S. Otto, A. Roodt, Unpublished results.
- ¹⁷ U. Frey, S. Elmroth, B. Moullet, L. I. Elding, A. E. Merbach, *Inorg. Chem.*, 1991, **30**, 5033.
- ¹⁸ N. Hallinan, V. Besançon, M. Forster, G. Elbaze, Y. Ducommun, A. Merbach, *Inorg. Chem.*, 1991, **30**, 1112.
- ¹⁹ P. M. Treichel, R. W. Hess, *J. Chem. Soc., Chem. Commun.*, 1970, 1626.
- ²⁰ S. Otto, A. Roodt, *Inorg. Chem. Commun.*, 2001, **4**, 49.

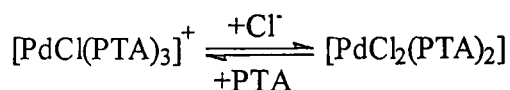
5 Evaluation and Future Research

The evaluation of this study is briefly discussed in Par. 5.1 in terms of the pre-set aims as outlined in Chapter 1, while some future research aspects are also presented in Par. 5.2.

5.1 Evaluation of the study

The aim of this study was discussed in Chapter 1 and the evaluation of the success will be discussed in this section:

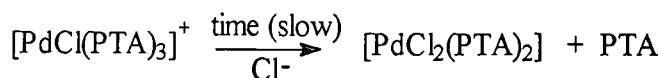
- (i) The complexes $[\text{PdCl}(\text{PTA})_3]\text{Cl}$ and *cis*- $[\text{PdCl}_2(\text{PTA})_2]$ were prepared and characterised as described in literature. As anticipated both complexes were water-soluble with the $[\text{PdCl}(\text{PTA})_3]^+$ complex more so than the *cis*- $[\text{PdCl}_2(\text{PTA})_2]$.
- (ii) The stability of these complexes in aqueous solution were investigated. In solution, a dynamic equilibrium exists between $[\text{PdCl}(\text{PTA})_3]^+$ and *cis*- $[\text{PdCl}_2(\text{PTA})_2]$.



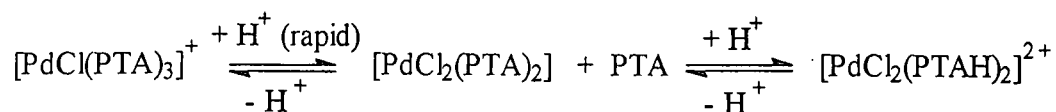
Therefore, for the reactions involving these complexes were investigated in parallel. The ratio of $[\text{PdCl}(\text{PTA})_3]^+$ to *cis*- $[\text{PdCl}_2(\text{PTA})_2]$ could not be determined exactly, because of the limitations of characterisation methods for the palladium complexes. It is concluded that the ratio is dependent on the following: $[\text{PTA}]$, pH and $[\text{Cl}^-]$. The ratio of $[\text{PdCl}(\text{PTA})_3]^+$ to *cis*- $[\text{PdCl}_2(\text{PTA})_2]$ is larger if an excess (5 equivalents) of PTA is used to force the equilibrium to the side of $[\text{PdCl}(\text{PTA})_3]^+$, than if a stoichiometric amount of PTA is used, while an excess of Cl^- has the opposite effect. Unprotonated PTA has a better electron donating ability than protonated PTA (PTAH^+) has and therefore preparation/reactions must be performed at neutral pH. Using only 2 equivalents of PTA

results in the selective formation of *cis*-[PdCl₂(PTA)₂] and reactions thereof were investigated separately.

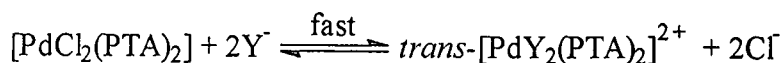
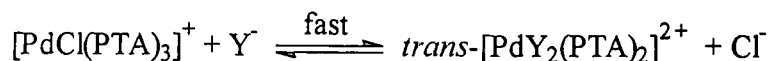
Both the [PdCl(PTA)₃]⁺ and *cis*-[PdCl₂(PTA)₂] complexes showed complicated solution behaviour and both the complexes hydrolyse and decompose in absence of excess chloride. In excess of chloride *cis*-[PdCl₂(PTA)₂] is stable and [PdCl(PTA)₃]⁺ is slowly converted to *cis*-[PdCl₂(PTA)₂].



The conversion of [PdCl(PTA)₃]⁺ to *cis*-[PdCl₂(PTA)₂] is, however, rapid upon the addition of H⁺. This is concluded to be due to protonation of one, or both, PTA ligands as can be confirmed by the pK_a determination. Similarly, in more acidic solution a protonated PTA complex is formed. The Pt analogue of *cis*-[PdCl₂(PTAH)₂]²⁺ was characterised crystallographically by Darensbourg.



(iii) High reactivity of complexes was observed upon addition of halide/pseudo-halide (Br⁻, I⁻, SCN⁻ and N₃⁻) forming the [Pd(PTA)₃]⁺ complexes; it was not possible to study the complexes by time-resolved spectroscopy.



Therefore, chloride exchange was studied with NMR spectroscopy. It was observed that the higher the chloride concentration, the slower the rate of exchange becomes, thus indicative of a hydrolysed species participating in the reaction.



(iv) Characterization of the starting complexes, intermediates and products were done with IR- and UV-Vis spectrophotometry, multinuclear NMR (^{31}P and ^{35}Cl) spectrometry and X-ray crystallography. Unfortunately no crystal structure of the actual $[\text{Pd}(\text{Y})(\text{PTA})_3]^+$ complex could be obtained since consecutive substitution reactions were encountered. Nevertheless two crystal structures of two reaction products, *trans*- $[\text{Pd}(\text{SCN})_2(\text{PTA})_2](\text{SCN})_2$ and *trans*- $[\text{PdBr}_2(\text{PTA})_2]$ were determined successfully. Both structures revealed the *trans* isomers were isolated, therefore *cis-trans* isomerization must occur at some stage during the reaction process. The crystal structures provides useful information on protonation behaviour ($\text{p}K_{\text{a}1}$ and $\text{p}K_{\text{a}2}$ calculated), isomerization (*cis-trans* isomerization as observed from the crystal structures reported) and substitution behaviour of ligands (for both PTA and Cl^-) of the complexes.

A significant drawback of this study was the reactivity of the Pd(II) centre which prohibited the isolation of single step products and more detailed reactivity studies. However, it is specifically this characteristic that needs to be exploited in future for possible application.

5.2 Future research

The use of PTA as water-soluble ligand provides a large scope wherein these type of complexes could be investigated, also with respect to possible catalytic applications.

The investigations conducted during of this study, where Pd is used as metal, could be extended by doing substitution kinetics at low temperatures and NMR chloride exchange at a wider range of temperatures. The complexes could also be evaluated for catalytic properties.

The crystal structure, *trans*- $[\text{Pd}(\text{SCN})_2(\text{PTA})_2](\text{SCN})_2$ was reported and it was observed that the thiocyanate ligand coordinates *via* the S atom. S coordination is an indication that the complex is the product of the *cis*- $[\text{PdCl}_2(\text{PTA})_2]$ and SCN^- and not *trans*- $[\text{PdCl}_2(\text{PTA})_2]$. Therefore, Cl^- substitution first takes place and thereafter isomerization

occurs. The preparation and isolation of a Pd(NCS) species, where the thiocyanate coordinates *via* the N-atom, could deliberately be done by starting from *trans*-[PdBr₂(PTA)₂] or *trans*-[PdI₂(PTA)₂] and SCN⁻.

The preparation of [PdCl₃(PTA)]⁻ complexes and substitution of the Cl⁻ *trans* of the PTA could also be investigated, including hydrolysed/ solvated species.

All of the above mentioned points can also be extended to other metal centres, for instance Rh and Pt, to further evaluate the properties of PTA as ligand.

Appendix A

A Crystallographic data for *trans*-[Pd(SCN)₂(PTAH)₂](SCN)₂.

Table A1: Atomic coordinates ($\times 10^4$) and equivalent isotropic displacement parameters ($\text{\AA}^2 \times 10^3$) for *trans*-[Pd(SCN)₂(PTAH)₂](SCN)₂. U(eq) is defined as one third of the trace of the orthogonalized U_{ij} tensor.

	x	y	z	U(eq)		x	y	z	U(eq)
Pd(1)	0	0	5000	18(1)	C(1)	-648(3)	34(2)	2210(2)	23(1)
P(1)	927(1)	171(1)	3367(1)	16(1)	C(11)	1952(3)	-2651(2)	6196(2)	27(1)
S(10)	2637(1)	831(1)	5682(1)	27(1)	N(11)	1013(3)	-3260(2)	6530(2)	50(1)
S(11)	3284(1)	-1797(1)	5732(1)	33(1)	C(6)	1567(4)	-670(2)	1154(2)	27(1)
N(2)	3152(3)	-558(2)	1965(2)	22(1)	C(4)	1119(4)	1169(2)	1186(2)	30(1)
C(2)	2629(3)	-774(2)	3034(2)	22(1)	C(5)	3938(4)	537(2)	1877(2)	25(1)
C(3)	2046(3)	1390(2)	3021(2)	24(1)	N(10)	1693(3)	2981(2)	5752(2)	52(1)
N(1)	278(3)	140(2)	1262(2)	25(1)	C(10)	2030(4)	2097(2)	5713(2)	32(1)
N(3)	2626(3)	1337(2)	1969(2)	24(1)					

Table A2: Bond lengths [\AA] and angles [$^\circ$] for *trans*-[Pd(SCN)₂(PTAH)₂](SCN)₂

Bond	\AA	Bond	\AA
Pd(1)-P(1)	2.2940(8)	N(2)-C(5)	1.522(3)
Pd(1)-P(1)#1	2.2940(8)	N(2)-C(6)	1.526(3)
Pd(1)-S(10)#1	2.3509(8)	C(3)-N(3)	1.467(3)
Pd(1)-S(10)	2.3509(8)	N(1)-C(6)	1.431(3)
Pd(1)-S(11)	3.4381(9)	N(1)-C(4)	1.461(3)
P(1)-C(2)	1.835(2)	N(1)-C(1)	1.469(3)
P(1)-C(1)	1.837(3)	N(3)-C(5)	1.430(3)
P(1)-C(3)	1.839(2)	N(3)-C(4)	1.470(3)
S(10)-C(10)	1.676(3)	C(11)-N(11)	1.158(3)
S(11)-C(11)	1.628(3)	N(10)-C(10)	1.155(3)
N(2)-C(2)	1.498(3)		

APPENDIX A

Bond lengths [\AA] and angles [$^\circ$] for *trans*-[Pd(SCN)₂(PTAH)₂](SCN)₂

Angle	$^\circ$	Angle	$^\circ$
P(1)-Pd(1)-P(1)#1	180.0	C(2)-N(2)-C(5)	111.9(2)
P(1)-Pd(1)-S(10)#1	90.55(3)	C(2)-N(2)-C(6)	111.61(19)
P(1)#1-Pd(1)-S(10)#1	89.45(3)	C(5)-N(2)-C(6)	108.6(2)
P(1)-Pd(1)-S(10)	89.45(3)	N(2)-C(2)-P(1)	109.93(16)
P(1)#1-Pd(1)-S(10)	90.55(3)	N(3)-C(3)-P(1)	111.49(16)
S(10)#1-Pd(1)-S(10)	180.0	C(6)-N(1)-C(4)	109.8(2)
P(1)-Pd(1)-S(11)	92.83(3)	C(6)-N(1)-C(1)	113.0(2)
P(1)#1-Pd(1)-S(11)	87.17(3)	C(4)-N(1)-C(1)	112.2(2)
S(10)#1-Pd(1)-S(11)	111.47(3)	C(5)-N(3)-C(3)	111.9(2)
S(10)-Pd(1)-S(11)	68.53(3)	C(5)-N(3)-C(4)	109.6(2)
C(2)-P(1)-C(1)	99.16(11)	C(3)-N(3)-C(4)	112.03(19)
C(2)-P(1)-C(3)	98.80(11)	N(1)-C(1)-P(1)	110.78(16)
C(1)-P(1)-C(3)	99.03(12)	N(11)-C(11)-S(11)	179.6(2)
C(2)-P(1)-Pd(1)	115.36(8)	N(1)-C(6)-N(2)	111.1(2)
C(1)-P(1)-Pd(1)	121.19(8)	N(1)-C(4)-N(3)	113.3(2)
C(3)-P(1)-Pd(1)	119.14(8)	N(3)-C(5)-N(2)	111.8(2)
C(10)-S(10)-Pd(1)	102.70(10)	N(10)-C(10)-S(10)	176.8(3)
C(11)-S(11)-Pd(1)	95.55(9)		

Symmetry transformations used to generate equivalent atoms: #1 -x,-y,-z+1

Table A3: Anisotropic displacement parameters ($\text{\AA}^2 \times 10^3$) for *trans*-[Pd(SCN)₂(PTAH)₂](SCN)₂. The anisotropic displacement factor exponent takes the form: $-2\pi^2[h^2 a^{*2}U11 + \dots + 2hka^*b^*U12]$

	U11	U22	U33	U23	U13	U12
Pd(1)	17(1)	21(1)	15(1)	-3(1)	3(1)	-6(1)
P(1)	15(1)	19(1)	15(1)	-1(1)	2(1)	-2(1)
S(10)	23(1)	30(1)	28(1)	-1(1)	0(1)	-5(1)
S(11)	36(1)	25(1)	38(1)	0(1)	6(1)	-7(1)
N(2)	21(1)	23(1)	25(1)	-2(1)	8(1)	4(1)
C(2)	24(1)	21(1)	20(1)	1(1)	2(1)	0(1)
C(3)	28(1)	18(1)	28(2)	-2(1)	6(1)	-2(1)
N(1)	24(1)	36(1)	15(1)	2(1)	0(1)	-3(1)

APPENDIX A

N(3)	25(1)	22(1)	25(1)	3(1)	7(1)	-2(1)
C(1)	18(1)	32(1)	19(1)	2(1)	1(1)	-2(1)
C(11)	22(1)	26(2)	34(2)	5(1)	2(1)	9(1)
N(11)	27(1)	45(2)	78(2)	28(2)	9(1)	1(1)
C(6)	30(2)	33(2)	18(2)	-6(1)	6(1)	-5(1)
C(4)	32(2)	34(2)	26(2)	11(1)	6(1)	3(1)
C(5)	21(1)	32(2)	24(2)	2(1)	7(1)	-4(1)
N(10)	44(2)	34(2)	77(2)	-11(2)	9(2)	-6(1)
C(10)	28(2)	36(2)	32(2)	-6(1)	3(1)	-12(1)

Table A4: Hydrogen coordinates ($\times 10^4$) and isotropic displacement parameters ($\text{\AA}^2 \times 10^3$) for *trans*-[Pd(SCN)₂(PTAH)₂](SCN)₂

	x	y	z	U(eq)
H(2A)	3670	-720	3529	26
H(2B)	2162	-1482	3067	26
H(3B)	1233	1976	3066	29
H(3A)	3076	1512	3511	29
H(1A)	-1223	-647	2217	27
H(1B)	-1566	569	2218	27
H(6A)	1060(3)	-1343(18)	1236(17)	14(6)
H(5B)	4860(3)	583(18)	2387(19)	19(7)
H(5A)	4390(3)	550(18)	1227(19)	18(6)
H(2)	4010(3)	-960(2)	1820(19)	30(8)
H(6B)	2010(3)	-628(19)	490(2)	27(7)
H(4B)	1560(3)	1230(19)	540(2)	32(7)
H(4A)	250(3)	1690(2)	1254(19)	32(8)

Table A5: Torsion angles [$^\circ$] for *trans*-[Pd(SCN)₂(PTAH)₂](SCN)₂

S(10)-Pd(1)-P(1)-C(1)	-162.90(10)
S(10)-Pd(1)-P(1)-C(2)	77.57(9)
S(10)-Pd(1)-P(1)-C(3)	-39.70(10)

Symmetry transformations used to generate equivalent atoms: #1 -x,-y,-z+1

APPENDIX A

B Crystallographic data for *trans*-[PdBr₂(PTA)₂]

Table B1: Atomic coordinates ($\times 10^4$) and equivalent isotropic displacement parameters ($\text{\AA}^2 \times 10^3$) for *trans*-[PdBr₂(PTA)₂]. U(eq) is defined as one third of the trace of the orthogonalized U_{ij} tensor.

	x	y	z	U(eq)		x	y	z	U(eq)
Pd(1)	0	0	5000	20(1)	C(1)	2746(6)	1785(4)	7054(5)	30(1)
Br(1)	2402(1)	-457(1)	3594(1)	37(1)	C(3)	-10(6)	3041(4)	5678(5)	28(1)
P(1)	1359(2)	1745(1)	5480(1)	22(1)	C(2)	3067(6)	2343(4)	4464(5)	33(1)
N(1)	3615(5)	2890(3)	7321(4)	27(1)	C(4)	2225(6)	3779(4)	7350(5)	32(1)
N(3)	1182(5)	4004(3)	6107(4)	26(1)	C(5)	2484(6)	4264(4)	5127(5)	31(1)
N(2)	3900(5)	3392(3)	5020(4)	29(1)	C(6)	4835(6)	3186(4)	6307(5)	32(1)

Table B2: Bond lengths [\AA] and angles [$^\circ$] for *trans*-[PdBr₂(PTA)₂].

Bond/Angle	$\text{\AA}/^\circ$	Bond/Angle	$\text{\AA}/^\circ$
Pd(1)-P(1)#1	2.3200(11)	N(2)-C(5)	1.467(5)
Pd(1)-P(1)	2.3200(11)	N(2)-C(2)	1.474(5)
Pd(1)-Br(1)	2.4270(8)	C(1)-H(1A)	0.9700
Pd(1)-Br(1)#1	2.4270(8)	C(1)-H(1B)	0.9700
P(1)-C(2)	1.835(4)	C(3)-H(3A)	0.9700
P(1)-C(1)	1.837(5)	C(3)-H(3B)	0.9700
P(1)-C(3)	1.846(4)	C(2)-H(2A)	0.9700
N(1)-C(4)	1.460(6)	C(2)-H(2B)	0.9700
N(1)-C(1)	1.465(5)	C(4)-H(4A)	0.9700
N(1)-C(6)	1.472(6)	C(4)-H(4B)	0.9700
N(3)-C(4)	1.457(6)	C(5)-H(5A)	0.9700
N(3)-C(3)	1.475(5)	C(5)-H(5B)	0.9700
N(3)-C(5)	1.476(5)	C(6)-H(6A)	0.9700
N(2)-C(6)	1.459(6)	C(6)-H(6B)	0.9700

P(1)#1-Pd(1)-P(1)	180.0	N(3)-C(3)-H(3B)	109.4
P(1)#1-Pd(1)-Br(1)	89.45(3)	P(1)-C(3)-H(3B)	109.4
P(1)-Pd(1)-Br(1)	90.55(3)	H(3A)-C(3)-H(3B)	108.0
P(1)#1-Pd(1)-Br(1)#1	90.55(3)	N(2)-C(2)-P(1)	112.2(3)
P(1)-Pd(1)-Br(1)#1	89.45(3)	N(2)-C(2)-H(2A)	109.2

APPENDIX A

Br(1)-Pd(1)-Br(1)#1	180.0	P(1)-C(2)-H(2A)	109.2
C(2)-P(1)-C(1)	98.5(2)	N(2)-C(2)-H(2B)	109.2
C(2)-P(1)-C(3)	98.2(2)	P(1)-C(2)-H(2B)	109.2
C(1)-P(1)-C(3)	98.1(2)	H(2A)-C(2)-H(2B)	107.9
C(2)-P(1)-Pd(1)	121.12(15)	N(3)-C(4)-N(1)	115.0(4)
C(1)-P(1)-Pd(1)	113.76(14)	N(3)-C(4)-H(4A)	108.5
C(3)-P(1)-Pd(1)	122.39(14)	N(1)-C(4)-H(4A)	108.5
C(4)-N(1)-C(1)	110.8(3)	N(3)-C(4)-H(4B)	108.5
C(4)-N(1)-C(6)	107.7(3)	N(1)-C(4)-H(4B)	108.5
C(1)-N(1)-C(6)	110.8(3)	H(4A)-C(4)-H(4B)	107.5
C(4)-N(3)-C(3)	111.8(3)	N(2)-C(5)-N(3)	113.7(3)
C(4)-N(3)-C(5)	108.9(4)	N(2)-C(5)-H(5A)	108.8
C(3)-N(3)-C(5)	110.5(3)	N(3)-C(5)-H(5A)	108.8
C(6)-N(2)-C(5)	108.8(4)	N(2)-C(5)-H(5B)	108.8
C(6)-N(2)-C(2)	111.0(4)	N(3)-C(5)-H(5B)	108.8
C(5)-N(2)-C(2)	110.6(4)	H(5A)-C(5)-H(5B)	107.7
N(1)-C(1)-P(1)	112.6(3)	N(2)-C(6)-N(1)	115.1(3)
N(1)-C(1)-H(1A)	109.1	N(2)-C(6)-H(6A)	108.5
P(1)-C(1)-H(1A)	109.1	N(1)-C(6)-H(6A)	108.5
N(1)-C(1)-H(1B)	109.1	N(2)-C(6)-H(6B)	108.5
P(1)-C(1)-H(1B)	109.1	N(1)-C(6)-H(6B)	108.5
H(1A)-C(1)-H(1B)	107.8	H(6A)-C(6)-H(6B)	107.5
N(3)-C(3)-P(1)	111.3(3)	N(3)-C(3)-H(3A)	109.4
P(1)-C(3)-H(3A)	109.4		

Symmetry transformations used to generate equivalent atoms: #1 -x,-y,-z+1

Table B3: Anisotropic displacement parameters ($\text{\AA}^2 \times 10^3$) for *trans*-[PdBr₂(PTA)₂]. The anisotropic displacement factor exponent takes the form: $-2\pi^2[h^2a^{*2}U_{11} + \dots + 2hka^*b^*U_{12}]$

	U11	U22	U33	U23	U13	U12
Pd(1)	20(1)	17(1)	23(1)	-4(1)	0(1)	0(1)
Br(1)	39(1)	29(1)	47(1)	-7(1)	19(1)	3(1)
P(1)	20(1)	18(1)	27(1)	-4(1)	2(1)	-1(1)
N(1)	31(2)	18(2)	30(2)	-1(2)	-7(2)	-6(2)
N(3)	25(2)	17(2)	35(2)	-2(2)	1(2)	1(2)
N(2)	28(2)	23(2)	36(2)	-3(2)	8(2)	-7(2)

APPENDIX A

C(1)	34(3)	21(2)	35(3)	7(2)	-3(2)	-7(2)
C(3)	22(2)	22(2)	40(3)	-3(2)	-2(2)	4(2)
C(2)	36(3)	33(3)	31(3)	-11(2)	12(2)	-5(2)
C(4)	39(3)	24(2)	32(3)	-10(2)	1(2)	-5(2)
C(5)	35(3)	21(2)	38(3)	7(2)	1(2)	-2(2)
C(6)	20(2)	20(2)	54(3)	3(2)	-4(2)	-1(2)

Table B4: Hydrogen coordinates ($\times 10^4$) and isotropic displacement parameters ($\text{\AA}^2 \times 10^3$) for *trans*-[PdBr₂(PTA)₂]

	x	y	z	U(eq)
H(1A)	1961	1608	7741	39(4)
H(1B)	3697	1209	7064	39(4)
H(3A)	-694	3226	4857	39(4)
H(3B)	-891	2904	6314	39(4)
H(2A)	4032	1789	4372	39(4)
H(2B)	2477	2501	3604	39(4)
H(4A)	1367	3569	7977	39(4)
H(4B)	2832	4473	7653	39(4)
H(5A)	1794	4355	4286	39(4)
H(5B)	3087	4979	5350	39(4)
H(6A)	5525	3861	6581	39(4)
H(6B)	5717	2577	6240	39(4)

Table B5: Torsion angles [$^\circ$] for *trans*-[PdBr₂(PTA)₂]

Br(1)-Pd(1)-P(1)-C(1)	-100.19(17)
Br(1)-Pd(1)-P(1)-C(2)	16.8(2)
Br(1)-Pd(1)-P(1)-C(3)	142.35(19)

Symmetry transformations used to generate equivalent atoms: #1 -x,-y,-z+1

C Supplementary material reported for Chapter 4

Table C1 Absorbance and pH values obtained for the reaction of $[\text{PdCl}(\text{PTA})_3]^+$ and HClO_4 at 245 nm, 275 nm and 315 nm, respectively

pH	A 245 nm	A 275 nm	A 315 nm	pH	A 245 nm	A 275 nm	A 315 nm
6.17	1.452	0.635	0.649	2.57	0.888	0.776	0.280
5.50	1.406	0.608	0.541	2.25	0.770	0.793	0.283
4.84	1.365	0.605	0.429	1.98	0.689	0.808	0.284
4.40	1.328	0.611	0.352	1.69	0.632	0.815	0.285
4.15	1.314	0.619	0.328	1.42	0.598	0.820	0.287
3.85	1.278	0.636	0.303	1.21	0.579	0.825	0.286
3.51	1.214	0.700	0.287	0.96	0.567	0.826	0.288
3.21	1.043	0.697	0.281	0.73	0.556	0.822	0.289
2.95	1.045	0.744	0.281				

Derivation of Eq. 4.44 for the determination of equilibrium constants



$$\text{Equilibrium constant is defined as } K = \frac{[\text{PdP}_2][\text{Cl}^-]}{[\text{PdP}_3][\text{Y}^-]} \quad (2)$$

at any given time, t , the total concentration of PdP_3 is given as:

$$[\text{PdP}_3]_t = [\text{PdP}_3]_e + [\text{PdP}_2]_e \quad (3)$$

From (2) after equilibrium is reach :

$$[\text{PdP}_3]_t = \frac{[\text{PdP}_2]_e[\text{Cl}^-]_e}{k[\text{Y}^-]_e} \quad (4)$$

.....where k = rate constant of forward reaction

Substitute (3) in (4)

$$[\text{PdP}_3]_t = \frac{[\text{PdP}_2]_e[\text{Cl}^-]_e}{k[\text{Y}^-]_e} + [\text{PdP}_2]_e$$

$$[\text{PdP}_3]_t = [\text{PdP}_2]_e \left(\frac{[\text{Cl}^-]_e}{k[\text{Y}^-]_e} + 1 \right)$$

$$[\text{PdP}_2]_e = [\text{PdP}_3]_t \left(\frac{k[\text{Y}^-]_e}{[\text{Cl}^-]_e + k[\text{Y}^-]_e} \right)$$

$$[\text{PdP}_3]_e = \left(\frac{[\text{PdP}_3]_t K[\text{Y}^-]_e}{[\text{Cl}^-]_e + k[\text{Y}^-]_e} \right) \left(\frac{[\text{Cl}^-]_e}{K[\text{Y}^-]_e} \right)$$

$$[\text{PdP}_3]_e = \frac{[\text{PdP}_3]_t [\text{Cl}^-]_e}{[\text{Cl}^-]_e + k[\text{Y}^-]_e}$$

If $[\text{PdP}_3]$ and $[\text{PdP}_2]$ absorbs light at equilibrium then the total absorbance at equilibrium is:

$$A_e = \epsilon_{[\text{PdP}_3]} [\text{PdP}_3]_e + \epsilon_{[\text{PdP}_2]} [\text{PdP}_2]_e$$

$$A_e = \epsilon_{[\text{PdP}_3]} \left(\frac{[\text{PdP}_3]_t [\text{Cl}^-]_e}{[\text{Cl}^-]_e + k[\text{Y}^-]_e} \right) + \epsilon_{[\text{PdP}_2]} \left(\frac{[\text{PdP}_3]_t K[\text{Y}^-]_e}{[\text{Cl}^-]_e + k[\text{Y}^-]_e} \right)$$

since $A = \epsilon cl$ then

$$A_b = \epsilon_{[\text{PdP}_3]} [\text{PdP}_3]_e \quad \text{and} \quad A_f = \epsilon_{[\text{PdP}_2]} [\text{PdP}_2]_e$$

$$A_e = \frac{A_b [\text{Cl}^-]_e}{[\text{Cl}^-]_e + k[\text{Y}^-]_e} + \frac{A_f K [\text{Y}^-]_e}{[\text{Cl}^-]_e + k[\text{Y}^-]_e}$$

$$A_e = \frac{A_b [\text{Cl}^-]_e + A_f K [\text{Y}^-]_e}{[\text{Cl}^-]_e + k[\text{Y}^-]_e}$$

APPENDIX A

Table C2 Determination of equilibrium constants, K_{14} , for $[\text{PdCl}(\text{PTA})_3]\text{Cl}$ and Y^- . Absorbances as a function of added ligand concentration in water at 298 K.

$[\text{I}]^a$ (mM)	A^{400}	$[\text{SCN}]^b$ (mM)	A^{380}	$[\text{Br}]^c$ (mM)	A^{265}
0	0.118	0.10	0.196	0.00	0.929
0.05	0.119	0.15	0.195	0.10	0.928
0.10	0.125	0.20	0.196	0.30	0.932
0.15	0.125	0.30	0.196	0.70	0.928
0.20	0.130	0.40	0.194	0.99	0.928
0.25	0.133	0.60	0.192	4.00	0.932
0.30	0.139	1.00	0.185	8.00	0.932
0.35	0.144	1.50	0.206	10.00	0.934
0.40	0.149	2.00	0.195	20.01	0.950
0.43	0.151	4.00	0.216	60.03	0.994
0.45	0.154	4.00	0.216	100.00	1.050
0.48	0.154	6.01	0.217	200.01	1.136
0.50	0.161	8.01	0.230	400.02	1.223
0.75	0.178	10.01	0.242	600.03	1.276
1.00	0.200	20.02	0.276	800.04	1.299
4.00	0.283	40.05	0.331	1000.05	1.324
6.00	0.300	60.07	0.353		
10.01	0.315	80.10	0.373		
20.01	0.326	100.01	0.398		
40.03	0.328	100.01	0.395		
		200.02	0.439		
		400.05	0.468		
		600.07	0.475		

 $C_{\text{Pd}}^a = 0.062 \text{ mM (as NaI)}$ $C_{\text{Pd}}^b = 0.056 \text{ mM (as KSCN)}$ $C_{\text{Pd}}^c = 0.07 \text{ mM as LiBr}$

APPENDIX A

Table C3 Determination of equilibrium constants, K_{24} , for *cis*-[PdCl₂(PTA)₂] and Y. Absorbances as a function of added ligand concentration in water at 298 K.

[I] ^a (mM)	A^{400}	[SCN] ^b (mM)	A^{300}	[Br] ^c (mM)	A^{265}	[N ₃] ^d (mM)	A^{300}
0	0.270	0	0.374	0	0.379	0	0.462
0.01	0.263	0.01	0.381	0.10	0.363	0.10	0.454
0.02	0.264	0.02	0.375	0.20	0.365	0.20	0.459
0.03	0.267	0.03	0.379	0.30	0.359	0.30	0.448
0.04	0.270	0.04	0.396	0.40	0.360	0.39	0.454
0.06	0.277	0.05	0.400	0.50	0.362	0.39	0.455
0.07	0.277	0.06	0.398	0.60	0.361	0.49	0.456
0.08	0.287	0.07	0.403	0.80	0.358	0.59	0.456
0.10	0.295	0.08	0.403	1.00	0.363	0.79	0.472
0.12	0.297	0.10	0.415	2.00	0.361	0.98	0.482
0.14	0.304	0.12	0.418	5.00	0.360	4.99	0.641
0.16	0.315	0.14	0.418	10.00	0.366	4.99	0.637
0.20	0.326	0.16	0.420	20.01	0.370	9.98	0.771
0.30	0.367	0.20	0.429	50.02	0.392	19.95	0.917
0.40	0.391	0.30	0.455	100.00	0.414	49.88	1.081
0.50	0.422	0.40	0.463	150.00	0.442	99.99	1.185
0.60	0.441	0.50	0.475	200.00	0.468	149.98	1.223
1.00	0.471	0.71	0.502	250.00	0.478	199.98	1.254
1.00	0.470	1.01	0.544	300.00	0.486	249.97	1.270
2.00	0.488	1.51	0.567	350.00	0.494	299.96	1.285
4.00	0.505	2.02	0.597	400.00	0.504	599.93	1.313
6.00	0.516	4.03	0.713	600.00	0.519	799.90	1.342
10.00	0.536	6.05	0.786	800.00	0.526		
15.00	0.537	8.06	0.847	1000.00	0.537		
20.00	0.542	12.09	0.940				
		20.15	1.058				
		40.00	1.180				

APPENDIX A

80.01 1.256

160.02 1.322

300.03 1.330

$C_{Pd}^a = 0.062 \text{ mM (as NaI)}$ $C_{Pd}^b = 0.057 \text{ mM (as KSCN)}$

$C_{Pd}^c = 0.07 \text{ mM (as LiBr)}$ $C_{Pd}^d = 0.07 \text{ mM (as NaN}_3\text{)}$

An expression of the observed rate constant, $(k_{obs})_{Cl}$, (Eq. 4.48 and 4.49) as derived from the mechanism presented in Scheme 4.3.

The rate is given as

$$R = (k_e[PdCl^*(PTA)_3] + k_s[Pd(OH_2)(PTA)_3])[Cl^-] \quad (A)$$

The equilibrium constant is given as

$$K_{Cl} = [Pd(OH_2)(PTA)_3] [Cl^-] / [PdCl(PTA)_3] \quad (B)$$

rearrangement of (B) gives

$$[Pd(OH_2)(PTA)_3] = (K_{Cl} [PdCl(PTA)_3]) / [Cl^-] \quad (C)$$

$$\text{and } [PdCl(PTA)_3] = ([Pd(OH_2)(PTA)_3] [Cl^-]) / K_{Cl} \quad (D)$$

The total palladium concentration, $[Pd]_T$, is given as

$$[Pd]_T = [PdCl(PTA)_3] + [Pd(OH_2)(PTA)_3] \quad (E)$$

Substitution of (D) into (E) gives

$$[Pd]_T = ([Pd(OH_2)(PTA)_3] [Cl^-]) / K_{Cl} + [Pd(OH_2)(PTA)_3] \quad (F)$$

$$\text{and } [Pd(OH_2)(PTA)_3] = [Pd]_T / (1 + [Cl^-] / K_{Cl})$$

Multiplication of (F) with $K_{Cl}/[Cl^-]$ gives

$$[Pd(OH_2)(PTA)_3] = [Pd]_T (K_{Cl}/[Cl^-]) / (1 + K_{Cl}/[Cl^-]) \quad (G)$$

Substitution of (C) into (E) gives

$$[Pd]_T = [PdCl(PTA)_3] + (K_{Cl} [PdCl(PTA)_3]) / [Cl^-] \quad (H)$$

$$\text{and } [PdCl(PTA)_3] = [Pd]_T / (1 + K_{Cl}/[Cl^-])$$

APPENDIX A

Substitution of (G) and (H) into (A) gives

$$R = (k_e ([Pd]_T / (1 + K_{Cl}/[Cl^-])) + k_s ([Pd]_T (K_{Cl}/[Cl^-]) / (1 + K_{Cl}/[Cl^-])) [Cl^-]$$
$$= (k_e ([Pd]_T + k_s ([Pd]_T (K_{Cl}/[Cl^-])) [Cl^-] / (1 + K_{Cl}/[Cl^-]))$$

By definition, the rate constant observed (as a function of line-width) on the free Cl^- peak, is given by:

$$d[PdCl]/dt[Cl^-] = (k_{obs})_{Cl} = ((k_e + k_s (K_{Cl}/[Cl^-])) / (1 + K_{Cl}/[Cl^-])) [Pd]_T \quad (I)$$

If $[Cl^-] \gg K_{Cl}$ then

$$(k_{obs})_{Cl} = ((k_e + k_s (K_{Cl}/[Cl^-])) [Pd]_T) \quad (J)$$

$$(k_{obs})_{Cl} / [Pd]_T = (k_{obs})' = k_e + k_s (K_{Cl}/[Cl^-]) \quad (K)$$

Abstract

The aim of this study was to prepare complexes of the type $[\text{PdCl}(\text{PTA})_3]\text{Cl}$ and *cis*- $[\text{PdCl}_2(\text{PTA})_2]$ (PTA = 1,3,5-triaza-7-phosphaadamantane) and to investigate i) the stability, ii) protonation behaviour, and iii) the substitution behaviour with halides/pseudo-halides, of these complexes in aqueous solution.

Structure determinations were done by X-ray crystallography and two square planar complexes, *trans*- $[\text{Pd}(\text{SCN})_2(\text{PTA})_2](\text{SCN})_2$ and *trans*- $[\text{PdBr}_2(\text{PTA})_2]$ were reported. Both crystallize in the monoclinic space group, $P2_1/n$, refined to final R values of 2.88 % and 4.15 %, respectively. For the *trans*- $[\text{Pd}(\text{SCN})_2(\text{PTA})_2](\text{SCN})_2$ complex it was observed that both the PTA ligands are protonated at one of the N atoms, while two thiocyanate moieties acts as counterions and occupy the axial positions.

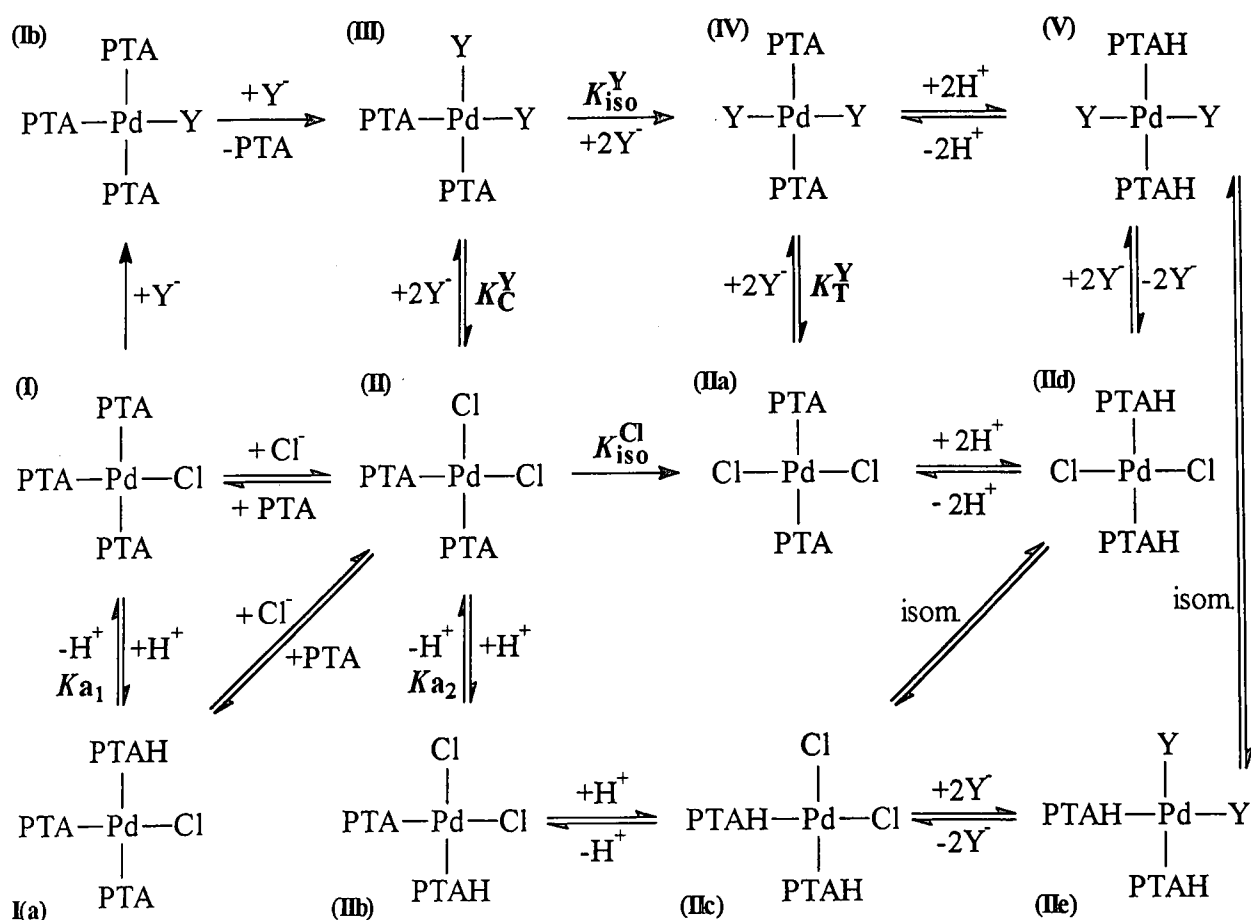
Both the $[\text{PdCl}(\text{PTA})_3]^+$ and *cis*- $[\text{PdCl}_2(\text{PTA})_2]$ complexes hydrolyze and decompose when dissolved in water. However, in an excess of chloride hydrolysis is prevented to a large extent. In solution, a dynamic equilibrium exists between $[\text{PdCl}(\text{PTA})_3]^+$ and *cis*- $[\text{PdCl}_2(\text{PTA})_2]$ and over a period of time, depending on the chloride concentration added, $[\text{PdCl}(\text{PTA})_3]^+$ slowly converts to *cis*- $[\text{PdCl}_2(\text{PTA})_2]$.

In acidic medium $[\text{PdCl}(\text{PTA})_3]^+$ rapidly converts to *cis*- $[\text{PdCl}_2(\text{PTA})_2]$ and two pH dependences are observed; *i.e.*, $\text{p}K_{a1} = 5.11(4)$ and $\text{p}K_{a2} = 2.92(6)$, which are assumed to represent the protonation of the $[\text{PdCl}(\text{PTA})_3]^+$ and $[\text{PdCl}_2(\text{PTA})_2]$ complexes respectively.

The addition of a halide/pseudo-halide, Y^- ($Y^- = \text{Br}^-, \text{I}^-, \text{SCN}^-$ and N_3^-) to $[\text{PdCl}(\text{PTA})_3]^+$ in neutral solution (pH = 5.0-6.5), results in the rapid substitution of the chloride to form, as final product, *trans*- $[\text{Pd}Y_2(\text{PTA})_2]$. Similarly, upon addition of a halide/pseudo-halide, Y^- , to *cis*- $[\text{PdCl}_2(\text{PTA})_2]$, the *trans* product is formed. Larger equilibrium constants were obtained for *cis*- $[\text{PdCl}_2(\text{PTA})_2]$ and Y^- (K_{24}), than for $[\text{PdCl}(\text{PTA})_3]^+$ and Y^- (K_{14}) ($K_{24} = 3.0(3) \times 10^3$, $1.1(6) \times 10^2$, $6.0(4) \times 10$ and $4.1(3) \text{ M}^{-1}$, for I^- , SCN^- , N_3^- and Br^- , respectively, and $K_{14} = 5.8(4) \times 10^2$, $1.9(4) \times 10$ and $3.0(3) \text{ M}^{-1}$, for I^- , SCN^- and Br^- , respectively).

High reactivity of all the complexes investigated was observed and it was not possible to study these complexes by time-resolved spectroscopy. Significant line-broadening on ^{35}Cl NMR was observed which enabled the study of the rapid chloride exchange for $[\text{PdCl}(\text{PTA})_3]^+$. It was observed that the higher the concentration of the chloride, the smaller the rate of chloride exchange becomes. It is concluded that two species contributed to the exchange, the $[\text{PdCl}(\text{PTA})_3]^+$ and a palladium-aqua species, probably $[\text{Pd}(\text{OH})_2(\text{PTA})_3]^+$. The chloride exchange rate constant for the $[\text{PdCl}(\text{PTA})_3]^+$, at 22 °C, was determined as $1.64(8)\times 10^5 \text{ M}^{-1}\text{s}^{-1}$.

Both the $[\text{PdCl}(\text{PTA})_3]^+$ and *cis*- $[\text{PdCl}_2(\text{PTA})_2]$ complexes showed complicated solution behaviour as indicated in the scheme* below:



*Aqua species and charges omitted, PTAH = protonated PTA, isom. = isomerization

Opsomming

Die primêre doel van hierdie studie was die bereiding van komplekse van die tipe $[\text{PdCl}(\text{PTA})_3]\text{Cl}$ en $\text{cis}-[\text{PdCl}_2(\text{PTA})_2]$ (PTA = 1,3,5-triaza-7-fosfaadamantaan), asook om die volgende eienskappe van hierdie komplekse in waterige oplossing te ondersoek: i) stabiliteit, ii) protoneringsgedrag, en iii) substitusiegedrag met haliede en pseudo-haliede.

Struktuurbevestigings is gedoen met behulp van X-straal kristallografie en twee vierkantig planêre komplekse, $\text{trans}-[\text{Pd}(\text{SCN})_2(\text{PTA})_2](\text{SCN})_2$ en $\text{trans}-[\text{PdBr}_2(\text{PTA})_2]$, is gerapporteer. Beide kristalliseer in die monokliniese ruimte groep, $P2_1/n$, en onderskeidelike R-waardes van 2.88% en 4.15% is verkry. Vir die $\text{trans}-[\text{Pd}(\text{SCN})_2(\text{PTA})_2](\text{SCN})_2$ kompleks is waargeneem dat beide die PTA ligande geprotoneer is by een van die N atome, terwyl twee tiosianaatanione as teenione optree en die aksiale posisie beset.

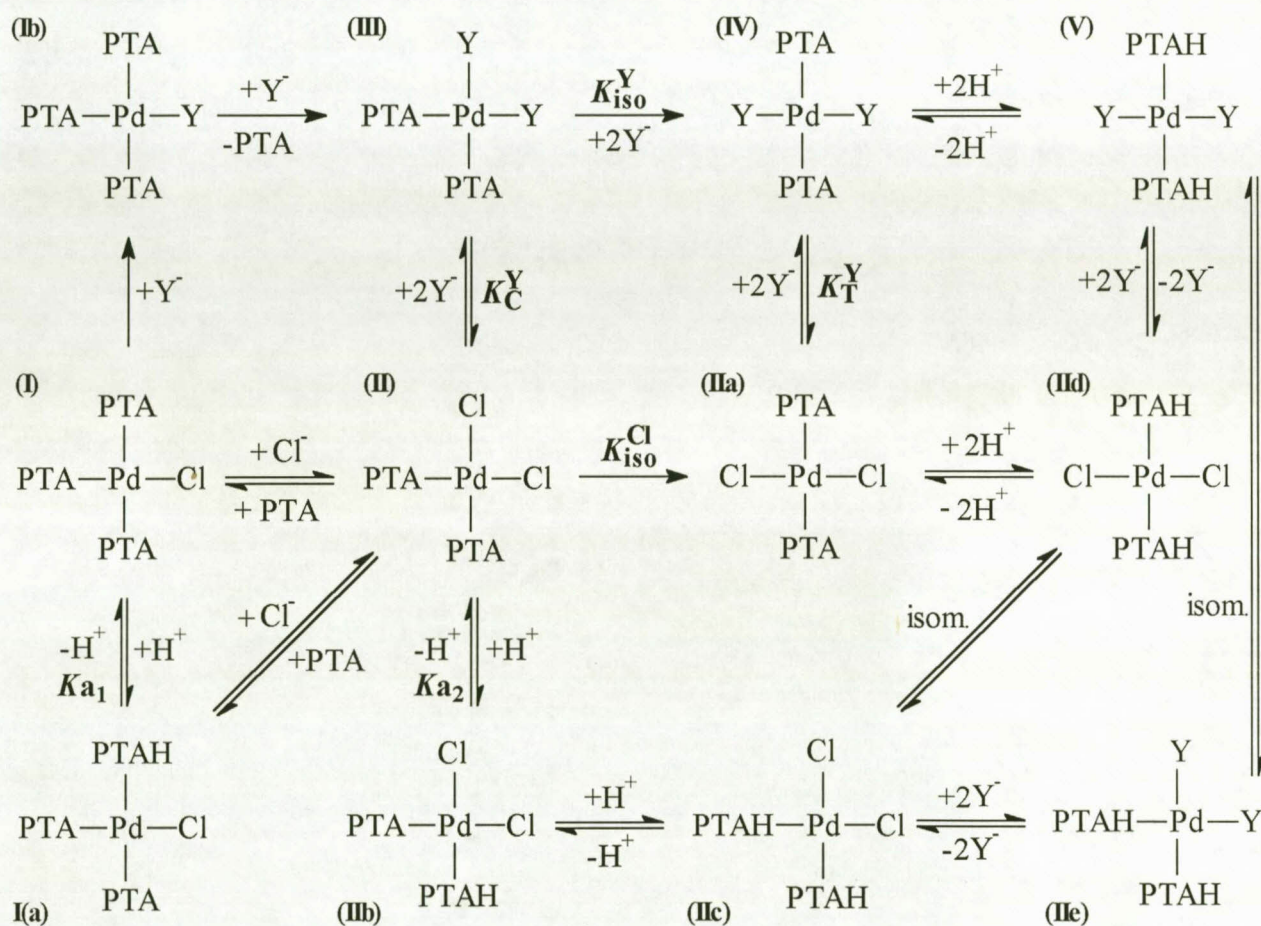
Beide die $[\text{PdCl}(\text{PTA})_3]^+$ en $\text{cis}-[\text{PdCl}_2(\text{PTA})_2]$ komplekse hidroliseer en ontbind wanneer dit opgelos word in waterige media. Hidrolise word egter tot 'n groot mate beperk indien 'n oormaat chloried teenwoordig is. 'n Dinamiese ewewig bestaan in oplossing tussen $[\text{PdCl}(\text{PTA})_3]^+$ en $\text{cis}-[\text{PdCl}_2(\text{PTA})_2]$ en afhangend van die chloriedkonsentrasie wat bygevoeg is, ontbind $[\text{PdCl}(\text{PTA})_3]^+$ stadig om die $\text{cis}-[\text{PdCl}_2(\text{PTA})_2]$ kompleks te vorm.

In suurmedium ontbind $[\text{PdCl}(\text{PTA})_3]^+$ vinnig om die $\text{cis}-[\text{PdCl}_2(\text{PTA})_2]$ kompleks te vorm en twee pH afhanklikhede is waargeneem; *nl.*, $\text{p}K_{a1} = 5.11(4)$ en $\text{p}K_{a2} = 2.92(6)$ en dit word aanvaar dat dit onderskeidelik die protonering van die $[\text{PdCl}(\text{PTA})_3]^+$ en $[\text{Pd}(\text{Cl})_2(\text{PTA})_2]$ komplekse, verteenwoordig.

Die byvoeging van 'n halied/pseudo-halied, Y, ($Y = \text{Br}, \text{I}, \text{SCN}$ and N_3) by $[\text{PdCl}(\text{PTA})_3]^+$, in neutrale oplossing, (pH = 5.0-6.5), lei tot die vinnige substitusie van die chloried om $\text{trans}-[\text{PdY}_2(\text{PTA})_2]$ as finale produk te gee. Soortgelyk, met die byvoeging van 'n halied/pseudo-halied, Y, by $\text{cis}-[\text{PdCl}_2(\text{PTA})_2]$ word die trans produk gevorm. Groter ewewigkonstantes is verkry vir $\text{cis}-[\text{PdCl}_2(\text{PTA})_2]$ met Y (K_{24}), as vir $[\text{PdCl}(\text{PTA})_3]^+$ met Y (K_{14}) ($K_{24} = 3.0(3) \times 10^3$, $1.1(6) \times 10^2$, $6.0(4) \times 10$ en $3.0(3) \text{ M}^{-1}$ vir I^- , SCN^- , N_3^- en Br^- , onderskeidelik en $K_{14} = 5.8(4) \times 10^2$, $1.9(4) \times 10$ en $3.0(3) \text{ M}^{-1}$ vir I^- , SCN^- en Br^- , onderskeidelik).

Vir al die komplekse wat ondersoek is, is gevind dat dit hoogs reaktief is en dit was gevolglik nie moontlik om die komplekse met behulp van konvensionele metodes van spektroskopie (bv. stop-vloei) te bestudeer nie. Betekenisvolle lynverbreding op ^{35}Cl KMR is waargeneem wat die bestudering van vinnige chlorieduitruiling vir $[\text{PdCl}(\text{PTA})_3]^+$ moontlik gemaak het. Daar is gevind dat hoe hoër die konsentrasie van die chloried, hoe kleiner die tempo van chlorieduitruiling word. Die gevolgtrekking kan gemaak word dat twee spesies bydraes maak tot die uitruiling, nl., die $[\text{PdCl}(\text{PTA})_3]^+$ en die palladium-akwa spesie, waarskynlik $[\text{Pd}(\text{OH}_2)(\text{PTA})_3]^+$. Die tempokonstante vir die chlorieduitruiling van die $[\text{PdCl}(\text{PTA})_3]^+$, by 22°C , is bereken as $1.64(8)\times 10^5 \text{ M}^{-1}\text{s}^{-1}$.

Beide die $[\text{PdCl}(\text{PTA})_3]^+$ en *cis*- $[\text{PdCl}_2(\text{PTA})_2]$ het komplekse oplossingsgedrag getoon, soos aangedui in die volgende skema*:



*Ladings en akwaspesie is weggelaat, PTAH = geprotoneerde PTA, isom. = isomerisasie.